

Final Technical Report

Paleoseismic Investigation of the Idalia Hill Fault along the Commerce Geophysical Lineament Idalia, Missouri



Prepared for:

U.S. Geological Survey
National Earthquake Hazards Reduction Program
Award No. 03-HQ-GR-0095

Prepared by:

William Lettis & Associates, Inc.
1777 Botelho Drive, Suite 262
Walnut Creek, CA 94596

June 2004



FINAL TECHNICAL REPORT

PALEOSEISMIC INVESTIGATION OF THE IDALIA HILL FAULT ALONG THE COMMERCE GEOPHYSICAL LINEAMENT, IDALIA, MISSOURI

Recipient:

William Lettis & Associates, Inc.,
1777 Botelho Dr., Ste. 262, Walnut Creek, CA 94596
(925) 256-6070; (925) 256-6076 fax; URL www.lettis.com

Principal Investigators:

John N. Baldwin and Robert Witter
William Lettis & Associates, Inc.
1777 Botelho Drive, Suite 262, Walnut Creek, CA 94596
(925) 256-6070; (925) 256-6076 (fax)
Email: baldwin@lettis.com; witter@lettis.com

Contributors:

James D. Vaughn
KeenGeoserve; 325 East Vine Street; Dexter, Missouri, 63841

James Harris
Millsaps College, Geology Department; Jackson, Mississippi, 39210

John Sexton and Marshall Lake
Southern Illinois University, Geology Department; Carbondale, IL 62901

Steve Forman
University of Illinois, Chicago, Department of Geological Sciences; Chicago, IL 60607

Program Elements II

Keywords:

Quaternary fault behavior, neotectonics, paleoseismology

U. S. Geological Survey
National Earthquake Hazards Reduction Program
Award Number 03-HQ-GR-0095

June 30, 2004

This research was supported by the U.S. Geological Survey (USGS), Department of the Interior, under USGS Award 03-HQ-GR-0095. The views and conclusions contained in this document are those of the authors and should not be interpreted as necessarily representing the official policies, either expressed or implied, of the U.S. Government.

Award 03-HQ-GR-0095

**PALEOSEISMIC INVESTIGATION OF THE IDALIA HILL FAULT ALONG THE
COMMERCE GEOPHYSICAL LINEAMENT, IDALIA, MISSOURI**

Baldwin¹, J.N., Witter¹, R.C., Vaughn², J.D., Harris³, J.B., Sexton⁴, J., Lake⁴, M., and Forman⁵, S.

Principal Investigators:

¹William Lettis & Associates, Inc., 1777 Botelho Drive, Suite 262 Walnut Creek, CA 94596
balwin@lettis.com; witter@lettis.com; phone: 925-256-6070, fax: 925-256-6076

Contributors:

²Keen GeoServe, 325 E. Vine, Dexter, MO 63841

³Millsaps College, Geology Department, Jackson, Mississippi, 39210

⁴Southern Illinois University, Geology Department, Carbondale, IL 62901

⁵University of Illinois, Chicago, Department of Geological Sciences, Chicago, IL 60607

ABSTRACT

The Commerce geophysical lineament (CGL) is a 600-km-long, 5- to 10-km-wide, northeast-trending magnetic and gravity anomaly that extends from northeastern Arkansas to central Indiana. Recent geomorphic mapping, seismic reflection and ground penetrating radar data, paleoseismic trenching, and borehole information collected at the South Holly Ridge site near Idalia, southeastern Missouri, provide evidence of late Pleistocene to possibly early Holocene deformation aligned with the Idalia Hill fault zone which overlies the CGL. At the South Holly Ridge site, we investigated a prominent, northeast-trending linear swale that is bounded on the south by a 2- to 3-m-high north-facing escarpment and an apparent right-laterally deflected creek. The site geomorphology aligns with regional northeast-trending linear valleys, escarpments, linear and deflected drainages, springs and bedrock notches mapped northeast and southwest of the site. At South Holly Ridge, seismic reflection data acquired across the mapped CGL image near-vertical faults offsetting Tertiary/Cretaceous and Tertiary/Quaternary stratigraphic contacts that project up dip toward the mapped surface trace of the Idalia Hill fault zone. Also, the faults imaged at depth coincide with mapped faults interpreted from ground penetrating radar surveys, and faults exposed in excavations performed at the site.

Trenches excavated across a 2- to 3-m-high linear escarpment expose faulted and warped Tertiary deposits, Pleistocene reworked Mounds Gravel, the Sangamon Geosol, and Pleistocene Peoria loess. Warping and possible faulting of late Pleistocene to early Holocene soil(s) developed in scarp-derived colluvium and loess coincide with the linear scarp. Preliminary analyses of trench, borehole and GPR data constrain the most recent event at the site between the late Pleistocene (about 18 ka) and early Holocene (pre-7.7 ka), and an earlier event that predates 23 to 18 ka. Although poorly constrained, the timing of these events overlaps with late Pleistocene to early Holocene faulting and paleoliquefaction events evaluated elsewhere along the CGL in southeastern Missouri. Lastly, the combined results suggest that deformation observed at the site and coincident with the CGL is of primary tectonic origin based on: (1) deep-seated faults coincident with near-surface faulting and folding exposed in excavations at the site, (2) an absence of reverse faulting at the hypothetical “toe bulge” of a hypothetical landslide, (3) lateral continuity of prominent northeast-trending geomorphic lineaments, and (4) lateral continuity (3 km) of Quaternary faulting and folding along the eastern ridge margin.

TABLE OF CONTENTS

ABSTRACT.....	i
1.0 INTRODUCTION	1
2.0 REGIONAL TECTONIC SETTING.....	3
3.0 LOCAL GEOLOGIC SETTING	4
3.1 Idalia Hill Fault Zone.....	4
3.2 Approach and Methodology.....	5
3.3 Seismic Reflection Data Acquisition	6
3.4 Paleoseismic Trenching and Drilling.....	6
3.5 Age Dating.....	6
3.6 Geotechnical Analyses.....	7
4.0 REGIONAL GEOMORPHOLOGY.....	8
5.0 SOUTH HOLLY RIDGE SITE.....	10
5.1 Seismic Reflection Survey.....	10
5.1.1 Faulting and Folding Interpreted from Seismic Lines	10
5.1.2 Ground Penetrating Radar Studies.....	11
6.0 PALEOSEISMIC TRENCHING AND DRILLING	12
6.1 Site Stratigraphy.....	12
6.2 Eocene Wilcox Formation	12
6.3 Pleistocene Reworked Mounds Gravel with Sangamon Geosol.....	13
6.4 Pleistocene Colluvium/Reworked Mounds Gravel.....	13
6.5 Loess	13
6.6 Buried Soils (Q_{s1} , Q_{s2} , and Q_{s3}).....	13
6.6.1 Holocene Surficial Deposits	15
6.7 Fault Zone Characteristics	16
6.7.1 Deformation Northeast of Pennington Creek.....	16
6.7.1.1 Primary Zone of Northeast- Striking Faults.....	16
6.7.1.2 Folding of Units Q_{s1} and Q_{s2}	17
6.7.1.3 Southwest Dipping Low Angle Faults	17
6.7.1.4 Absence of Reverse Faulting in Trench T-7	18
6.7.1.5 Absence of Faulting Southwest of Pennington Creek.....	18
7.0 DISCUSSION.....	20
7.1 Basal Slide Plane.....	20
7.2 Map Pattern and Sense of Slip of Boundary Faults	21

7.2.1 Headscarp and Margin Faulting.....	21
7.2.2 Reverse Faulting at Toe Bulge.....	21
7.2.3 Sinuous Bulging Ridges.....	22
7.3 Lateral Continuity of Features	22
7.4 Strain Rates	23
7.5 Seismic Implications if Deformation is Tectonic in Origin	23
8.0 TIMING OF DEFORMATION	24
8.1 Regional Comparison of Event Timing Information	25
9.0 SUMMARY OF FINDINGS	27
10.0 ACKNOWLEDGEMENTS	28
11.0 REPORTS/ABSTRACTS PUBLISHED	29
12.0 REFERENCES	31

LIST OF TABLES

Table 1. Radiocarbon Analyses, South Holly Ridge Site Idalia, Missouri	30
--	----

LIST OF FIGURES

Figure 1	Regional location map of the New Madrid seismic zone and the commerce section of the geophysical lineament. Commerce geophysical lineament. Lineament location based on latitude and longitude coordinates provided by Hildenbrand (personal communication, 2002) and, in part, modified from Stephenson et al. (1999). Historical seismicity (1974 to 1991) after Rhea and Wheeler, 1995, and Johnston and Schweig (1996). IHF = Idalia Hill fault; CF = Commerce fault; CGL = Commerce geophysical lineament (Hildenbrand and Ravat, 1997). Stars represent epicenters of M4.8 earthquakes (after Stephenson et al., 1999).
Figure 2	Geologic and site map of the Bloomfield Hills, Missouri (geology modified from Saucier, 1964; Farrar and McManamy, 1937; Stewart, 1942; Satterfield and Ward, 1978).
Figure 3	Seismic reflection profile IDAL-2 along Road E, near Idalia (see Figure 2 for location). Quaternary (Q), Tertiary (T), Cretaceous (K), and Paleozoic (P _z) strata labeled; interpreted faults shown by heavy black lines (modified from Stephenson et al., 1999). Deformation near Idalia Hill fault resembles transpressional deformation.
Figure 4	Seismic reflection profile IDAL-1 along Road AB, near Guam (see Figure 2 for location). Quaternary (Q), Tertiary (T), Cretaceous (K), and Paleozoic (P _z) strata labeled; interpreted faults shown by heavy black lines (modified from Stephenson et al., 1999).
Figure 5	Geomorphic lineament map of eastern margin of the Bloomfield Hills, southeast Missouri.
Figure 6	Site map showing trench, borehole, seismic reflection survey, and GPR survey locations. Location of stream bank thalweg estimated from mapping.

- Figure 7 Interpreted shear-wave seismic reflection profiles from South Holly Ridge site, Idalia, MO. See Figure 5 for section locations.
- Figure 8 GPR-1 is interpreted as imaging moderately dipping Eocene Wilcox (T_w) and Pleistocene (Q_p) loess that are inset by a sequence of buried paleochannel deposits and undeformed overlying alluvium. Parabolic feature in GPR-1 interpreted as an artifact from a telephone pole. GPR-2 depicts folded and faulted bedding along the southeast part of the profile and a sequence of nested paleochannel deposits in the axis of the linear valley. See Figure 6 for section location.
- Figure 9 Log of Trenches T-1 and T-2.
- Figure 10 Log of Trenches T-3 and T-4.
- Figure 11 Log of Trench T-5.
- Figure 12 Log of Trench T-6.
- Figure 13 Log of Trench T-7.
- Figure 14 Schematic cross section A-A' across North and South Holly Ridge sites showing shallow surface faults connecting with faults interpreted from seismic profiles HR-1 and HR-2. See Figure 6 for section location. Tectonic model assumes deformation as primary tectonic deformation. Landslide model assumes faulting interpreted at both sites is related to landsliding.

LIST OF APPENDICES

- Appendix A Detailed Pedologic Descriptions of Trench T-5
- Appendix B Results of Partical Size Analyses

1.0 INTRODUCTION

The CGL is a 600-km-long, 5- to 10-km-wide northeast-trending gravity and aeromagnetic anomaly that trends subparallel to and west of the Reelfoot rift and extends from northeast Arkansas to central Indiana (Figure 1). The Holly Ridge site is located along the 150-km-long Commerce section of the CGL within the northwestern Mississippi embayment about 40 to 50 km northwest of the active New Madrid seismic zone (NMSZ) (Figure 1). Recent geologic, geomorphic and geophysical studies performed along the CGL in southeastern Missouri provide direct and indirect evidence indicative of late Quaternary activity along faults coincident with the lineament. This evidence includes: (1) anomalous west-flowing drainages on Crowley's Ridge (Cox, 1988; Fischer-Boyd and Schumm, 1995) and the Bloomfield and Benton Hills; (2) displacement of late-Tertiary and Pleistocene to Holocene deposits (Groshkopf, 1955; Satterfield and Ward, 1978; Thompson, 1981; Harrison et al., 1999; Harrison et al., 2002) along NE-striking faults that are consistent with the present-day stress field (Zoback, 1992); (3) paleoliquefaction features within the Western Lowlands that overlie the CGL (Figure 1; Vaughn, 1991; 1992; 1994; and Vaughn et al., 2002); (4) presence of diffuse microseismicity consisting of low to moderate magnitude earthquakes spatially associated with the CGL (Harrison and Schultz, 1994; Langenheim and Hildenbrand, 1997; Hildenbrand and Ravat, 1997); (5) geophysical evidence of about 20 m of vertical separation of the Paleozoic/Cretaceous boundary, as well as poorly constrained Tertiary-Quaternary deformation coincident with the surface traces of previously mapped faults in the Bloomfield and Benton Hills (Stephenson et al., 1999); and (6) a prominent tonal lineament developed in late Wisconsin braided stream deposits that aligns partly with the Commerce and Idalia Hill faults (Heyl and McKeown, 1978). Furthermore, similar geologic, geophysical, and seismologic data collected in Illinois and Indiana provide further support for Quaternary active structures spatially coincident with the CGL (Odum, et al., 2002, McBride et al., 2002).

Combined, this body of evidence strongly implies that previously mapped northeast-striking faults that overlie the surface projection of the CGL in southeast Missouri, but are outside of the active NMSZ, represent poorly characterized seismogenic structures that are capable of generating moderate to large magnitude earthquakes. A preliminary review, interpretation and correlation of limited earthquake timing data collected from paleoseismic and paleoliquefaction studies appears to indicate that northeast-striking faults coincident with the CGL were active up to at least the late Pleistocene and early Holocene (Vaughn, 1994), and possibly into the middle to late Holocene (Harrison et al., 1999). Clearly, the possible existence of a significant seismic source spanning up to 600 km in length from Arkansas to Indiana, poses a major seismic hazard to the population, infrastructure, and lifelines of the central U.S., and thus, requires characterization of the style, timing and rate of deformation, and rupture boundaries for input into probabilistic earthquake hazard models.

The objective of this study is to evaluate the seismogenic potential of the Commerce geophysical lineament (CGL) by assessing the late Pleistocene and Holocene deformation associated with the northeast-striking Idalia Hill fault located along the CGL in southeastern Missouri (Figure 1). The 0.5-km wide Idalia Hill fault zone bounds the southeastern margin of the Bloomfield Hills, and exhibits direct and indirect evidence of Quaternary deformation based on the alignment of topographic escarpments, deflected drainages, photolineaments, and subsurface faulting of Paleozoic through late Quaternary deposits.

This research expands the regional coverage of paleoseismic investigations outside of the New Madrid seismic zone (NMSZ) to locate and assess other possible seismic sources, and to evaluate the spatial and temporal characteristics of prehistoric earthquakes in the central United States. The Idalia Hill fault zone intersects the Holly Ridge site (herein referred to as the North Holly Ridge site) previously investigated

by the Missouri Department of Natural Resources (Hoffman, 1997). The site of this current study is located directly south of the North Holly Ridge site and herein is referred to as the South Holly Ridge site. Together these two sites define the Holly Ridge sites (Figure 2). Data collected previously by Hoffman (1997) at the North Holly Ridge site are combined with subsurface and geomorphic information collected as part of the South Holly Ridge site assessment to characterize the Idalia Hill fault zone and its potential down-dip connection with the Commerce geophysical lineament.

2.0 REGIONAL TECTONIC SETTING

The CGL is hypothesized to represent a 600-km-long series of mafic dike intrusions emplaced along pre-existing or coeval faults between Arkansas and southern Illinois during the Early Cambrian (intrusions accompanying origin of the Reelfoot rift), or possibly Precambrian (Langenheim and Hildenbrand, 1997). The CGL coincides with the northwest margin of the Reelfoot rift, as identified by gravity and aeromagnetic data. Faulting along the CGL appears to be complex and long-lived, and includes both dip-slip and strike-slip faulting. Hildenbrand et al., (2002) speculate that the Commerce geophysical lineament evolved in the Mesoproterozoic (1.1 to 1.5 Ga) as a major cratonic rheological boundary that was reactivated during varying stress regimes throughout its history.

On the basis of variations in gravity, magnetic and geologic characteristics, portions of the CGL have been differentiated into the Newport, Commerce and Junction sections (Langenheim and Hildenbrand, 1997). The Commerce section exhibits the most prominent gravity and magnetic anomalies and extends from the Arkansas-Missouri border across Thebes Gap and into southern Illinois (Figure 1). The northern part of the Commerce section is associated with the mapped trace of the Commerce fault, near Commerce, Missouri, where recent neotectonic studies provide evidence of Pleistocene and Holocene deformation (Figure 1; Harrison and Schultz, 1994; Harrison et al., 1999; Harrison et al., 2002). To the southwest of Commerce, a well-defined photo-lineament and topographic escarpment along the southeastern margins of the Benton and Bloomfield Hills coincide with the Commerce section of the CGL (Heyl and McKeown, 1978). This photolineament is parallel to the Idalia Hill fault in the Bloomfield Hills, which offsets deposits as young as Quaternary in age (Figure 1; Stephenson et al., 1999; Palmer et al., 1997).

Geophysical surveys at the south end of the Benton Hills (Anderson, 1997) and the northern part of the Bloomfield Hills (Stephenson et al., 1999) image extensive faulting aligned with the CGL, and the Idalia Hill and Commerce faults. Between the Benton and Bloomfield Hills, the CGL underlies both the Quaternary-Holocene active Commerce fault and the inferred Quaternary active Idalia Hill fault (Stephenson et al., 1999) (Figure 1). Furthermore, northeast across Thebes Gap and into southern Illinois, more recent geophysical investigations link faults imaged in high-resolution seismic reflection and microgravity surveys with near surface faults that possibly offset Quaternary deposits directly east of the Cache River (Odum et al., 2002). Collectively, the data strongly suggest a correlation between structural anomalies interpreted from geophysical profiles and near-surface northeast-striking faults and interpreted Quaternary deformation.

Diffuse contemporary seismicity occurs beneath, along and adjacent to the CGL between Arkansas and southern Illinois (Harrison and Schultz, 1994; Langenheim and Hildenbrand, 1997). Focal mechanisms of 16 earthquakes that occurred between 1963 and 1990 are consistent with predominantly strike-slip and reverse modes of faulting along the entire length of the CGL. At least two M4.8 earthquakes with predominantly strike-slip components have occurred near or on the Commerce section of the CGL within this 17-year period (Figure 1). Investigators have shown that some of the focal mechanisms are consistent with NE-striking faults (Harrison and Schultz, 1994), and others have indicated that a few of the focal mechanisms are consistent with northwest-trending structures (Zoback, 1992). Further northeast, near Vincennes, Indiana, where it is hypothesized that the CGL forms a restraining left-step, the CGL is believed to be associated with the location of several large prehistoric earthquakes on the basis of a deflection in the Wabash River and a left-step in the magnetic anomaly (McNulty and Obermeier, 1999).

3.0 LOCAL GEOLOGIC SETTING

The Bloomfield Hills lie within the northwestern part of the Mississippi embayment, and average about 60 m above the adjacent alluvial lowlands. East of the Bloomfield Hills are the Eastern Lowlands consisting of Pleistocene braided stream channel and alluvial fan deposits, overlain by Holocene alluvium and/or inset Holocene meander deposits (Figure 1; Saucier, 1996). The Western Lowlands, that lie directly west of the Bloomfield Hills, consist of 24 to 18 ka Pleistocene braided stream channel deposits derived from the ancestral Mississippi River (Figure 1; Royall et al., 1991; Blum et al., 2000). The eastern margin of the ridge is bounded by slightly younger braided stream deposits that formed following the eastward diversion of the Mississippi River through the Bell City-Oran Gap at about 17 to 16 ka (Saucier, 1974; Royall et al., 1991), or possibly even later between 11 and 10.5 ka (Blum et al., 2000).

The geology of the Bloomfield Hills has been mapped by Farrar and McManamy (1937) and Stewart (1942) [in Nelson et al. (1999)], Grohskopf (1955), Satterfield and Ward (1978), and more recently by Thompson (1981) and Nelson et al. (1999) (Figure 2). The stratigraphy of the Bloomfield Hills consists of Paleozoic limestone and sandstone bedrock, unconformably overlain by Cretaceous McNairy Formation, which in turn is overlain by the Paleocene Midway Group. Unconformably overlying the Midway Group is the Paleocene-Eocene Wilcox Group and Porter Creek Clay, which consist of shallow-water and back-beach/deltaic sand and silt deposits, respectively. The Wilcox Group is unconformably overlain by Miocene to early Pleistocene Mounds Gravels. The late Pleistocene deposits include reworked Mounds Gravel, Roxana Silt (60 to 25 ka), and Peoria Loess (26 to 10 ka) (Nelson et al., 1999; Harrison et al., 1999). Regionally, the Tertiary beds are nearly flat, with a gentle (0.5°) southeast gradient (Grohskopf, 1955).

3.1 Idalia Hill Fault Zone

Faulting in southeastern Missouri was investigated first by Farrar and McManamy (1937) and Stewart (1942). This earlier work was revisited by Satterfield and Ward (1978) and Thompson (1981). Stewart (1942) described the Idalia Hill fault zone as a series of closely spaced parallel faults striking N50° to 60°E that displace Pliocene deposits between 15 and 30 m. Based on this earlier mapping the northeast-trending zone of faulting is about 0.5 km wide with the mapped trace of the Idalia Hill fault being very poorly constrained but trending parallel to the eastern margin of the Bloomfield Hills (Figure 2). The fault zone descriptions of Stewart (1942) are consistent with subsurface information interpreted from seismic reflection profiles crossing the eastern margin of the ridge that exhibit east-side down vertical separation of Paleozoic and Cretaceous rocks (Stephenson et al., 1999) (Figures 3 and 4). Recent seismic-reflection surveys acquired across the Idalia Hill fault zone image numerous high-angle west-dipping and east-dipping faults (Stephenson et al., 1999). Stephenson et al. (1999) also project the Idalia Hill fault upward through Tertiary deposits and intersecting the ridge margin midway up the slope.

In summary, the seismic reflection data of Stephenson et al. (1999) indicate that the eastern margin of the Bloomfield Hills may be fault controlled, and that warping and faulting of Paleozoic/Cretaceous and Cretaceous/Tertiary contacts is consistent with transpressional deformation and the existing orientation of the regional stress field. Profile IDAL-2, located along County Road E, 3-km northeast of the South Holly Ridge site, images a broad (< 1 km wide) zone of complex faulting and warping that includes a broad monocline, subsidiary anticlines bound by faults, and faults with apparent reverse separation (Figure 3). Total vertical separation across the top of Paleozoic bedrock is about 20 m. The overall sense of displacement from northwest to southeast is down to the east, which is consistent with the existing topography. Folding and faulting of the Cretaceous/Paleozoic, Tertiary/Cretaceous and Quaternary boundaries becomes most pronounced east of station 290. Near station 290 (Figure 3), a steep west-dipping fault projects updip toward the mapped surface trace of the Idalia Hill fault (Stephenson et al.,

1999). This fault shows west-side up vertical displacement, consistent with the overlying surface topography (Figure 3). East of station 290, where the subsurface distribution of Quaternary deposits is better constrained, Stephenson et al. (1999) show east-dipping faults vertically deforming Quaternary deposits within 30 m of the ground surface. This zone of Quaternary deformation is slightly east of the bluff line and mapped trace of the Idalia Hill fault.

Seismic line IDAL-1 is located about 5 km northeast of Idalia, and along a northeast projection of the mapped Idalia Hill fault zone (Figures 2 and 4). The seismic reflection line shows less deformation of the Tertiary and younger deposits than IDAL-2 with much of the interpreted deformation constrained prior to the Cretaceous. Stephenson et al. (1999) speculate that the absence of significant faulting along profile IDAL-1 may be due to (1) poor source and receiver coupling, (2) the short length of the profile, and (3) possible complex faulting relations that exhibit stepovers similar to the faulting observed in the Benton Hills (Harrison et al., 1999; Palmer et al., 1997). Seismic-reflection surveys (IDAL-1 and -2; Figures 2 and 5) that obliquely cross the CGL and Idalia Hill fault zone provide evidence of Quaternary deformation, and suggest that the eastern margin of the Bloomfield Hills may be controlled by moderate-to-steeply dipping faults (Figure 3; Stephenson et al., 1999).

The North Holly Ridge site evaluated previously by the Missouri Department of Natural Resources (Hoffman, 1997) and located directly north of the South Holly Ridge site (this study), also provides circumstantial evidence of Quaternary deformation along the Idalia Hill fault zone midway up the bluffs of the Bloomfield Hills (Figures 2, 5 and 6). Exposures developed within the cutslopes of a salvage yard at the site show a 30-m-wide complex fault zone comprised of strike-slip, reverse and extensional faults that strike both northwest-southeast and northeast-southwest, and offset Late Wisconsinan Peoria Loess (Hoffman, 1997; Nelson et al., 1999) (Figure 6). The faulting aligns with the Idalia Hill fault zone (Hoffman, 1997). A review of the logs that document the exposure shows at least one fault extending upward and offsetting inferred Holocene colluvium. However, it is unclear if the faulting is, in part, landslide related or primary tectonic in origin (Hoffman, 1997; Nelson et al., 1999).

3.2 Approach and Methodology

Our approach to evaluate the Idalia Hill fault with respect to the CGL included analysis of aerial photography, aerial reconnaissance, and field mapping along critical sections of the eastern margins of the Bloomfield Hills, and incorporates data obtained through seismic reflection, drilling, ground penetrating radar and paleoseismic trenching. Geomorphic lineaments were identified initially through the interpretation of aerial photography of the study area. Photographs analyzed included 1:40,000-scale U.S. Geological Survey (USGS) infrared photography, and black and white 1:24,000-scale photography from the U.S. Department of Agriculture. We reviewed LANDSAT satellite imagery provided by Mike Rymer (USGS, Menlo Park, California) of the upper Mississippi embayment to obtain a regional perspective of the Bloomfield Hills. The larger scale photography allowed more detailed analysis of potential tectonic-related geomorphic features and fluvial geomorphology. Geomorphic lineaments from the study area were compiled on parts of three 1:24,000-scale USGS 7.5-minute quadrangle maps (i.e., Dexter, Essex and Clines Island) and exist as a GIS digital database produced from the original 1:24,000-scale mapping (Figure 5).

Field reconnaissance included several traverses across the Bloomfield Hills to verify to the aerial photography interpretations and 1:24,000-scale mapping between Guam, Missouri, and Highway 60. Much of the reconnaissance was limited to traverses along public roads. We performed more detailed reconnaissance between Road E and the Holly Ridge site, where property owners granted access to private land. The public portions of the town of Dexter, Missouri, southwest of Highway 60 and near Dexter Creek also were field checked. From the geomorphic mapping we evaluated and ranked numerous

potential paleoseismic research sites along the eastern margin of the Bloomfield Hills, and settled on the South Holly Ridge site for more detailed subsurface investigation such as seismic reflection acquisition, trenching and drilling, and age-dating of surficial deposits (Figures 5 and 6).

3.3 Seismic Reflection Data Acquisition

Seismic reflection data for two profiles (HR-1 and HR-2) were collected in SH mode (sensitive to horizontally polarized shear waves) on a 12-channel engineering seismograph. Seismic line locations are shown on Figures 2, 5 and 6. The profiles intersect the Idalia Hill fault zone. The active spread consisted of 12 receivers (4.5 Hz horizontal geophones oriented perpendicular to the seismic line) spaced at 3-m intervals. The seismic profiles were shot off-end with 3-m shotpoint spacings and 3-m source offsets. Seismic energy was generated by five horizontal impacts of a 4.5-kg sledgehammer on a 10-kg steel I-beam oriented perpendicular to the spread. Acquisition parameters on the seismograph included filter settings of 20 Hz (lowcut) and 250 Hz (highcut), a 1.0 s record length, and 0.5 ms sampling interval. Processing followed a standard sequence for shallow common midpoint (CMP) reflection data included: data reformatting and editing, CMP sorting, elevation statics, bandpass filtering (8-64 Hz), automatic gain control, velocity analysis, NMO correction, surface-consistent residual statics, CMP Stacking (6-fold), and F-K filtering. The findings of the seismic reflection survey are provided in section 5.1.

3.4 Paleoseismic Trenching and Drilling

Paleoseismic trenches (T-1 to T-7) were excavated at the South Holly Ridge site to document near-surface stratigraphy and structure across the eastern part of the Idalia Hill fault zone and faults imaged in the seismic reflection survey (Figure 6). General stratigraphic and structural relations exposed in the trenches were cleaned, flagged, surveyed, and logged at a scale of 1 in. = 1m. Zones of faulting were logged at a scale of 1 in. = 0.5 m. Six boreholes (B-1 to B-3) were drilled using a Giddings rig operated by the United States Department of Agriculture. Continuous samples were obtained in three foot long core barrels, logged and correlated with existing trench stratigraphy as shown on the respective trench logs (see section 6.0). Pedologic descriptions also were made of trench T-5 and soil borings B-1 to B-3 for the purpose of correlating site-specific pedologic development with respect to age. The soil profile descriptions are presented in Appendix A.

Nearly all the trench locations and dimensions, with the exception of trench T-7, were surveyed using a Topcon GRS-303 total station relative to nearby cultural features, such as roads, drainage ditches, telephone poles, and the adjacent North Holly Ridge site (Hoffman, 1998). Trench T-7 and the exploratory borings were located using a Garmin GPS hand-held device, as well as a measuring tape and Brunton compass. Trench T-7 and boreholes B-1 to B-6 were located relative to previously surveyed landmarks (i.e., survey stakes and fences).

3.5 Age Dating

The ages of the sedimentary deposits at the site were estimated from radiocarbon dates, thermoluminescence dates and pedologic development. Twelve detrital charcoal samples collected from trenches and test pits were submitted for radiocarbon analysis to Beta Analytic Inc., in Miami, Florida. The radiocarbon dates were dendrochronologically corrected to calibrated years according to the procedure of Stuiver and Reimer (2000). Four thermoluminescence (TL) samples were collected from the trenches, to assess the age of the youngest exposed loess, as well as overlying colluvial deposits. The TL samples were submitted to the University of Illinois at Chicago for thermoluminescence analysis. The radiocarbon and thermoluminescence results are presented in Table 1.

3.6 Geotechnical Analyses

Lastly, four sediment samples were collected from anomalous fractures present in trench T-5 and submitted to Ray Fisher Geotechnical Engineering in Walnut Creek for particle-size analyses. The analyses performed included moisture content, dry density, Atterberg limits, and sieve analysis. The results of the analyses are presented in Appendix B.

4.0 REGIONAL GEOMORPHOLOGY

Prominent possible fault-related geomorphic lineaments, interpreted on aerial photography and verified by aerial reconnaissance, characterize the topography along the east-facing bluffs of the Bloomfield Hills. Between Guam, Missouri, and the South Holly Ridge site, several to many northeast-trending valleys and northwest- and southeast-facing escarpments are present near the base and along the eastern margin of the Bloomfield Hills (Figure 5). These features align with springs, bedrock notches, and zones of deflected drainages that all fall within the Idalia Hill fault zone. We also note that in some places these features intersect large arcuate lineaments that have been interpreted as landslide headscarps. The northeast-trending linear valleys and scarps are well-expressed in Pleistocene or older sedimentary deposits, but were observed less frequently and weakly expressed in Holocene alluvial fan material. Geomorphic features present on the younger surfaces (e.g., Holocene) typically include springs, vegetation lineaments, and very subtle topographic escarpments that may or may not correlate with the margins of interfingering alluvial fan and fluvial deposits.

The presence of relatively high topographic elevations at the ridge margin changes in the trend of the eastern Bloomfield Hills escarpment and the distribution of extensive alluvial fans southwest of the Holly Ridge sites suggest the presence of a restraining bend near the southwest end of the Idalia Hill fault zone (Figure 5). Between Pleasant Valley Church and Highway 60, the bend is defined from southwest to northeast as a 20° change in trend of the eastern margin of the Bloomfield Hills (part of the more extensive ridge) to the more easterly trend of the southeastern escarpment of the Bloomfield Hills (Figures 1 and 5). Well-expressed geomorphic lineaments along the escarpment to the northeast of Pleasant Valley Church do not continue to the southwest nor do they appear to cross extensive alluvial fans. Under the present-day, nearly east-west compressive stress regime (Zoback, 1992), the faults that parallel northeast-trending CGL should accommodate dextral slip. Therefore, if the eastern escarpment of the Bloomfield Hills reflects structural control, then the apparent 20° change in fault strike would result in a restraining geometry and produce contractional deformation uplift through folding and reverse faulting. Field reconnaissance, coupled with interpretation of aerial photography and existing USGS 7.5-minute topographic maps, within the region of the hypothetical restraining bend identified a broad alluvial surface with numerous south-flowing drainages.

We also track subtle geomorphic and tonal lineaments in the Bloomfield Hills southwest to Dexter, where Dexter Creek is anomalously right-laterally deflected at the surface projection of the CGL, and consists of at least two and potentially three flights of fluvial terraces (Figure 5). Seismic reflection surveys that image tilted and folded Tertiary to Quaternary bedrock at the eastern ridge margin is consistent with a transpressional deformation within a restraining bend in the Idalia Hill fault system. Alternatively, the apparent bend in the ridge margin may be the result of fluvial incision along the southeastern escarpment of the Bloomfield Hills.

Within the region of this hypothesized restraining bend are at least two generations of alluvial fans that post-date the Peoria Loess. We speculate that the development of numerous fans in this area may be in part fault-controlled along the CGL. The oldest alluvial surface (Qf1) extends easterly from the Bloomfield Hills and intersects undifferentiated Quaternary alluvium of the Castor River. On the basis of this mapping, the youngest fans (Qf2) typically are confined near the margin of the Bloomfield Hills and have a smaller regional extent. The southern part of the South Holly Ridge site is located on alluvial fan surface Qf2.

The geomorphology of the eastern slopes of the Bloomfield Hills also is dominated by the presence of large, arcuate landslide complexes. The landslide headwalls are typically broad arcs, some up to 1,000 m long, and have intermittent creeks that commonly erode headward from the base of the scarps, producing

radial drainage patterns. Many of these landslides are clearly visible in the digital electronic map of the area (Figure 5). Where the lateral margins of the slides can be reasonably inferred, the margins appear to coincide with creeks. The North Holly Ridge site of Hoffman (1997) falls within one of the mapped arcuate landslide-like features.

It is difficult to differentiate primary tectonic (faulting) from nontectonic (landsliding) structures along much of the eastern part of the Bloomfield Hills. On the basis of the size of the landslide features many of the landslide toes are assumed to project to the base of the mountain front near the present-day alluvial plain. Field reconnaissance confirmed the presence of hummocky topography, tilted trees, and abrupt, steep headscarps directly at the ridge margin, indicating that small active landslides nested within the larger slide complexes are presently active. However, on the basis of geomorphology, size of the landslides, and well-developed drainages that dissect the oldest complexes, we interpret that many of the large inferred landslides are inactive ancient features.

5.0 SOUTH HOLLY RIDGE SITE

We focused our study on the South Holly Ridge site directly adjacent to the North Holly Ridge site because of the presence of: (1) Holocene alluvial and colluvial deposits, (2) prominent inferred tectonic-related geomorphology, and (3) faulting previously documented in exposures directly to the northwest at the North Holly Ridge site. The South Holly Ridge site is bisected by a prominent, deeply incised creek (herein designated Pennington Creek) that is deflected across a 2- to 3-m-high north-facing escarpment. The site is located near the southwest end of a prominent northeast-trending linear valley occupied by two small depressions near the northeast end of the valley, and is bounded on the southeast by a northeast-trending linear topographic escarpment (Figure 6). On the basis of field mapping geomorphic lineaments that characterize the site align with northeast-trending linear valleys and escarpments, linear drainages, springs and bedrock notches that occur to the northeast and southwest. Our field mapping also identified possible landslide-related geomorphology northwest of the site. Therefore, to evaluate whether geomorphic features at the South Holly Ridge site are best explained by a primary tectonic or landsliding mechanisms, we developed an integrated program that included the acquisition and interpretation of seismic reflection and ground penetrating radar data, followed by paleoseismic trenching and drilling.

5.1 Seismic Reflection Survey

Shallow seismic reflection imaging was used to characterize the significance of near-surface tectonic deformation associated with the northeast-trending Idalia Hill fault zone and to assess its association with the CGL. Two shear wave (S-wave) seismic reflection profiles (HR-1 and HR-2) were collected across the southeastern topographic escarpment of the Bloomfield Hills (Figure 2). Seismic profiles HR-1 and HR-2 were oriented nearly north-south, parallel to Stoddard County Road 537, and intersect the mapped location of the Idalia Hill fault zone, previously identified in exposures at North Holly Ridge (Hoffman, 1997), and possible fault-related geomorphology of the South Holly Ridge site (Figures 2 and 6). Both seismic reflection lines are located outside of the mapped boundaries of an arcuate-shaped landslide feature identified during the field mapping.

5.1.1 Faulting and Folding Interpreted from Seismic Lines

The processed seismic profiles, HR-1 and HR-2, show coherent seismic reflection energy to depths greater than 100 m and as shallow as 20 to 25 m (Figure 7). Based on correlation with local borehole data and previously acquired compressional-wave seismic reflection data (Stephenson et al., 1999), reflections from the Quaternary/Tertiary, Tertiary/Cretaceous and Cretaceous/Paleozoic boundaries were identified on the S-wave reflection profiles (Figure 7). Offset reflections and changes in reflection amplitude and coherency suggest the presence of high-angle faults in the subsurface. Two prominent high-angle, southeast-dipping faults interpreted from the seismic reflection profiles offset the Tertiary/Cretaceous and Quaternary/Tertiary boundaries (Figure 7). The northwestern-most southeast-dipping fault projects updip toward faulting observed in excavations at the North Holly Ridge site (Hoffman, 1997), and is coincident with the Idalia Hill fault (Figure 2). The updip projection of the prominent southeastern fault aligns with the tectonic-related geomorphology (e.g., linear valley and topographic escarpment) and faulting exposed in trenches at the South Holly Ridge site (see section on trenching and drilling). The Tertiary/Cretaceous boundary shows northwest side-up vertical separation across both faults that is consistent with the present-day regional topography. Upsection, southeast-vergent northwest-dipping faults are interpreted to splay or “flower” from the two main faults that exhibit southeast-side and northwest-side up vertical displacement.

In summary, the complex near-surface pattern of faulting interpreted from profiles HR-1 and HR-2 also aligns with the broad, complex faulting observed in excavations and trench exposures at the North (Hoffman, 1997) and South Holly Ridge (this study) sites, as well as previous seismic reflection surveys

across the ridge (IDAL-2 and IDAL-1 of Stephenson et al., 1999). Similar to previous studies performed along the ridge margin, the faulting and folding imaged in the seismic reflection profiles can be best explained in the present-day tectonic stress regime as transpressive structures accommodating both lateral and reverse components of deformation.

5.1.2 Ground Penetrating Radar Studies

Two ground penetrating radar (GPR) surveys (GPR-1 and GPR-2) were acquired to image near-surface stratigraphy and structure not resolvable with conventional seismic reflection techniques (Figure 6). Survey line GPR-1 is located southwest of Pennington Creek and consists of a 100-m-long northwest-southeast transect across a gently east sloping alluvial fan. GPR-1 also intersects faulting imaged at depth in seismic reflection lines HR-1 and HR-2. Survey line GPR-2 extends about 70 m across the prominent northeast-trending escarpment and linear valley located directly northeast of Pennington Creek and southeast of County Road 533.

Line GPR-1 shadows parts of seismic reflection lines HR-1 and HR-2, and intersects the updip projection of faults interpreted from the S-wave profiles (Figure 6). GPR-1 provides indirect evidence for unfaulted strata/reflectors to a depth of about 4.5 m below the ground surface (Figure 8). Preliminary interpretation of GPR-1 depicts moderately southeast-dipping stratigraphy in the northwest end of the profile, and several prominent “u-shaped” reflectors suggestive of channel morphology in the central and southeastern parts of the profile (Figure 8). The inferred paleochannel reflectors align with the linear valley northeast of Pennington Creek. Also, the reflectors in the northwestern end of the trench appear to dip slightly more steeply than similar reflectors located further to the southeast. The apparent change in bedding attitude from the northwest to southeast may represent either tilting, or a steeper pre-existing slope gradient due to the close proximity of the deposits to the margin of the ridge. The hyperbolic-shaped reflector near the center and base of the profile is interpreted as interference from a telephone pole directly north of the profile and does not reflect the underlying geologic structure.

The approximately 70-m-long GPR-2 line extends across the entire width of the northeast-trending, inferred tectonic-related linear valley (Figure 6). Preliminary interpretation of the GPR profile depicts several buried paleochannels along the axis of the narrow valley that are traceable to a depth of about 5 m below the ground surface (Figure 8). On the eastern margin of the valley, the GPR survey images steep northwest-dipping bedding directly underlying the 2- to 3-m-high linear escarpment overlain by the paleochannel deposits (Figure 8). No faulting is interpreted along the western margin of the valley; however, faulting and folding is interpreted along the southeastern part of GPR-2. A 20-m-wide zone of deformation aligns with the surface projection of faulting interpreted in the eastern part of seismic reflection surveys HR-1 and HR-2 (Figure 6). We preliminarily interpret faulting and folding along the linear escarpment based on prominent northwestward tilted stratigraphy overlain by more gently northwest-dipping colluvial and alluvial deposits.

6.0 PALEOSEISMIC TRENCHING AND DRILLING

Seven trenches (T-1 to T-7), six boreholes (B-1 to B-6) and one soil probe (T-5B) provide detailed information on the near-surface stratigraphy and structure at the South Holly Ridge site (Figure 6). The trenches intersect inferred tectonic-related geomorphology, and/or the surface projection of faults imaged from seismic reflection and GPR techniques. The boreholes provide additional subsurface information on the lateral and vertical continuity of deposits that extend beyond the ends of the trenches, or beyond the depth limitations of conventional trenching techniques. The trench and borehole data provide information on: (1) the presence or absence of late Quaternary tectonic deformation across the northeast-trending topographic escarpment and faults interpreted from S-wave and GPR profiles; (2) whether or not the prominent geomorphic features reflect primary tectonic deformation or landsliding, and (3) event timing to compare with regional paleoliquefaction and paleoseismic investigations conducted on the CGL in southeast Missouri (Western Lowlands and Benton Hills).

6.1 Site Stratigraphy

Stratigraphy exposed in the trenches at the South Holly Ridge site is consistent with local and regional geomorphology, and includes deposits associated with alluvial fans, fluvial channels, scarp-derived colluvium and older sedimentary bedrock units. In general, Eocene to Pleistocene marine and eolian (loess) deposits are unconformably overlain by Holocene alluvial and colluvial surficial material. The older Eocene to Pleistocene deposits typically are encountered along the margins of the site where topographic relief is greatest, whereas the topographic lows are buried by Holocene alluvial, fluvial and colluvial material.

The oldest deposits exposed in the trenches consist of Eocene sand and gravel of the Wilcox Formation, and Pleistocene reworked Mounds Gravel. The Sangamon Geosol is developed in the Wilcox Formation and Pleistocene reworked Mounds Gravel and is characterized by a distinct reddish-brown hue and well-developed clay films that enclose or underlie pebbles. All of these units are overlain by or are in fault contact with Pleistocene Peoria Loess. The loess deposits are unconformably overlain by Holocene colluvium and alluvium. Two moderately developed pedogenic B horizons (from oldest to youngest are designated paleosol units Q_{s1} and Q_{s2}) overprint the Peoria Loess and a Peoria Loess scarp-derived colluvium. A third younger pedogenic B-horizon (unit Q_{s3}) overprints much of the near-surface remnants of paleosol units Q_{s1} and Q_{s2} , as well as Peoria Loess. These strata and soil horizons provide stratigraphic markers for documenting the presence of surface fault rupture and/or tectonic warping along near-surface faults at the site.

6.2 Eocene Wilcox Formation

The Eocene Wilcox Formation, a near-shore deltaic deposit, is exposed in all the trenches (T-1 to T-7) at the site, and is characterized by both a reddish-orange and whitish or bleached medium- to coarse-grained sand. The sand is cross-bedded and finely laminated to massive. It typically is moderately consolidated, but also is friable in places, and contains rare thin lenses of bedded fine gravel, silt and clay. Reddish-brown silt lamellae developed by soil processes are common and produce a “tiger-stripe” effect throughout much of the exposed sections of the Wilcox Formation. In at least several locations near the northwestern end of trench T-5, veinlets initiate near the Wilcox Formation, and contain reddish-brown, fine-grained sand that cuts across reworked Mounds Gravel and Peoria Loess. Where the veinlets can be traced down into the Wilcox Formation, and shown to contain sand, we interpret these rare sand-filled fractures as potential earthquake-related liquefaction dikes.

6.3 Pleistocene Reworked Mounds Gravel with Sangamon Geosol

Trenches T-1, T-2, T-4 to T-6 expose reworked Mounds Gravel consisting of well-rounded, bedded clast-supported gravel lenses with stringers of reddish-orange fine to coarse-grained sand. Clasts range from 1 to 3 cm in diameter, with occasional clasts up to 10 to 20 cm in diameter. Clast composition includes abundant brown chert with lesser amounts of quartzite chert, and siltstone lithologies. The reworked Mounds Gravel appears to have been deposited by large braided rivers based on the bedded sand and coarse gravel lithology. In the eastern ends of trenches T-1, T-4, and T-6, as well as the western end of trench T-5, a Sangamon Geosol overprints the reworked Mounds Gravel as a well-developed 0.25 to 0.30-cm-thick patina noted by thick clay films and strong reddish hues.

6.4 Pleistocene Colluvium/Reworked Mounds Gravel

Pleistocene colluvium is present in the eastern end of trenches T-1, T-2, T-4 and T-6 and consists of reddish brown clayey gravelly, fine-grained sand and silt. The coarse-grained colluvium is most pervasive near the contact with reworked Mounds Gravel, and contains predominantly chert clasts of ≤ 2 cm in diameter sourced from reworked Mounds Gravel. The colluvium fines and becomes massive upsection and grades into a light yellowish-brown silt with fine to medium gravel, and about 10% clay. Near the crest of the topographic escarpment the colluvium coarsens slightly as it picks up a coarser fraction of reworked Mounds Gravel that is exposed near the surface directly southeast of the trench (e.g., trench WLA T-2). The Sangamon Geosol is absent in the colluvial deposits suggesting that the colluvium post-dates the Sangamon. On the basis of stratigraphic relations, the absence of the Sangamon Geosol, and thermoluminescence (TL) results for loess samples from trenches T-4 and T-6 that overlie the colluvial deposit, we estimate the age of the colluvium as Pleistocene.

6.5 Loess

In trenches T-1, and T-4 to T-6, a thick (≤ 3 m) massive silty loess conformably drapes either Pleistocene colluvium (trenches T-1, T-4, T-6) or reworked Mounds Gravel (trench T-5). The loess ranges from dark reddish brown (7.5YR 4/4 to 4/6) to yellowish-brown (10YR 5/6 to 5/8) in color, and contains very few, fine clasts except near the basal contact with the underlying coarser-grained Pleistocene colluvium or reworked Mounds Gravel. The darker hues tend to be located near the base of the trench where the moisture content increases. No clear sedimentary contact was visible between these changes in color, therefore, we interpret the entire package to be Peoria Loess. However, based on sedimentary interpretations made at the North Holly Ridge site by Hoffman (1997), it is possible that the darker loess present near the base of trenches T-1, T-4 and T-6 represents the slightly older Roxana Loess. The age of the youngest, light-colored loess, is based on two sediment samples collected from trench T-4 in the upper sections of the loess exposure. TL dating yields an age range of 19.9 to 23.6 ka, which is consistent with the Peoria Loess ages reported in this part of Missouri (Table 1). On the basis of the lighter-colored nature of the loess, and age of the deposit, we interpret much of the loess at the South Holly Ridge site as Peoria Loess.

6.6 Buried Soils (Q_{s1} , Q_{s2} , and Q_{s3})

We recognize at least three buried soil horizons developed in either Peoria Loess or Peoria Loess-derived colluvium in the trenches of the South Holly Ridge site. The lowermost soil (paleosol unit Q_{s1}), is defined as a poorly developed pedogenic B-horizon forming in Peoria Loess. Unit Q_{s1} is present in trenches T-1, T-4 and T-6. Paleosol unit Q_{s1} is characterized by massive yellowish-brown (10YR 4/6) to dark yellowish brown (10YR 5/6) silt with manganese staining, and numerous whitish spherical to oblong silt rinds or skeltans (zones of translocated and reduced clay), that are pervasive along fracture surfaces. To the southeast toward the crest of the northeast-trending linear escarpment, the fine gravel content

increases suggesting that part of the unit may be colluvial in origin. Unit Q_{s1} has a very diffuse basal contact with the underlying Peoria loess, making it difficult to trace laterally. A single thermoluminescence sample collected from unit Q_{s1} in trench T-6 provides an age of 19.2 ± 1.6 ka for unit Q_{s1} (Table 1). This age is stratigraphically consistent and similar to the age estimates for the Peoria Loess, and suggests that unit Q_{s1} either experienced rapid burial during the development of loess-derived colluvium, or alternatively, the soil formed in Peoria Loess, and thus for both cases the unit was not re-exposed to sunlight long enough to reset the luminescence signal. Therefore, we consider a Late Pleistocene age for paleosol unit Q_{s1} .

Paleosol Q_{s2} is a silt-rich deposit that conformably overlies unit Q_{s1} . On the basis of color, clay content, and pedologic textural characteristics, we interpret unit Q_{s2} to be a soil developed in a loess-derived colluvium. Unit Q_{s2} is exposed in trenches T-1, T-4 to T-6, and is characterized by massive dark reddish brown (7.5YR 4/4) silty clay to clayey silt (in trench T-5, this pedogenic horizon is designated unit D). Unit Q_{s2} contains well-developed prismatic pedologic fractures with traces of clay films and abundant powdery silt-rich skeltans accumulating along pedologic fractures. Traces of fine rounded gravel randomly distributed throughout the unit indicates a colluvial origin for the parent material. A thermoluminescence analysis of a sample collected from this unit yielded an age of 18.3 ± 1.5 ka (Table 1). This age is stratigraphically consistent with the estimated age of underlying unit Q_{s1} , and Peoria Loess and pedologic soil development features preserved in the colluvial deposit. Based on stratigraphic position, the colluvium of unit Q_{s2} is younger than unit Q_{s1} , but because the thermoluminescence ages between these two units overlap, it suggests that the age span between the two interpreted colluvial sediments is probably less than 1,500-3,000 years, and that the two units formed closely in time. Alternatively, the more well-developed soil of unit Q_{s2} indicates a longer duration of landscape stability and soil forming processes than experienced by unit Q_{s1} , and thus the age is likely a maximum. On the basis of the close thermoluminescence ages between the Peoria Loess and the colluvial deposits of Q_{s1} and Q_{s2} , coupled with the apparent well-developed soil profile throughout unit Q_{s2} , we interpret unit Q_{s2} to be a soil developed in reworked colluvial loess that is at least Late Pleistocene and probably early Holocene in age. The early Holocene age is based on to the minimum time necessary to develop a prominent prismatic soil structure, clay films, and dark hue typical of this unit.

Paleosol unit Q_{s3} represents a 0.5 to 1.0-m-thick soil that overprints fine-grained colluvium and paleosol units Q_{s1} and Q_{s2} in the eastern part of trenches T-1, T-4 and T-6. The paleosol deposit consists of strong reddish brown (7.5 YR 5/8) silt with a trace of clay comprised of reworked Peoria Loess, traces of fine sand, clay and stone lines. We interpret this unit as a Peoria Loess-derived colluvium overprinted by a moderately-developed clay-rich soil, similar to unit Q_{s2} . The moderately to well-developed pedogenic structures present in unit Q_{s3} extend downward and overprint, in part, the soil horizons of units Q_{s1} and Q_{s2} . Unit Q_{s3} dips gently northwest consistent with present-day topography, whereas the older buried soils of units Q_{s1} and Q_{s2} dip more steeply to the northwest. In trench T-1, unit Q_{s3} is truncated by late Holocene alluvial and colluvial deposits lining the valley floor.

Fractures are pervasive in units Q_{s2} and Q_{s3} , many of which are attributed to soil processes, and a few to secondary tectonic deformation. The fractures are near vertical, anastomosing in three dimensions, and cut across much of the Holocene alluvial and fluvial deposits exposed in the trenches. Most of the vertical fractures are characterized by grayish-white, silt-rich vienlets or “skeltans” (“bleached zones”). The skeltans are about 7 cm wide and as much as 1 to 2 m long. Several generations of skeltans are present, as noted by their truncation by overlying colluvial and alluvial deposits. Geotechnical laboratory analysis of the skeltans indicates that the material consists of a slightly coarser fraction of very fine sand and silt in comparison to the wall rock. Close examination of the fractures shows that the majority of the fractures are pedogenic and allow the translocation of clay vertically downward. After the clay has been relocated, the silt is left behind as granular to fine pebble-sized clumps that can be confused with liquefaction-related deposits. Laboratory data sheets of the skeltans (samples 1 and 3), wall (samples 2

and 4) samples are provided in Appendix B. Samples were collected from unit C (Peoria Loess) and unit D (unit Q_{s2}; reworked loess) of trench T-5.

6.6.1 Holocene Surficial Deposits

Northeast of Pennington Creek the Holocene surficial deposits are confined to the margins and axis of the narrow northeast-trending linear valley that is bounded by the bluffs of the Bloomfield Hills on the northwest and a 2- to 3-m-high linear escarpment on the southeast. Within the linear valley are bedded fine-grained silty sand and silt deposits, and minor interbeds of medium- to coarse-grained sand. Several coarse-grained sand interbeds containing very faint planar laminae near the basal contacts suggest fluvial deposition within the central axis of the linear valley followed by colluvial deposition along the west and east sides of the valley. This is consistent with GPR-2 profile that images paleochannel deposits at the center of the valley. Near the base of the linear escarpment, the fluvial and colluvial deposits incise into paleosol unit Q_{s3}. Radiocarbon dating of detrital charcoal collected from the bedded fluvial material from as much as 1.6 m deep provide calibrated ages ranging 5,020 ± 270 yrs B.P. to 1,930 ± 70 yrs B.P. (Table 1). Furthermore, based on the relatively older age of the radiocarbon samples obtained from the Holocene fluvial deposits, and the interpretation of line GPR-2, that images buried paleochannel deposits beyond the depth of trenching, we interpret fluvial incision of the north and south-facing escarpments likely occurred during the early to middle Holocene.

Southeast of Pennington Creek, unit Q_{s2} (or unit D) is unconformably overlain by an approximately 1-m-thick interbedded alluvial fan deposit consisting of flat-lying to gently east-dipping, silty gravelly sand to sandy gravel (units E, F, G and H). The oldest alluvial fan deposit encountered in the trench, unit E, cuts into colluvial-derived Pleistocene Peoria Loess (unit D) at the northwest end of trench T-5 and dips gently eastward throughout the length of the trench. The alluvial fan deposits (unit E) in turn, are truncated by early Holocene paleochannel deposits between stations 23 and 38 near the central part of the trench, and an inferred paleochannel at the east end of the transect (Figure 11). Three charcoal samples collected from unit E provide an average weighted calibrated age of 7640 ± 40 cal yrs B.P. (Table 1).

Inset into the sequence of early Holocene alluvial fan material is a 15-m-wide zone of nested paleochannel deposits (units I to M) that span the west-central part of trench T-5 and likely extend as much as 4.5 m below the ground surface (Figure 11). The 15-m-wide zone of nested paleochannel deposits align with the prominent linear valley to the northeast of Pennington Creek. Orientations of paleochannel flow directions and paleo-gradients indicate a predominantly southwest flow direction that is approximately parallel to subparallel to the northeast-trending linear valley, and oblique to the present-day more south-southeasterly flow direction of Pennington Creek. The former flow direction also is opposite to that of the present-day linear valley northwest of Pennington Creek which based on topography drains northeast. Although there is no evidence of a controlling structure (e.g., buried escarpment) in the trench exposure or interpolated from borehole and GPR data, the concentration of the paleochannel deposits within a relatively narrow zone fortuitously aligned with the northeast-trending valley is suspicious. On the basis of radiometric age dating of charcoal samples collected from units I, K and Q, the age of the paleochannel deposits are 7140 ± 120 cal yrs B.P. (unit I), 7005 ± 145 cal yrs B.P. (unit K), and 6885 ± 115 cal yrs B.P. (unit Q). The suite of ages and stratigraphic relations (channel truncations) indicate the paleochannels decrease in age from southeast to northwest.

A second set of buried paleochannel deposits (unit E1) are inferred at the southeast end of the trench and borehole transect (Figure 11). Interbedded fluvial deposits (unit E1) underlie the 1-m-thick alluvial package (units F, and H) directly southeast of trench T-5. Interpretation of line GPR-1 images a “u-shaped” feature at the southeast end of the trench that has similar morphology to the buried paleochannel deposits encountered in the west-central part of the trench. Because this deposit underlies the alluvial package of units F and H, the relative age of this deposit likely exceeds the estimated ages of similar

channels located in the central part of the trench which interfinger with the alluvial material (Figure 11). The age of this deposit is estimated as early Holocene.

Both northeast and southwest of Pennington Creek the youngest deposits consist of late Holocene colluvial and fluvial overbank deposits associated with discrete narrow paleochannels. Two charcoal samples collected from the fine-grained overbank deposits provide a wide range in ages between approximately 6,000 to 0 yrs B.P.; however, based on stratigraphic position, we estimate the age of the overbank and colluvial deposits as late Holocene to modern.

6.7 Fault Zone Characteristics

The South Holly Ridge trenches exposed moderate to excellent Tertiary to late Pleistocene stratigraphic horizons from which to assess the presence or absence of primary and secondary tectonic deformation, as well as style (e.g., faulting, folding and tilting) and lateral extent of deformation. Direct evidence of faulting and folding was encountered northeast of Pennington Creek, whereas trench exposures southwest of the creek only suggest subtle folding and minor faulting.

6.7.1 Deformation Northeast of Pennington Creek

Trenches excavated at the South Holly Ridge site provide evidence of near-surface faulting and folding. Faulting along the prominent northeast trenching escarpment can be traced at least into the late Pleistocene Peoria Loess, and possibly up into the late Pleistocene to early Holocene deposit of unit Q_{s2} . In the trenches we recognize: (1) a primary zone of northeast-striking vertical faults, (2) folding of units Q_{s1} and Q_{s2} , (3) southwest-dipping low angle faults, (4) an absence of faulting southwest of Pennington Creek, and (5) an absence of reverse faulting in trench T-7 at the base of a hypothetical landslide toe.

6.7.1.1 Primary Zone of Northeast- Striking Faults

The linear escarpment coincides with a predominantly N55°E-striking, near-vertical to steeply southeast-dipping fault zone that is exposed in trenches T-1, T-2, T-4 and T-6, and also imaged on the GPR-2 profile spanning the linear valley. A broad, 6- to 12-m-wide zone of northeast-striking, near-vertical faults offset Tertiary sedimentary rocks, Pleistocene colluvium and loess, as well as late Pleistocene to possible early Holocene soil horizons developed in Peoria Loess and colluvium (Figures 9 and 10). Measured across the width of the trench, individual shears strike between N46°E and N65°E, generally parallel to, and coincident with the crest and central portions of the fault scarp. In general, the fault zones encountered in trenches T-1, T-2, T-4 and T-6 consist of anastomosing, thin (1-2 mm wide) shears, that contain finely pulverized and brecciated Peoria Loess, occasional vertically aligned and rotated pebbles (trenches T-1 and T-2), and manganese staining. The shears are conspicuously absent of clay gouge, slickensides, and striations; however, in places, discontinuous manganese staining occurs along the shears suggesting some antiquity.

Review of apparent bedding dips in trenches T-1, T-2, T-4 and T-6, indicate that the faults at the base of the topographic escarpment exhibit an overall down to the northwest vertical separation. Faults within bedrock can be traced confidently up to at least the Peoria Loess, where they become obscured by pedogenic processes, such as subvertical fractures in units Q_{s1} and Q_{s2} that suspiciously align with the shears. Although the faults in the Peoria Loess align with prominent fractures upsection in the overlying deposits, we conservatively interpret primarily folding and north-directed tilting of units Q_{s1} and Q_{s2} . Trench T-4 provides the most compelling evidence of possible offset of buried soils Q_{s1} and Q_{s2} juxtaposed against Peoria Loess at depth (Figure 10). Faulting of Q_{s2} also is permissible in trench T-1 near stations 18 and 19 m (Figure 9).

Southwest along the southern edge of the escarpment, near Pennington Creek, as the linear ridge decreases in elevation and becomes level with the valley floor, the faulting of late Pleistocene to early Holocene deposits is buried by a thin veneer of Holocene alluvium. For instance, trench T-4 exposes a 7-m-wide zone of deformation that aligns with the southwest projection of the topographic escarpment and faults exposed in trenches T-1 and T-6 (Figure 10). The southern end of the linear escarpment consists predominantly of northeast striking vertical faults with a lesser amount of low-angle, southeast dipping faults that do not extend into units overlying the Peoria Loess (Figure 10). Stratigraphic truncations of the Peoria Loess at the east end of the trench indicate that the ridge formerly continued southwest along projection, but has been planated by Pennington Creek. A thin <0.5 m thick massive, undeformed Holocene alluvial deposit drapes the fault zone and is laterally continuous throughout the length of the trench. The westernmost fault exposed in trench T-4 that juxtaposes Peoria Loess against Eocene Wilcox Formation strikes more easterly (N65°E) than faults of similar appearance in trenches T-1, T-2, and T-6, suggesting that the fault zone may be bending or stepping to the west along fault strike.

In summary, the sense of apparent vertical displacement observed across the Tertiary to early Holocene geologic units is consistent with present-day topography within the linear valley. Several distinct shears located near the main fault zone of trenches T-1, T-4 and T-6 displace basal contacts of bedrock units between ≤ 0.1 and ≥ 0.5 m and exhibit a north-side down apparent vertical separation. Faulting can be traced confidently up through the Peoria Loess and across a weathering front developed in the loess, and may extend upward into the overlying Peoria Loess-derived colluvium of units Q_{s1} and Q_{s2} , although this is not definitive. Distinct shearing also does not appear to offset paleosol unit Q_{s3} or the present-day colluvium. Unit Q_{s3} , that overprints units Q_{s1} and Q_{s2} in the eastern and central parts of trenches T-1 and T-6, projects across the fault zone without deformation and dips westerly similar to the present-day slope geometry. Faulting does not extend upward into the late Holocene colluvial and alluvial deposits that mantle these older soils; thus deformation is constrained to deposits older than at least unit Q_{s2} (Pleistocene to early Holocene).

6.7.1.2 *Folding of Units Q_{s1} and Q_{s2}*

Associated with the fault zones of trenches T-1, T-2, T-4 and T-6 are broad north-facing monoclinical warps of both Tertiary deposits and late Pleistocene to early Holocene buried soils that are coincident with the present-day linear escarpment at the site. Based on the dip of basal contacts exposed in these trenches, Tertiary to Pleistocene deposits show greater northward directed tilting than younger overlying Late Pleistocene to early Holocene deposits providing evidence for multiple displacements (trenches T-1 and T-4). Using the basal contacts of units Q_{s1} and Q_{s2} as strain gauges, where they are exposed in trenches T-1, T-4, and T-6, these deposits are warped down to the northwest between a minimum of 2.5 and 2.6 m, and 1.8 and 2.2 m, respectively, across the broad fault zone that delineates the linear escarpment (Figures 9 and 10). The youngest warped paleosol, unit Q_{s2} , shows a minimum of about 1.8 m and possibly as much as 2.2 m of northwest-down vertical separation through warping across the 8-m-wide shear zones in trenches T-1 and T-6. In trenches T-1 and T-6, unit Q_{s2} is relatively thin (≤ 0.25 m) near the primary zone of deformation and thickens (≥ 1 m) near the base of the escarpment suggesting multiple episodes of uplift, erosion, and burial. The overlying younger soil, such as unit Q_{s3} , and colluvial deposits draping buried unit Q_{s2} show no direct evidence of warping (Figures 9 and 10).

6.7.1.3 *Southwest Dipping Low Angle Faults*

In addition to the prominent near-vertical faulting at the site, at least two low-angle south east-dipping shears are present in trenches T-3 and T-4 that provide some complexity to the near-surface structural relations of the site (Figure 10). For instance, in the northwest end of trench T-4, Peoria Loess is juxtaposed against Eocene Wilcox Formation across a low-angle fault oriented N71°E, 33°SE, and a

vertical fault striking N65°E. The low-angle fault is truncated upsection by the near-vertical fault indicating multiple episodes of faulting.

A low-angle shear also was encountered in trench T-3, that strikes N53°E and dips 34°SE. Striae preserved along a 0.2-to 0.3-m-thick clay gouge within the Wilcox Formation indicate dip-slip displacement (Figure 10). The slip plane projects updip toward County Road 533 where prior to grading of the road it would have intersected a pre-existing east-facing slope. The present-day slope east of the county road consists of the North Holly Ridge site and a complex zone of faulting that likely is associated with both primary faulting and landsliding. Projection of the slip plane down dip or toward the southeast shows that it extends beneath the present-day alluvium of the linear valley, and currently is buttressed by the alluvial-filled valley.

6.7.1.4 Absence of Reverse Faulting in Trench T-7

Trench T-7 was excavated across the backside (south and east) and base of the linear escarpment to assess the presence or absence of low-angle west-dipping shears related to landsliding. The purpose of the trench was to test a hypothetical model in which the faulting at the South Holly Ridge can be explained as landslide-related. Trench T-7 constrains the southeastern limit of faulting at the site. Trench T-7 exposed nearly laterally continuous, massive, Eocene Wilcox Formation unconformably overlain by Holocene colluvium and alluvium (Figure 13). A thin discontinuous gravel lense in the northern end of the trench suggests nearly flat-lying stratigraphy. Iron-oxide stained silt lamelle forming a “tiger-stripe” weathering pattern also are horizontal. The absence of faulting in trench T-7 indicates that either: (1) there is no fault present along the base of the escarpment, and thus it is a fluvial cut, (2) faulting lies further to the northwest in between trenches T-2 and T-7, or (3) faulting lies further southeast beyond the limits of the subsurface investigation. Borings B-5 and B-6 drilled in the central and eastern parts of trench T-7 encountered poorly bedded fluvial and colluvial deposits unconformably overlying the Eocene Wilcox Formation. Stratigraphic relations interpreted from the trench exposure and borehole data indicate that the eastern margin of the linear escarpment has been fluvially cut. No charcoal was recovered from these deposits, therefore there is no age on the incision.

6.7.1.5 Absence of Faulting Southwest of Pennington Creek

We found no evidence of deformation in 7,600 year old alluvial deposits southwest of Pennington Creek along a southwestern projection of the linear valley and escarpment. Near the surface projection of the near-vertical faulting imaged in seismic reflection profiles HR-1 and HR-2, and coincident, in part, with the northeast-trending linear valley east of Pennington Creek, we encountered a 15 m wide zone of early Holocene paleochannel deposits in trench T-5 (Figure 11). Although the position of the buried channels and their alignment with the linear valley implies pre-existing structural control on the paleo-fluvial geomorphology, the approximately 7,600 year old fluvial deposits generally are flat-lying and show no evidence of warping, faulting or pre-topography (e.g., scarp) influence on their depositional pattern. In addition, no liquefaction-related features were encountered in the loose, granular fluvial deposits to suggest the occurrence of nearby middle or late Holocene large earthquakes.

The only suggestion of near-surface deformation southwest of Pennington Creek exists in the western end of trench T-5 within the Eocene to Pleistocene-aged deposits. Evidence for deformation includes poorly expressed folding of Eocene Wilcox Formation, reworked Mounds Gravel, and Peoria Loess. For example, anomalous vertically displaced silt lamelle developed in the Wilcox Formation coincide with the same sense of apparent vertical truncations within the overlying reworked Mounds Gravel and Peoria Loess (Figure 11). The features are visible in both trench walls, along with subtle folds trending and plunging northeast across the trench. Although no distinct shears were visible in the Wilcox Formation, or the thin gravel lenses of reworked Mounds Gravel, the apparent sense of displacement across basal and

weathering contacts of these units is consistent with both down-to-the-west and -east vertical separation, with an overall down to the southeast vertical separation (consistent with HR-1 and HR-2). Across one possible shear zone, the reworked Mounds Gravel deposit exhibits between 0.2 to 0.3 m of apparent vertical separation (Figure 11). In summary, stratigraphic and structural relations are permissive of subtle Pleistocene folding and faulting, as well as liquefaction. The inferred southeast-side-down vertical separation aligns with the surface projection of similar faulting and folding of bedrock imaged in profiles HR-1 and HR-2 (Figures 6 and 7).

7.0 DISCUSSION

Our review of aerial photography and field reconnaissance, coupled with geophysical and paleoseismic data, provide indirect and direct evidence for extensive Pleistocene and Holocene deformation aligned with the Idalia Hill fault zone and CGL. However, many geomorphic features (e.g., ridges, depressions, deflected drainages) and microstratigraphic deposits exposed in trenches (e.g., juxtaposed strata, buried soils, etc.) identified and interpreted during this investigation also can be produced by landslide processes. We recognize that landslide processes generate a multitude of brittle and ductile deformation phenomena, such as normal, reverse and strike-slip faults and folds that can be confused with primary tectonic features. To help differentiate between landslide-related features from earthquake-related features at the South and North Holly Ridge sites, we use criteria developed by the Nuclear Regulatory Commission (Hanson et al., 1999). These criteria for landslide-induced faults include:

- (1) presence of a shallow, listric basal slide plane subparallel to topography;
- (2) map pattern and sense of slip of boundary faults;
- (3) lack of lateral continuity of fault features; and
- (4) high strain rates and anomalous recurrence intervals.

7.1 Basal Slide Plane

According to Hanson et al., (1999) the presence of a shallow (<200m) basal slide plane is a highly diagnostic feature of landsliding phenomena. The criteria state: “If a fault merges with a shallow listric basal slide plane subparallel to topography, then the fault most likely is related to landsliding rather than tectonic surface rupture.” Because of limited site-specific geotechnical borehole data from the North and South Holly Ridge sites, evaluating the presence of a basal listric slide plane is difficult. Using borehole, trench, and GPR data from the North and South Holly Ridge sites, we developed a generalized geologic cross-section A-A’ to evaluate plausible hypothetical failure plane geometry (Figure 14). Using cross-section A-A’, we assume a listric geometry for the basal slide plane to test the plausibility of landsliding extending beneath both sites (Figure 14). By projecting a hypothetical listric slide plane downdip (southerly direction) near the graben structures (e.g., at or near a hypothetical headwall of a landslide) exposed at the North Holly Ridge site, and inferring that the topographic escarpment at the South Holly Ridge site represents the toe bulge of a landslide, cross-section A-A’ depicts a failure plane between 20 and 30 m below the ground surface (Figure 14). Based on review of regional borehole data, the most probable location for a basal shear plane would be within the highly plastic clay seams of the Wilcox Formation, or at the contact between the Wilcox Formation and Porter Creek Formation. The Porters Creek Formation is not exposed at either of the sites, but borehole data from wells located northeast of the site in alluvial fan surface Qf2, encounter the Porters Creek clay at a depth of ≥ 15 m (Figure 5). Thus, the regional depth of the Porters Creek clay is compatible with having a basal slide plane at or near 20 to 30 m below the ground surface. Such a landslide geometry predicts that the slide plane should daylight east of the present-day escarpment at the South Holly Ridge site (see below).

Alternatively, interpretation of seismic reflection profiles collected at the site shows faulting extending upward to within about 20 m (limit of resolution) of the ground surface, presumably across the hypothetical slide boundary, and coinciding with the shallow surface faulting encountered in excavations at the North and South Holly Ridge sites (Figures 3 and 6). The seismic profiles appear to link deformation interpreted in the subsurface with complex faulting and folding exposed near the ground surface, thus providing strong evidence of a deep-seated tectonic origin, in part, for the faulting and folding observed at both sites.

We acknowledge that some of the shallow, dip-slip faulting exposed along the northwestern margin of the site, such as in trench T-3, is probably landslide-related. This is further supported by the presence of

hummocky topography near the North Holly Ridge site, coupled with back-tilted trees suggesting recent landslide activity directly west of the site. Ongoing excavations and grading of the North Holly Ridge site may partly be the cause of the present-day slope instabilities. On the other hand, trees lining the northeast-trending, 2- to 3-m-high linear scarp of the South Holly Ridge site are not leaning or back-tilted, thus indicating a relatively stable slope geometry for the South Holly Ridge site.

7.2 Map Pattern and Sense of Slip of Boundary Faults

The map pattern typically associated with landslides includes the presence of: (1) normal faulting at the headscarp associated with graben formation; (2) strike-slip faulting along the margins; (3) thrust or reverse faulting near the toe of the landslide associated with a toe bulge; and (4) sinuous bulging ridges that overrun the former topographic surface (Hanson et al., 1999). No trenches were excavated along the margin of the hypothetical landslide, however, our research addresses the three other typical map patterns characterizing landslides.

7.2.1 Headscarp and Margin Faulting

The North Holly Ridge site exposes moderate- to steep-dipping faults with primarily apparent normal separation and to a lesser extent east-dipping reverse faults. In a landslide scenario, the normal faults would be most closely associated with the formation of the headscarp and lateral translation of the landslide downslope (Figure 14), whereas the reverse faults typically are associated with the toe of the slide and project back toward the landslide headwall. No margin faults oriented oblique to the ridge and with a strike-slip component were encountered, nor were thrust or reverse faults dipping westerly into the slope associated with a zone of bulging.

7.2.2 Reverse Faulting at Toe Bulge

Trenches T-1, T-2, T-4 and T-7 excavated across the hypothetical toe bulge provide evidence for the absence of southeast-vergent (downslope) reverse faulting. Trenches T-1, T-2 and T-4 excavated across the crest and backside of the “toe bulge” exposed primarily near vertical faults exhibiting apparent normal vertical displacement. Trench T-7 excavated near the topographic break in slope on the east-side of the escarpment and partly within the alluvial plain of modern Pennington Creek exposed nearly laterally continuous, massive, Eocene Wilcox Formation unconformably overlain by Holocene colluvium and alluvium (Figure 13). A thin discontinuous gravel lense in the northern end of the trench suggests nearly flat-lying stratigraphy compared to east dipping stratigraphy on the opposite side of the linear scarp. Iron-oxide stained lamella essentially are horizontal. The trench provides direct evidence for the absence of low-angle reverse faults or folding near the hypothetical leading edge of the “toe bulge”. Borehole and trench data provide evidence in support of a fluvial origin and incision by Pennington Creek, in part, for the eastern margin of the linear topographic escarpment (Figure 13).

The absence of faulting in trench T-7 indicates that either: (1) there is no fault present along the base of the escarpment, (2) reverse faulting lies further upslope to the northwest between trenches T-2 and T-7, or (3) the fault lies further east beyond the limits of the subsurface investigation. Based on site geomorphology and the relatively small size of Pennington Creek, we believe that scenario two is unlikely since there is little geomorphic evidence to support the presence of a mid-level topographic step suggestive of a higher low-angle reverse fault. Also, review of aerial photography and site reconnaissance indicates that there is no strong geomorphic evidence of a reverse fault or buried “toe bulge” present east of the existing topographic high at the site. Lastly, the escarpment is relatively linear with little sinuosity along its length, with the exception of where creeks erode into the east side of the

scarp (Figure 6). The strong linearity of the scarp, coupled with the absence of reverse faulting at the base of the hypothetical “toe bulge”, favors a tectonic origin for the linear escarpment.

7.2.3 Sinuous Bulging Ridges

A relatively consistent orientation for faults encountered in trenches T-1, T-2, T-4 and T-6, of about N40°E to N56°E, as well as fault orientations striking parallel to regional faults, argues in favor of a tectonic origin. A very important observation regarding the faults exposed at both sites is that the average orientation of the faults is consistent with: (1) the regional tectonic framework (subparallel to the CGL and Reelfoot Rift), (2) faults imaged and interpreted from seismic reflection profiles crossing the ridge, and (3) previously mapped faults in the Bloomfield Hills (i.e., Idalia Hill fault). Also, seismic reflection profiles acquired at the site and 3 km to the northeast (Stephenson et al., 1999) indicate the presence of steeply dipping faults extending upward into the Tertiary and Quaternary sections and having both normal and reverse senses of displacement. We speculate that a left step geomorphically expressed, in part, by the eastern margin of the Bloomfield Hills, near the South Holly Ridge site, produces a restraining bend geometry that is reflected in the subsurface and near-surface geology. Seismic reflection profiles by Stephenson et al. (1999) and this study show that deformation of the Quaternary section is complex and broad, and appears to “flower” upsection into splay faults that exhibit both normal and reverse offset, as well as folds that warp stratigraphy down to the north and south (Figures 3, 4, and 7). The observed folding and apparent sense-of-slip of the faults exposed at the North and South Holly Ridge sites is compatible with the complex pattern of deformation imaged from seismic reflection profiles, and the existing regional stress regime. We speculate that the complex pattern of folding and faulting at the South Holly Ridge site reflects structural complexities imparted by the hypothetical restraining bend, or the complexities associated with transpressive faulting as is interpreted elsewhere along the Bloomfield and Benton Hills (Palmer et al., 1997; Stephenson et al., 1999; Harrison et al., 1999). Collectively, this data strongly supports a tectonic origin for the faulting observed at the site.

7.3 Lateral Continuity of Features

The lateral continuity of landslide features generally is limited in length compared to seismogenic faults that rupture the ground surface. The NRC uses the following criterion for lateral continuity associated with landsliding: *If a fault is greater than 3 km long, it probably is not related to landsliding. If a fault is discontinuous or less than 3 km long, it may be related to landsliding.* This criteria is appropriate for late Holocene features (faults and landslides); however, older tectonic faults (e.g., early- to middle-Holocene) may have discontinuous surficial patterns if recent deposition and erosion has obscured or altered evidence of past surface-fault rupture. For instance, aligned northeast-trending geomorphic lineaments mapped along the eastern margin of the Bloomfield Hills extend discontinuously as a combination of one or more geomorphic features (e.g., not as a single unbroken topographic escarpment) for at least 6 km between Highway E, near Idalia, to Pleasant Valley Church southwest of the Holly Ridge sites (Figure 5). When considering the possible right-lateral separation of Dexter Creek and its associated fluvial terraces, as well as weak tonal lineaments preserved in Quaternary alluvial deposits northeast of Guam, Missouri, the geomorphic expression of these lineaments may be as long as 20 to 25 km. In reference to the northwest-facing escarpment at the South Holly Ridge site, this feature appears as a continuous escarpment with differences in height and slope face direction for at least 1.4 km and is aligned with a series of northeast trending lineaments to the north and south over a distance of at least 6 km. Lastly, seismic profiles that cross the eastern bluff line of the Bloomfield Hills at Holly Ridge and Idalia (Stephenson et al., 1999) provide evidence of late Quaternary faulting and folding along fault strike for at least 3 km. On the basis of its lateral continuity over distances greater than 3 km, we infer that the Idalia Hill fault zone is a tectonic feature and not related to landslides.

7.4 Strain Rates

Differences in strain rates and recurrence intervals also are potentially diagnostic criteria for differentiating landslide-induced faulting from tectonic faulting. The criterion used by the NRC to differentiate landslides from tectonic faults states: *If a fault has an anomalously high strain rate for the regional or local tectonic setting, then it is unlikely to be related to tectonic faulting and more likely to be related to landsliding or some other non- tectonic process. If a fault has an anomalously short recurrence interval between surface rupturing events for the regional or local tectonic setting (e.g., years or tens of years vs. hundreds to thousands of years), then it may be related to landsliding or some other non-tectonic process.* Strain rates along the Idalia Hill fault zone can be estimated using the apparent vertical displacement of buried soil Q_{s2} . The apparent vertical displacement of this unit is at least 2.2 m based on stratigraphic and structural relations exposed in trench T-6 (Figure 12). Using a minimum age of 10,000 years (early Holocene) for buried soil Q_{s2} , the minimum uplift rate is at least 0.22 mm/yr. As a comparison, this uplift rate is less than the estimated uplift rate of about 3 mm/yr for the late Holocene-active Reelfoot fault in the NMSZ (Mueller et al., 1999). This low uplift across one strand of the Idalia Hill fault zone and absence of prominent tectonic geomorphology preserved in the younger Holocene alluvium directly east of the site implies that the slip rate associated with this fault zone is likely lower than the deformation rates of the NMSZ. If the uplift rates were higher or close to the rates estimated in the NMSZ, one would be suspicious of landsliding. We acknowledge that the time-average strain rates for large dormant landslides may approach the strain rates for active tectonic faults, thus eliminating the usefulness of high strain rates as compelling criterion for differentiating the two processes.

7.5 Seismic Implications if Deformation is Tectonic in Origin

We believe that collectively the findings from the geomorphic, geophysical, and subsurface investigations at the South Holly Ridge site strongly support a model in which the deformation observed at the South Holly Ridge site is primarily of tectonic origin. If not, the size and dimension of the hypothetical landslide intersecting the North and South Holly Ridge sites strongly implies a groundshaking-induced origin possibly associated with a CGL structure such as the Idalia Hill fault. Thus data on the age of deformation may be applicable to assessing the earthquake potential of the Idalia Hill fault, and in turn the Commerce section of the CGL. However, we believe that the deformation observed at the South Holly Ridge site is likely of primary tectonic origin based on: (1) deep-seated faults closely coinciding with near-surface faulting and folding exposed in excavations at the site, (2) an absence of reverse faulting at the hypothetical “toe bulge” of the landslide, (3) lateral continuity of northeast-trending lineaments and geomorphology, and (4) lateral continuity (3 km) of Quaternary faulting and folding along the eastern ridge margin. Assuming that the faulting is tectonic, then the timing information obtained from this site can be used to assess recency of activity of the Idalia Hill fault zone, and can be compared to other similar paleoseismic studies performed along the CGL in southeast Missouri.

8.0 TIMING OF DEFORMATION

Assuming that the deformation exposed in the South Holly Ridge site excavations is primarily tectonic related, stratigraphic and structural relations interpreted from near-surface ground penetrating radar data and paleoseismic trenches at the South Holly Ridge site provide further age constraints on the long-term behavior and timing of Quaternary deformation of the Idalia Hill fault zone. From these data we infer the presence of at least two poorly constrained Late Quaternary surface-rupturing events at the South Holly Ridge site.

The earliest event at the site is based on the presence of a scarp-derived Pleistocene colluvium that directly overlies reworked Mounds Gravel in trenches T-1 and T-6, and possibly T-4. We interpret the Pleistocene colluvium to have formed during a surface-faulting event that would have produced vertical displacement across the prominent, northeast-trending fault scarp. For instance, the colluvium is coarse-grained near the easternmost fault and becomes finer grained and massive to the northwest or away from the scarp. In trench T-1, the Pleistocene colluvium dips more steeply to the northwest than the overlying Peoria Loess indicating the Pleistocene colluvium has undergone recurrent deformation. The upper part of the Pleistocene colluvium appears to be mixed with Peoria loess, thus providing a minimum age for the inferred faulting. A composite sample of detrital charcoal (HR-T2-LO-BLK-3) from the Pleistocene colluvium, yielded an anomalous calibrated C^{14} age of $10,920 \pm 200$ yrs B.P. (Table 1). It is likely that some of the very small detrital charcoal collected from this unit near the scarp crest has been contaminated by bioturbation and soil forming processes. Thermoluminescence analysis of two samples collected from the loess yielded an age ranging from ≥ 19.9 to ≤ 23.6 ka (Table 1). Therefore, the age of the event pre-dates the age of the Peoria Loess, and likely occurred prior to 19.9 to 23.6 ka.

The second event post-dates deposition of the Peoria Loess and subsequent burial of the Pleistocene scarp-derived colluvium. The event is based on vertical separation across relatively distinct near-vertical faults exposed near the base of trenches T-1, T-4 and T-6 that offset Pleistocene colluvium, Peoria Loess, as well as a weathering front developed in the upper part of the loess. This event may also be correlative with displacement on the easternmost fault exposed in trench T-1/T-2 that offsets Pleistocene colluvium and projects upsection to the ground surface (Figure 9). Based on the offset weathering patterns of the loess, faulting can be traced upsection to within 1.5 m of the ground surface, where it becomes obscured by soil processes from paleosol units Q_{s1} to Q_{s3} . However, where faulting clearly displaces the weathering front, the shear planes coincide with prominent fractures cutting across units Q_{s1} and Q_{s2} suggesting that the faulting also may continue upsection. Unfortunately, because of the strong-overprinting from soil pedogenic textures, recognition of faulting across the soils boundaries is unclear. Although less definitive than faulting, the inferred liquefaction vents in the northwest end of trench T-5 that extend into overlying Peoria Loess may be correlative with this earlier event. Lastly, the late Pleistocene to early Holocene paleosols of units Q_{s1} and Q_{s2} exhibit westward-directed tilting across the scarp in trenches T-1, T-4 and T-6. Both diffuse basal contacts of paleosol units Q_{s1} and Q_{s2} dip steeply to the northwest at slope angles that exceed the present-day slope.

Paleosol unit Q_{s3} partly overprints tilted units Q_{s1} and Q_{s2} , and appears to continue laterally undeformed across the zone of faulting and tilting in trenches T-1, T-4 and T-6, thus providing a constraint on the minimum age of deformation. Thermoluminescence dates from units Q_{s1} and Q_{s2} provide ages that are slightly younger than deeper and unweathered loess deposits exposed in trench T-4, and provide a maximum age for the deformation of 18.3 ± 1.5 ka. However, based on the well-developed soil profile of paleosol unit Q_{s2} , compared to the soil profile of the approximately 7.5 ka alluvial and fluvial deposits exposed in trench T-5 southwest of Pennington Creek, it is permissible to assume that the textures present in unit Q_{s2} required thousands of years to develop. If this is true, then based on pedochronology (e.g., clay film development, pedogenic structures, depth of the soil profile), and hue, paleosol unit Q_{s2} is

at least early Holocene in age, and extends the age of deformation along the fault scarp into the early Holocene. Lastly, the age of the undeformed alluvial and fluvial deposits exposed southwest of Pennington Creek and crossing the southwest projection of near-surface faulting, indicate that deformation associated with the fault scarp predates 7.6 ka.

In summary, we recognize at least two poorly constrained surface deforming events of Quaternary age at the South Holly Ridge site. The oldest event likely occurred prior to deposition of the Peoria Loess (≥ 23 ka) and is based on the presence of a scarp-derived colluvium. On the basis of the warped soil horizons Q_{s1} and Q_{s2} , the minimum age of deformation at the site ranges between 18 ka and 7.6 ka.

8.1 Regional Comparison of Event Timing Information

The ages of the events interpreted from stratigraphic and structural relations at the South Holly Ridge site overlap with existing paleoliquefaction (Vaughn, 1994) and paleoseismic (Harrison et al., 1994; 1999; 2002) event timing data collected in the Western Lowlands along the Commerce section of the CGL (Figure 1). Paleoliquefaction studies performed in the Western Lowlands, several tens of kilometers from the NMSZ, and about 30 km southwest of the South Holly Ridge site provide evidence for at least four poorly constrained prehistoric events (individual earthquakes or sequences of earthquakes), some of which may be related to the NMSZ, or structures associated with the CGL (Vaughn; 1994; Tuttle et al., 1998; Tuttle, 1999) (Figure 1). Evidence of prehistoric earthquakes is derived from the interpretation of numerous northeast-trending liquefaction-related dikes and surficial and buried sand blow deposits (Figure 1). Vaughn (1994) estimates the timing of four prehistoric events occurring between 23,000-17,000 yr B.P., 13,400-9000 yr B.P., A.D. 240-1020, and A.D. 1440-1540. The two most recent events of Vaughn (1994) likely are related to paleoearthquakes associated with seismic sources within the New Madrid seismic zone (Tuttle et al., 2002); whereas, the two earliest paleoliquefaction events may correlate with nearby CGL structures. Correlation of the older events to unidentified CGL structures is based on the event's apparent older age and the greater size of the liquefaction feature relative to similar liquefaction-related deformation correlative with New Madrid-like events (i.e., the size of the dike is used to infer proximity of the earthquake-induced liquefaction with respect to the seismogenic source). Interestingly, the two older events of Vaughn (1994) are close in age to the two poorly constrained events interpreted at the South Holly Ridge site.

Detailed geologic mapping, structural analyses, and paleoseismic trenching performed by Harrison et al. (1994; 1999; and 2002) approximately 50 km northeast of the South Holly Ridge site, in the Benton Hills, provide additional timing information on surface-deforming events believed to be associated with faults overlying the CGL (Figure 1). Harrison et al. (1999) interpret episodic faulting throughout the Cenozoic, and as many as four faulting events occurring during the late Quaternary. The surface faulting events are broadly estimated to have occurred between 60 to 50 ka, 35 to 25 ka, $4,860 \pm 120$ yrs B.P. and $1,270 \pm 60$ yrs B.P., respectively (Harrison et al., 1999). Only the second event interpreted at South Holly Ridge roughly correlates with one of the poorly constrained older events (60 to 50 ka and 35 to 25 ka) of Harrison et al. (1999). The two younger events at Commerce are believed to be correlative with NMSZ events.

Paleoseismic and paleoliquefaction event timing data from the Western Lowlands provide evidence for about four poorly constrained pre-historic events, two of which are roughly correlative with poorly constrained event chronology data from the South Holly Ridge site. The oldest events of Vaughn (1994) are possibly correlative with the late Pleistocene to early Holocene deformation interpreted from trench exposures at the South Holly Ridge site and some of the early deformation interpreted at the Commerce site (Harrison et al., 1999) site. Correlation of the late Holocene events interpreted by Vaughn (1994) and Harrison et al. (1999) can not be deciphered at the South Holly Ridge site because of the poor stratigraphic and structural control of middle to late Holocene faulting in trenches located northeast of

Pennington Creek. However, trench T-5 located southwest of Pennington Creek, and shadowing the observed faulting and folding to the northeast, provides valuable information on the absence of middle to late Holocene faulting along the eastern part of the Idalia Hill fault zone. Trench T-5 provides direct evidence for the absence of middle to late Holocene faulting and folding along the easternmost strands of the Idalia Hill fault zone. If the absence of middle to late Holocene faulting reflects the behavior of the entire Idalia Hill fault zone, then the earthquake timing information from the South Holly Ridge site, coupled with paleoliquefaction and paleoseismic data from elsewhere along the CGL in the Western Lowlands, can be interpreted to suggest that the CGL was active into at least the early Holocene, but does not appear to have been active in the middle to late Holocene between Vaughn's (1994) paleoliquefaction sites in southeast Missouri and the South Holly Ridge site.

9.0 SUMMARY OF FINDINGS

Our investigation of the Idalia Hill fault zone and its inferred connectivity with the Commerce geophysical lineament provides additional circumstantial evidence for linking observed Pleistocene-Holocene surficial deformation with previously mapped faults directly overlying the CGL. Although our study documents the presence of large and numerous landslides along the eastern margin of the Bloomfield Hills, shallow surface deformation observed at the North and South Holly Ridge sites is most consistent with primary tectonic-related deformation. The seismic reflection data acquired during this study image steeply dipping faults, closely coinciding with near-surface faulting and folding expressed in trenches at the North and South Holly Ridge sites, that in turn closely align with the Idalia Hill fault zone. Also, the near-vertical faults exposed in the trenches at the South Holly Ridge site strike parallel to the Idalia Hill fault zone and Commerce geophysical lineament. The northeast strike of the Idalia Hill fault zone is preferentially aligned in today's central U.S. stress regime to accommodate transpressive deformation.

Interpretation of stratigraphic and structural relations at South Holly Ridge provide evidence for at least two poorly constrained faulting events, with one occurring in the late Pleistocene (predates 23.6 to 18.9 ka), and the other in the late Pleistocene to early Holocene (18.5 to 7.6 ka). The poorly constrained ages of these faulting events generally overlap with the two pre-historic events interpreted by Vaughn (1994) that occurred 23 to 17 ka and 13.4 to 9 ka and one event recognized by Harrison et al. (1999) that occurred 35 to 25 ka. The events interpreted by others are believed to be associated with structures overlying the CGL. Furthermore, interpretation and correlation of event stratigraphy from the South Holly Ridge site to possible CGL-related paleoliquefaction features near the Arkansas-Missouri state border, coupled with similar event timing information from Commerce, provides evidence of late Pleistocene to early Holocene deformation along an approximately 75 km reach of the CGL.

Because the South Holly Ridge site intersects only one of potentially numerous fault strands associated with the Idalia Hill fault, it is unclear if other fault strands located to the west near the bluff line of the Bloomfield Hills ruptured more recently in the middle to late Holocene and would correlate with events at Commerce (Harrison et al., 1999). We speculate, that based on the absence of prominent geomorphology northeast of the northern margin of the Bloomfield Hills, that if rupture were to have occurred in the last 5,000 years or so, features suggestive of surface faulting likely would be preserved in the alluvial and fluvial deposits of the Castor River. Currently, the photolineament of Heyl and McKeown (1978), which lies west of the Idalia Hill fault and the alluvial plain near the Bell City-Oran Gap is the only geomorphic evidence linking faults between Commerce and Idalia.

This geologic and paleoseismic investigation of the eastern margin of the Bloomfield Hills improves our understanding of the likelihood of potentially active seismogenic sources existing outside of the NMSZ and in the mid continental United States. The existing paleoseismic and paleoliquefaction event timing data for pre-historic large magnitude earthquakes in the Western Lowlands is sparse and poorly constrained, but collectively, the data indicate that future earthquakes on northeast-striking faults aligned with the CGL should be considered in probabilistic seismic hazard studies of the central United States. Additional event timing information are needed along the Commerce section of the CGL to ascertain the possibility of middle to late Holocene earthquakes along structures aligned with the CGL, assess temporal clustering of large earthquakes in the upper Mississippi embayment between the NMSZ and CGL structures, and refine the initial late Pleistocene to early Holocene event chronology for the Commerce section of the CGL.

10.0 ACKNOWLEDGEMENTS

This research was supported by the U.S. Geological Survey's National Earthquake Hazard Reduction Program, under Award No's. 01-HQ-GR-0055 and 03-HQ-GR-0095. The views and conclusions contained in this document are those of the authors and should not be interpreted as necessarily representing the official policies, either expressed or implied, of the U.S. Government. Additional support for this study was provided by the Professional Development Program of William Lettis & Associates, Inc. We also are thankful to those people who made this project possible, including David Hoffman formerly of Missouri Department of Natural Resources (MDNR), and Jim Palmer of MDNR who provided copies of original logs prepared for the North Holly Ridge site, reviewed the South Holly Ridge trenches, and provided critical review. Bruce Harrison of the U.S. Geological Survey provided encouragement and lively discussion throughout the field stages of this investigation, and reviewed some of the trenches during the first year of study. Mr. Jim Burton kindly provided access to the existing exposures at the North Holly Ridge site. Dan Childress and his members of the U.S. Department of Agriculture provided use of the Giddings rig, and helped describe the soils encountered in the cores. A very special thanks to Billy and Deana Pennington who allowed us the opportunity to conduct this research on their property. Without the Pennington's generosity, this study would not have been possible. Lastly, we are grateful to Lori and Lynn Brotherton who housed our gear and provided a shelter during our studies in southeast Missouri. Hamilton Plumbing provided excellent backhoe service and excavated the trenches at the site.

11.0 REPORTS/ABSTRACTS PUBLISHED

As part of this U.S. Geological Survey NEHRP-funded research two abstracts were presented to discuss the initial findings of the study:

Baldwin, J.N., Witter, R.C., Vaughn, J.D., Harris, J.B., Sexton, J., Lake, M., and Forman, S.L., 2004, Quaternary deformation associated with the Commerce geophysical lineament, Holly Ridge, Idalia, Missouri [abs.]: Geological Society of America Abstract and Programs North-Central Section 38th Annual Meeting, St. Louis, Missouri.

Lake, M., Sexton, J., Mueller S.E., McClain, J., **Baldwin, J.**, Carpenter, P., and Harris, J., 2004, Georadar profile studies of Quaternary deformation associated with the Farrenburg and Commerce geophysical lineaments in the New Madrid seismic zone, [abs.]: Geological Society of America Abstract and Programs North-Central Section 38th Annual Meeting, St. Louis, Missouri.

Baldwin, J.N., Barron, A.D., Harris, J.B., Vaughn, J.D., and Forman, S., 2002, Geophysical and paleoseismic investigation of the Commerce geophysical lineament, Idalia, Missouri: Deformation associated with primary tectonic faulting? [abs.]: Geological Society of America Abstract and Programs North-Central Section (36th) and Southeastern Section (51st), GSA Joint Annual Meeting, v. 34, n.2, p. A15.

Vaughn, J.D., **Baldwin, J.N.**, and Barron, A.D., 2002, Recurrent Late-Quaternary deformation within the Dexter Tectonic Zone, upper Mississippi embayment [abs.]: International Basement Tectonics Association 16th Annual Conference, Rolla, MO., May 19 to 24, 2002.

Table 1. Radiocarbon Analyses, South Holly Ridge Site Idalia, Missouri

Unit	Sample	Lab Number (Beta)	Sample Material	Conventional Radiocarbon age $\pm 1\sigma$ (yr BP) ^a	$^{13}\text{C}/^{12}\text{C}$ (‰) ^b	Calibrated Age ^c (calibrated 2 σ) (yrBP)	TL Age of Unit	Interpreted Age of Unit
<u>Northeast of Creek</u>								
H _{c3}	HR-T1-RC-5	161504	Charred material	240 \pm 40	26.2	420 to 0		Holocene Colluvial
H _{a3}	HR-T1-RC-10E	161503	Charred material	1980 \pm 40	25.8	1930 \pm 70		Holocene Alluvial
H _{a3}	HR-TP-1-RC-3	161502	Charred material	4420 \pm 40	25.9	5070 \pm 220		Holocene Alluvial
Q _p	HR-T1-UP BLK - 1	161505	Charred material	3280 \pm 40	27.5	3500 \pm 100		Pleistocene - Holocene
PC	HR-T2-LO BLK - 3	161500	Plant Material	9570 \pm 40	NA	10920 \pm 200		Pleistocene
Peoria derived colluvium (Qs ₂)	CGL-T6-Sample 2	UIC 1272	Colluvium	-	-	-	18.3 \pm 1.5 ka	Pleistocene to early Holocene
Peoria derived colluvium (Qs ₁)	CGL-T6-Sample 1	UIC 1271	Colluvium	-	-	-	19.2 \pm 1.6 ka	Pleistocene
Peoria Loess	TL-1-T4	UIC 900	Loess	-	-	-	21.4 \pm 1.5 ka	Pleistocene
Peoria Loess	TL-2-T4	UIC 901	Loess	-	-	-	21.9 \pm 1.7 ka	Pleistocene
<u>Southwest of Creek</u>								
Unit Sall	CGL-T5-RC33	182907	Charcoal	190 \pm 40	-26.5	0 to 300		Late Holocene
Unit Sall	CGL-T5-RC13	182903	Charcoal	6020 \pm 40	-28.3	6855 \pm 105		Late Holocene
Unit Q	CGL-T5-RC41	182909	Charcoal	6050 \pm 40	-24.9	6885 \pm 115		Early Holocene
Unit K	CGL-T5-RC24	183545	Charcoal	6100 \pm 40	-24.0	7005 \pm 145		Early Holocene
Unit I	CGL-T5-RC18	182905	Charcoal	6260 \pm 40	-25.1	7140 \pm 120		Early Holocene
Unit E	CGL-T5-RC43	182910	Charcoal	6390 \pm 40	NA	7335 \pm 85		Early Holocene
Unit E	CGL-T5-RC44	182911	Charcoal	6370 \pm 40	NA	7325 \pm 85		Early Holocene
Unit E	CGL-T5-RC11	182902	Charcoal	7670 \pm 40	NA	8455 \pm 65		Early Holocene
<u>Average</u>								
Unit E	CGL-T5-RC43 & RC44		Averaged Age	6380 \pm 28		7251 - 7333		Early Holocene
Unit E	CGL-T5-RC43, RC44 & RC11		Averaged Age	6810 \pm 23		7608 - 7680		Early Holocene

a) Reported ages are corrected for $\delta^{13}\text{C}$ and include a laboratory error multiplier of 1.0 in reported laboratory uncertainty; samples analyzed by Beta Analytic, Inc. (radiocarbon years before present; "present"=1950AD)

b) Read -25 as value of 25% measured for $^{13}\text{C}/^{12}\text{C}$ ratio.

c) Calibrated using Stuiver and Reimer (2000)

12.0 REFERENCES

- Anderson, N.L., 1997, Subsurface structure of the Commerce English Hill and related faults in the Benton Hills of southeastern Missouri: collaborative research, University of Missouri-Rolla, Department of Geology and Geophysics, and Missouri Department of Natural Resources Division of Geology and Land Survey, U.S. Geological Survey Award No. 1434-HQ-97-GR-03038, Project Summary, 4 p.
- Blum, M.D. Guccione, M.J., Wysocki, D.A., Dobret, P.C., and Rutledge, E.M., 2000, Late Pleistocene evolution of the lower Mississippi River Valley, southern Missouri to Arkansas: *GSA Bulletin*, v. 112, no. 2, p. 221-235.
- Cox, R.T., 1988, Evidence of Quaternary ground tilting associated with the Reelfoot rift zone, northeast Arkansas: *Southeastern Geology*, v. 28, no. 4, p. 211-224.
- Farrar, W. and McManamy, 1937, The geology of Stoddard County, Missouri: Missouri Geological Survey and Water Resources, 59th Biennial Report, 92 p.
- Fischer-Boyd, K.F., and Schumm, S.A., 1995, Geomorphic evidence of deformation in the northern part of the New Madrid seismic zone: U.S. Geological Survey Professional Paper 1538-R, 35 p.
- Grohskopf, J.G., 1955, Subsurface geology of the Mississippi Embayment of southeast Missouri: Missouri Geological Survey and Water Resources, v. 37, 2nd Series, 133 p.
- Hanson, K.L., Kelson, K.I., Angell, M., Lettis, W.R., 1999, Techniques for Identifying Faults and Determining Their Origins: U.S. Nuclear Regulatory Commission, NUREG/CR-5503, 5 chapters + apps.
- Harrison, R.W., Palmer, J.R., Hoffman, D., Vaughn, J.D., Repetski, J.E., Frederiksen, N.O., and Forman, S.L., 2002, Geologic map of the Scott City 7.5 minute Quadrangle, Scott and Cape Girardeau Counties, Missouri: U.S. Geological Survey, Geological Investigations Series Map I-2744.
- Harrison, R.W., Hoffman, D., Vaughn, J.D., Palmer, J.R., Wiscombe, C.L., McGeehin, Stephenson, W.J., Odum, J.K., Williams, R.A., and Forman, S.L., 1999, An example of neotectonism in a continental interior-Thebes Gap, Midcontinent, United States.
- Harrison, R.W. and Schultz, A., 1994, Strike-slip faulting at Thebes Gap, Missouri and Illinois: Implications for New Madrid tectonism: *Tectonics*, v.13, no. 2, p. 246-257.
- Heyl, A.V., and McKeown, F.A., 1978, Preliminary seismotectonic map of central Mississippi Valley and environs: U.S. Geological Survey Miscellaneous Investigations Map MF-1011, scale 1:250,000, 2 sheets.
- Hildebrand, T.G., and Ravat, D., 1997, Geophysical setting of the Wabash Valley fault system: *Seismological Research Letters*, v. 68, no. 4, p. 567-585.
- Hoffman, D., 1997, Another possible new earthquake fault found: Missouri Department of Natural Resources Division of Geology and Land Survey, Outlook, v. 10, no. 3.
- Langenheim, V.E., and Hildenbrand, T.G., 1997, Commerce geophysical lineament-Its source, geometry, and relation to the Reelfoot rift and New Madrid seismic zone: *GSA Bulletin*, v. 109, no. 5, p 580-595.
- McBride, J.H., Nelson, W.J., and Stephenson, W.J., 2002, Integrated Geological and Geophysical Study of Neogene and Quaternary-age Deformation in the Northern Mississippi Embayment: *Seismological Research Letters*, v 73, no. 5, P. 597-627.

- McNulty, W.E., and Obermeier, S.F., 1999, Liquefaction evidence for at least two strong Holocene paleo-earthquakes in central and southwestern Illinois, USA: *Environmental and Engineering Geoscience*, v. 5, p. 133-136.
- Nelson, J.W., Harrison, R.H., and Hoffman, D., 1999, Neotectonics of the northern Mississippi Embayment, Illinois State Geological Survey Guidebook 30, 33rd Annual Meeting, April 1999, GSA Field Trip, p. 34.
- Nelson, W.J., Denny, F.B., Devera, J.A., Follmer, L.R., Masters, J.M., 1997, Tertiary and Quaternary tectonic faulting in southernmost Illinois: *Engineering Geology*, v. 46, p. 235-258.
- Odum, J.K., Stephenson, W.J., Williams, R.A., Devera, J.A., and Staub, J.R., 2002, Near-surface Faulting and Deformation Overlying the Commerce Geophysical Lineament in Southern Illinois: *Seismological Research Letters*, v. 73, no. 5, p. 687-697.
- Palmer, J.R., Hoffman, D., Stephenson, W.J., Odum, J.K., and Williams, R.A., 1997, Shallow seismic reflection profiles and geological structure in the Benton Hills, southeast Missouri: *Engineering Geology*, v. 46, p. 217-233.
- Pratt, T.L., 1994, How old is the New Madrid Seismic Zone: *Seismological Research Letters*, v. 65, no. 2, p. 172-179.
- Royall, P.D., Delcourt, P.A., and Delcourt, H.R., 1991, Late Quaternary paleocology and paleoenvironments of the Central Mississippi alluvial valley: *Geological Society of America Bulletin*, v. 103, p. 157-170.
- Satterfield, I.R., and Ward, R.A., 1978, Structural geologic study of southeast Missouri: Summary of Annual Progress Report-Phase 1-Fiscal Year 1978, Contract No. NRC-04078-206; *in*, New Madrid Seismotectonic Study-Activities during Fiscal Year 1978, ed. Buschbach, T.C., Illinois State Geological Survey, p. 53-63.
- Saucier, R.T., 1996, Geomorphology and Quaternary geologic history of the lower Mississippi Valley, Army Engineering Waterways Experiment, v. 1 and 2, Vicksburg, Mississippi, U.S. Department of Commerce.
- Saucier, R.T., 1974, Quaternary geology of the Lower Mississippi Valley: *Arkansas Arch. Survey Res. Series* 6, 26 p.
- Saucier, R.T., 1964, Geological investigation of St. Francis Basin, U.S. Army Eng. Waterways Exp. Stat., Corps of Eng., Vicksburg, Miss., Tech. Rpt. No. 3-659, Distribution of Alluvial Deposits, scale 1:62,500.
- Schweig, E.S., and Ellis, M.A., 1994, Reconciling Short Recurrence Intervals with Minor Deformation in the New Madrid Seismic Zone: *Science*, v. 264, p. 1308-1311.
- Stephenson, W.J., Odum, J.K., Williams, R.A., Pratt, T.L., Harrison, R.W., and Hoffman, D., 1999, Deformation and Quaternary faulting in southeast Missouri across the Commerce Geophysical Lineament: *Bulletin of Seismological Society of America*, v. 89, no. 1, p. 140-155.
- Stewart, D.R., 1942, The Mesozoic and Cenozoic geology of southeastern Missouri: Internal report, Missouri Division Geological Survey and Water Resources, Rolla, Mo., 115 p.
- Stuiver, M., and Reimer, D.J., 2000, Radiocarbon calibration program, CALIB rev. 4.3: *Radiocarbon*, v. 35, p. 215-230.
- Thompson, T.L., 1981, Structural geologic study of southeastern Missouri: Division of Reactor Safety Research, Nuclear Regulatory Commission, Contract No. NRC-04-78-206, 25 p.

- Vaughn, J.D., 1994, Oaleoseismological studies in the western lowlands of southeast Missouri: Report to NEHRP Annual External Program, contract no. 14-08-0001-G1931, 27 pp.
- Vaughn, J.D., 1992, Active tectonics in the Western Lowlands of southeast Missouri: An initial assessment; *in*, Missouri Department Natural Resources Special Publication No. 8, 54-59.
- Vaughn, J.D., 1991, Evidence for multiple generations of seismically induced liquefaction features in the Western Lowlands, southeast Missouri [abs.]: Seismological Research Letters, v. 62, p. 189.
- Vaughn, J.D., Baldwin, J.N., and Barron, A.D., 2002, Recurrent Late-Quaternary deformation within the Dexter Tectonic Zone, upper Mississippi embayment [abs.]: International Basement Tectonics Association 16th Annual Conference, Rolla, MO, May 19 to 24, 2002.
- Zoback, M.L., 1992, Stress field constraints on intraplate seismicity in eastern North America: Journal Geophysical Resources, v. 97, p. 11,761-11,782.

FIGURES

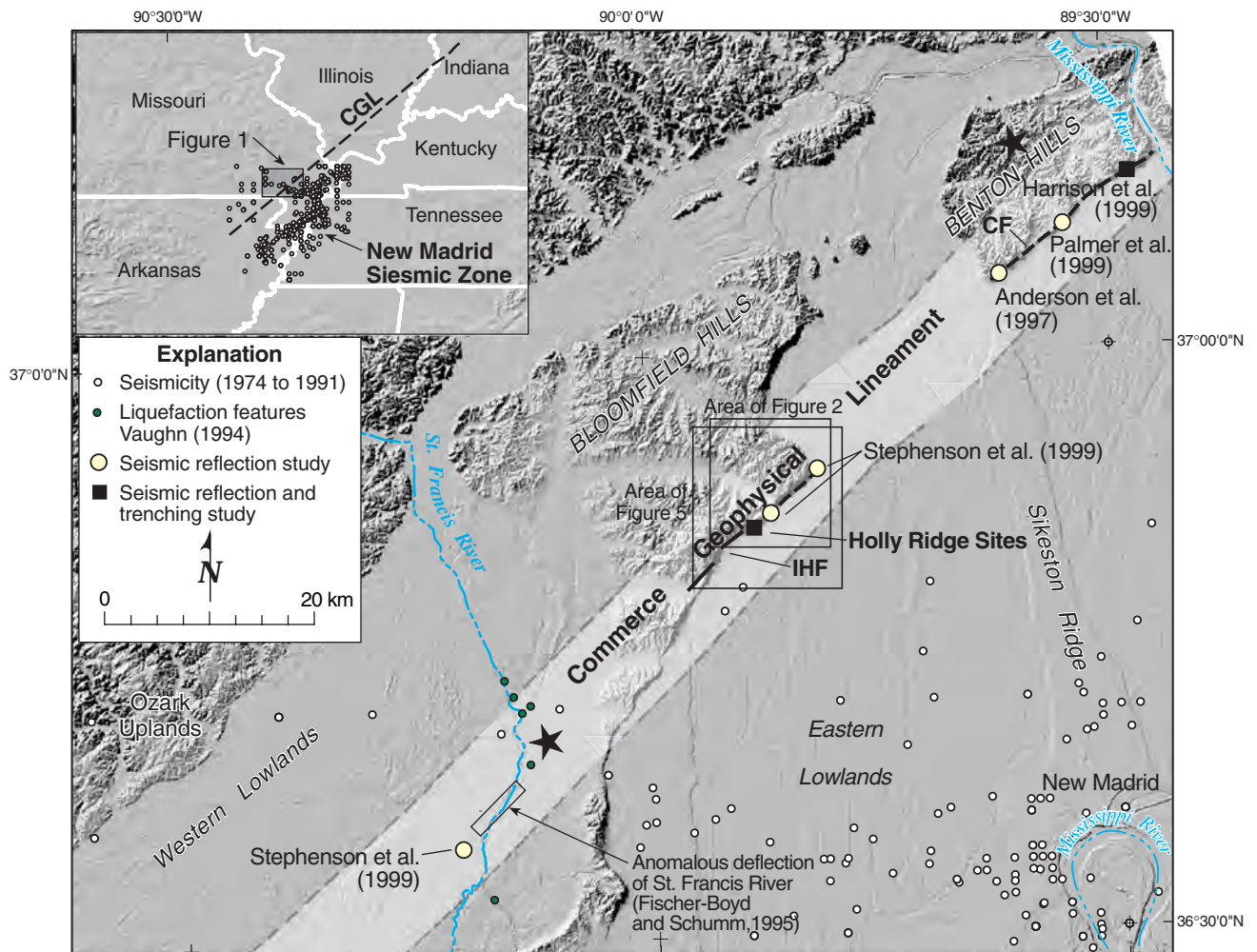


Figure 1. Regional location map of the New Madrid seismic zone and the Commerce section of the Commerce geophysical lineament. Lineament location based on latitude and longitude coordinates provided by Hildenbrand (personal communication, 2002) and, in part, modified from Stephenson et al. (1999). Historical seismicity (1974 to 1991) after Rhea and Wheeler, 1995, and Johnston and Schweig (1996). IHF = Idalia Hill fault; CF = Commerce fault; CGL = Commerce geophysical lineament (Hildenbrand and Ravat, 1997). Stars represent epicenters of $M_{4.8}$ earthquakes (after Stephenson et al., 1999).

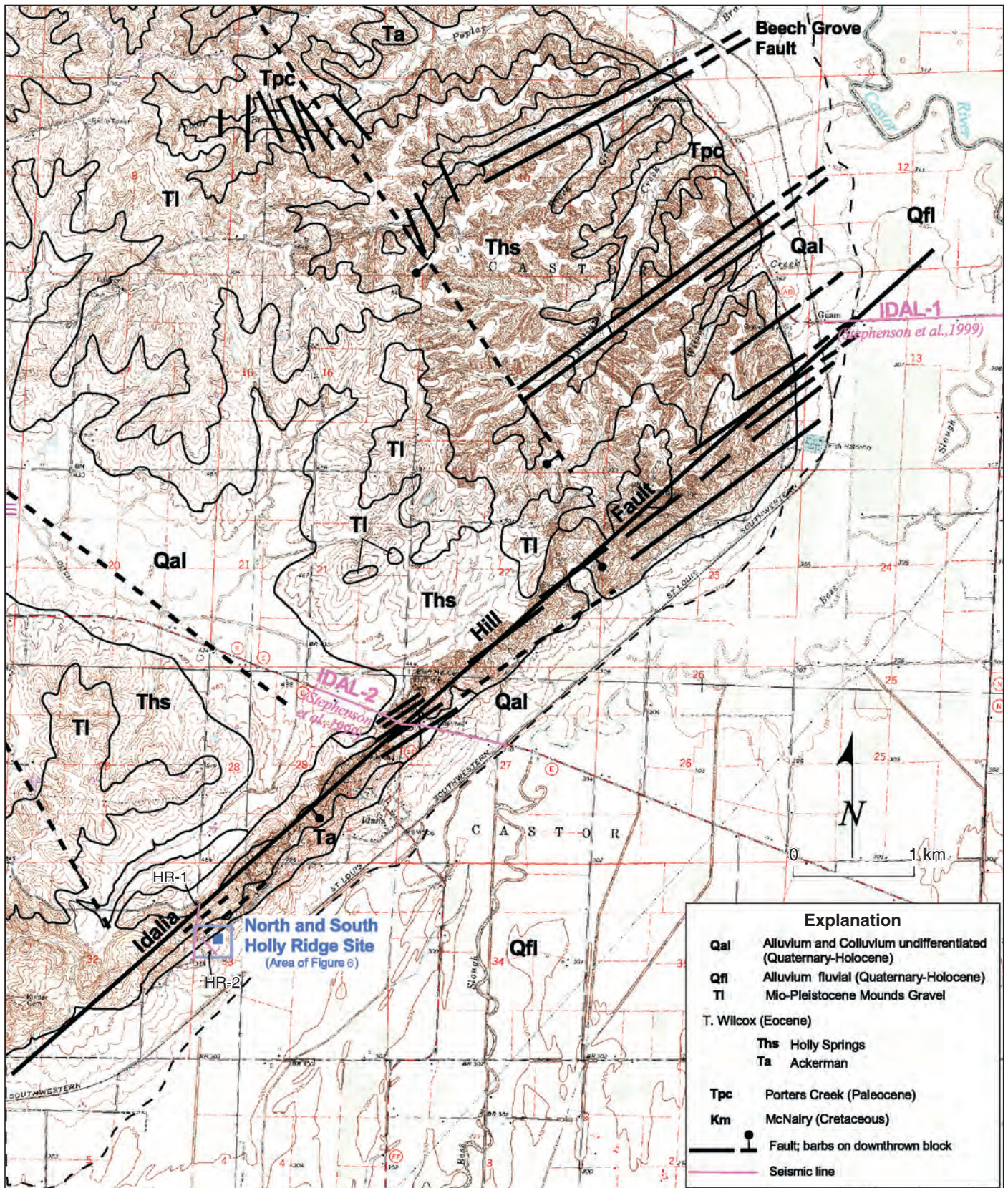


Figure 2. Geologic and site map of the Bloomfield Hills, Missouri, (geology modified from Saucier, 1964; Farrar and McManamy, 1937; Stewart, 1942; Satterfield and Ward, 1978).

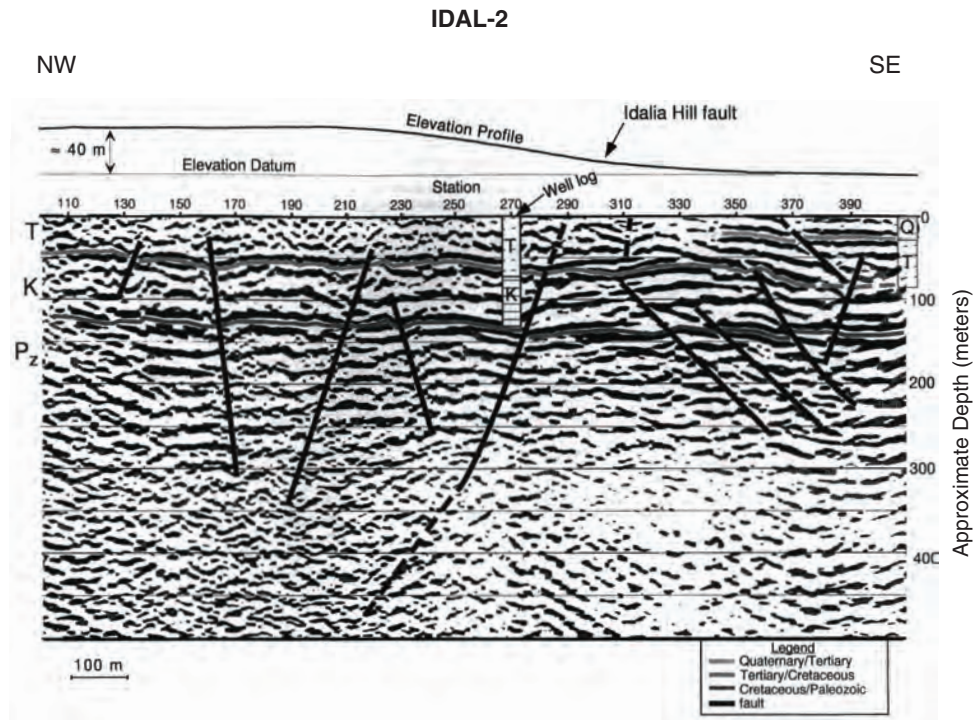


Figure 3. Seismic reflection profile IDAL-2 along Road E, near Idalia (see Figure 2 for location). Quaternary (Q), Tertiary (T), Cretaceous (K), and Paleozoic (P_z) strata labeled; interpreted faults shown by heavy black lines (modified from Stephenson et al., 1999). Deformation near Idalia Hill fault resembles transpressional deformation.

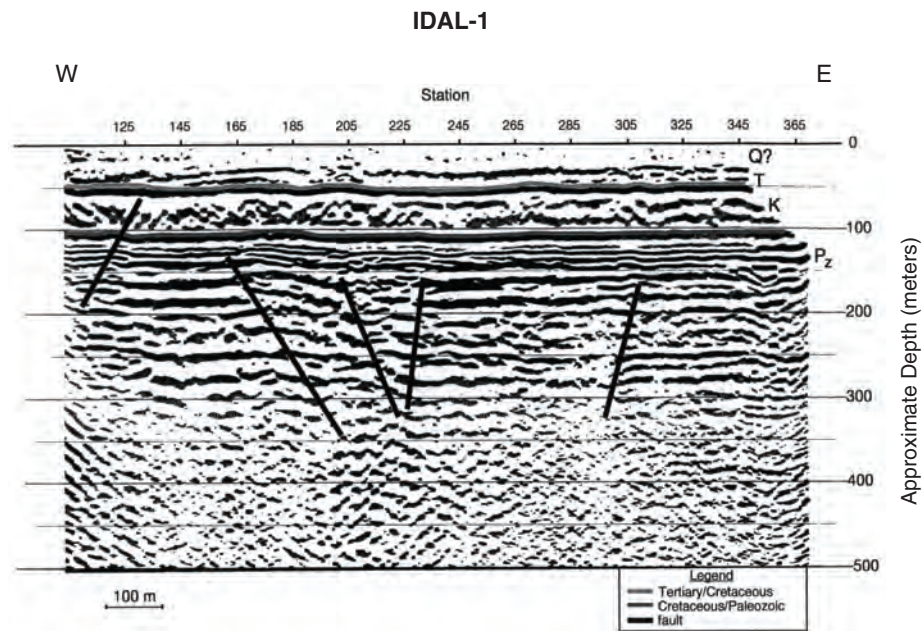


Figure 4. Seismic reflection profile IDAL-1 along Road AB, near Guam (see Figure 2 for location). Quaternary (Q), Tertiary (T), Cretaceous (K), and Paleozoic (P_z) strata labeled; interpreted faults shown by heavy black lines (modified from Stephenson et al., 1999).

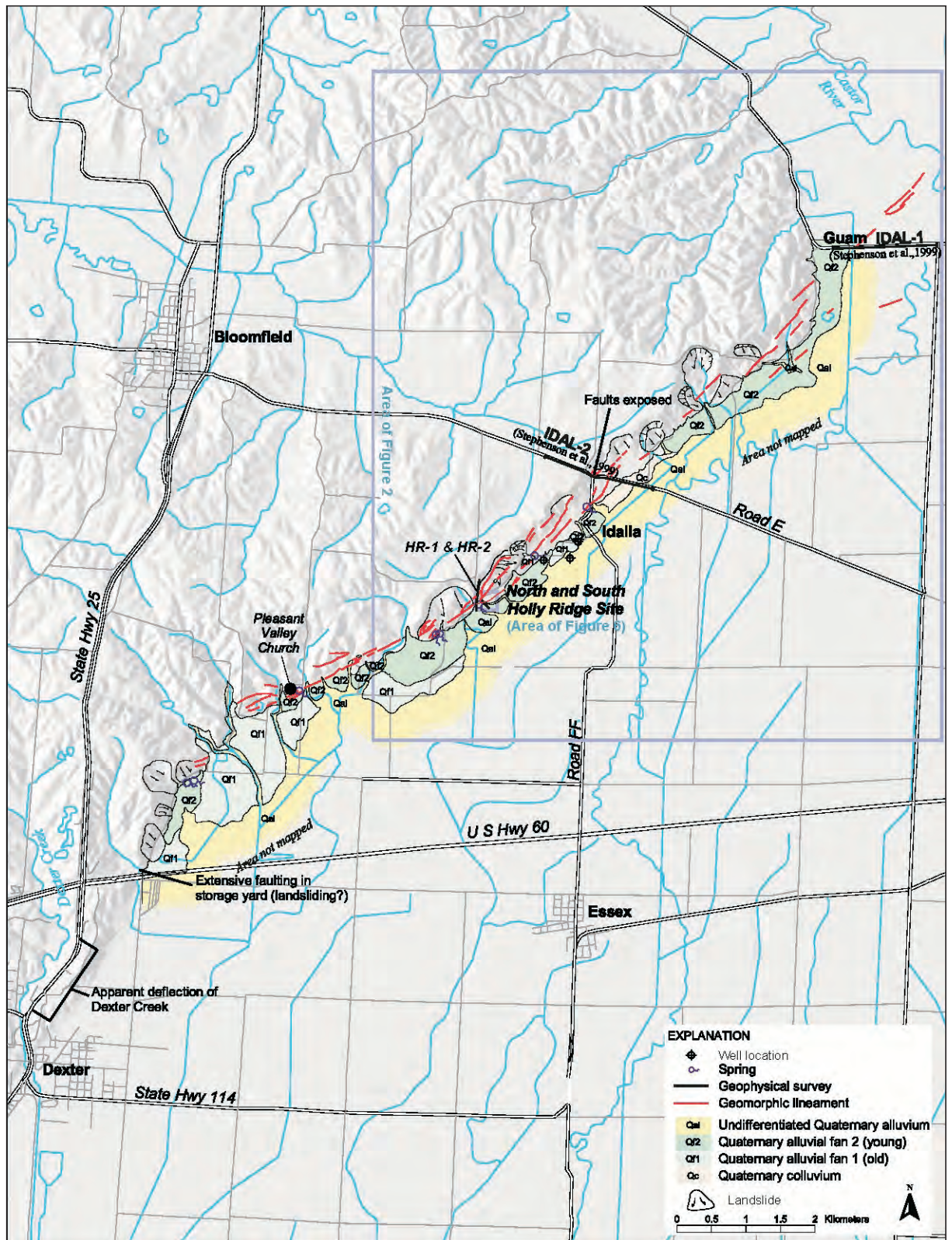


Figure 5. Geomorphic lineament map of the eastern margin of the Bloomfield Hills, southeast Missouri.

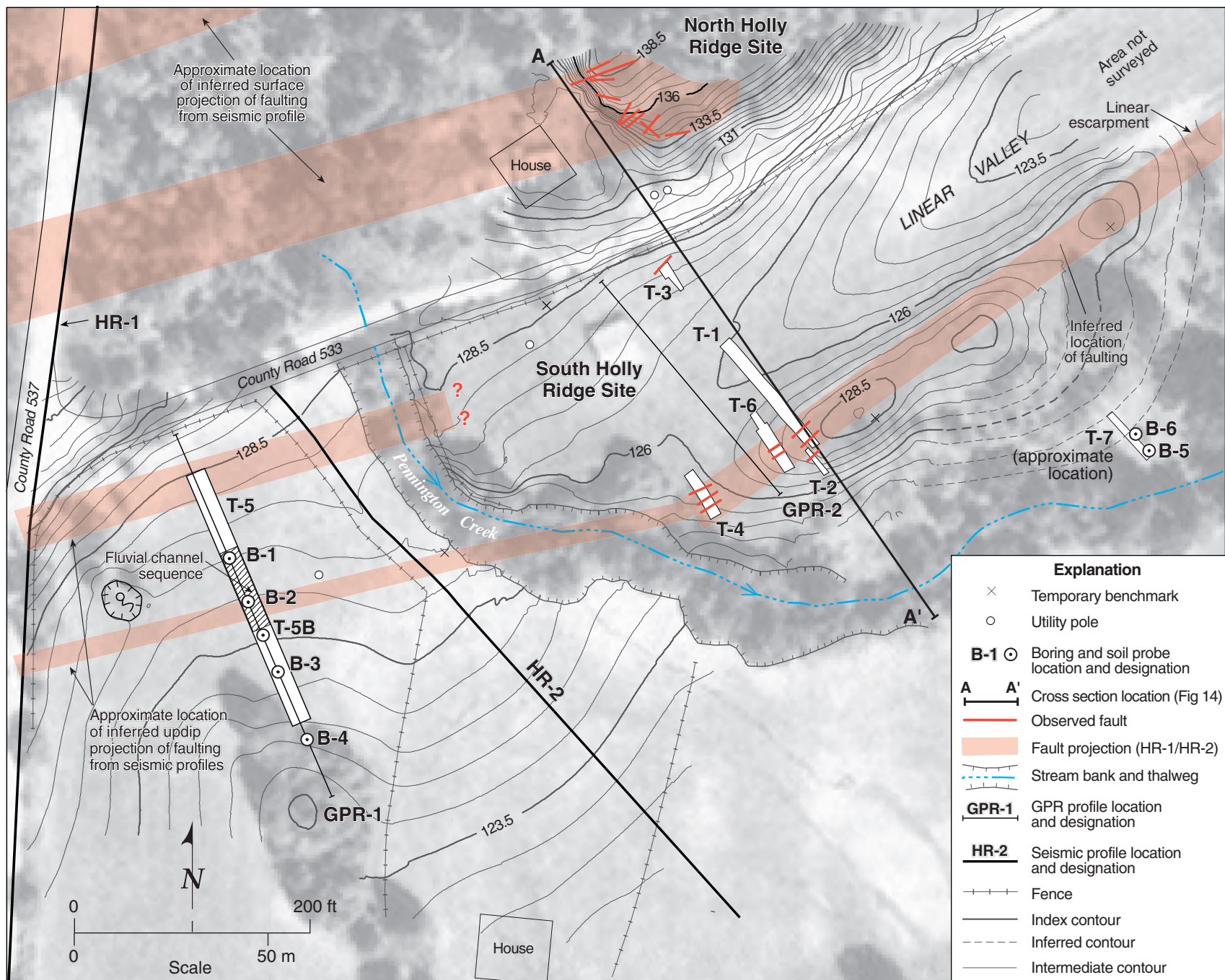


Figure 6. Site map showing trench, borehole, seismic reflection survey, and GPR survey locations. Location of stream bank thalweg estimated from mapping.

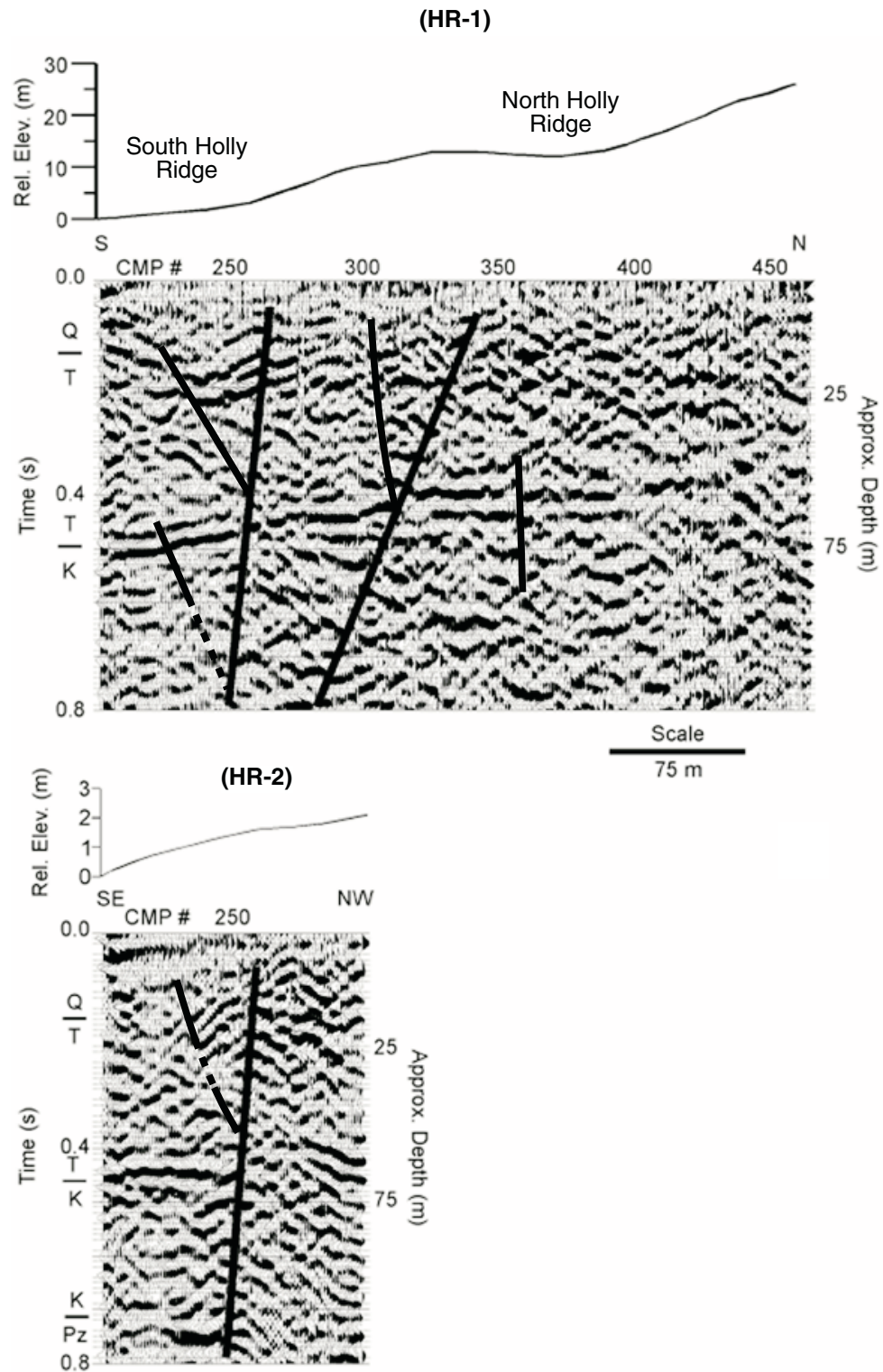


Figure 7. Interpreted shear-wave seismic reflection profiles from South Holly Ridge site, Idalia, Missouri. See Figure 5 for section locations.

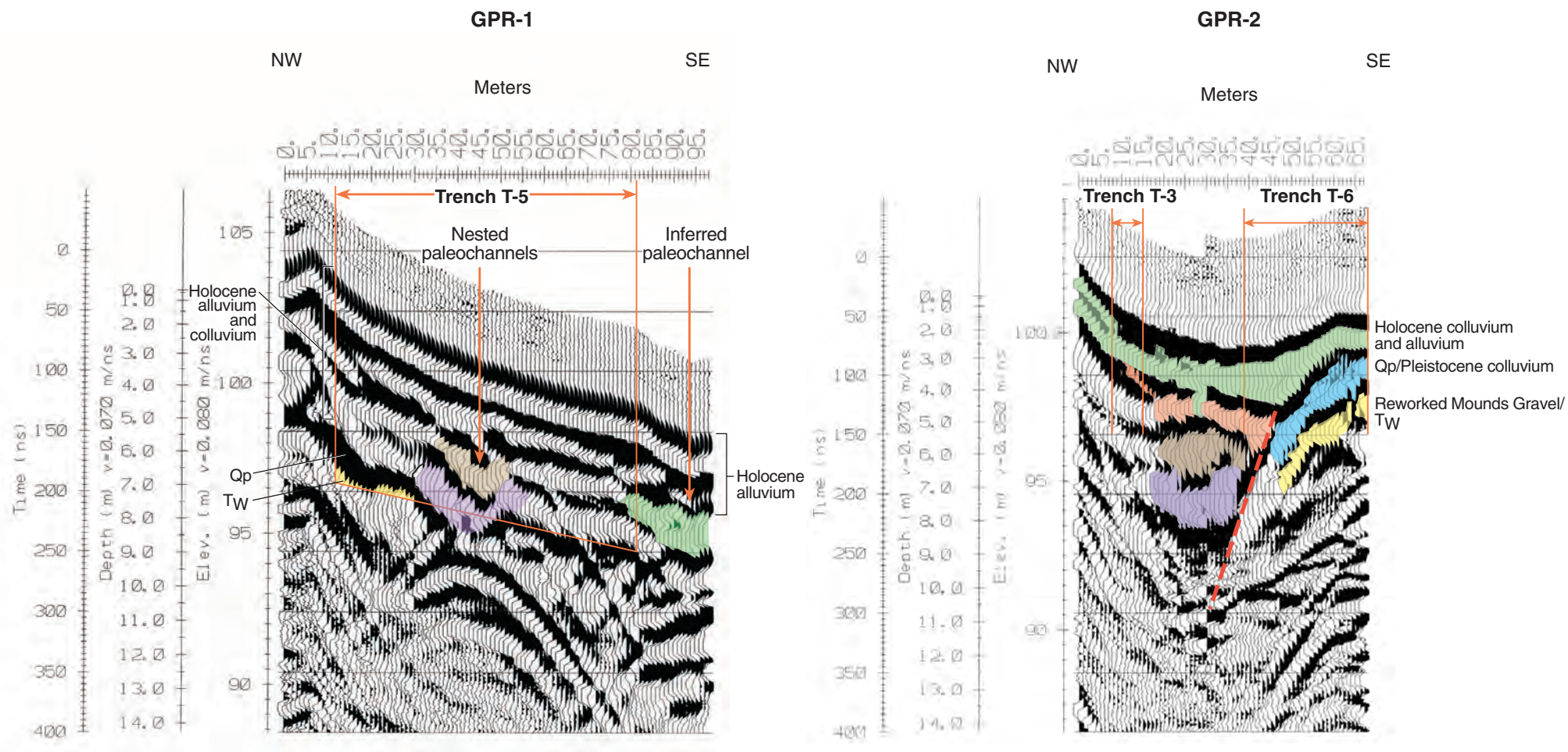
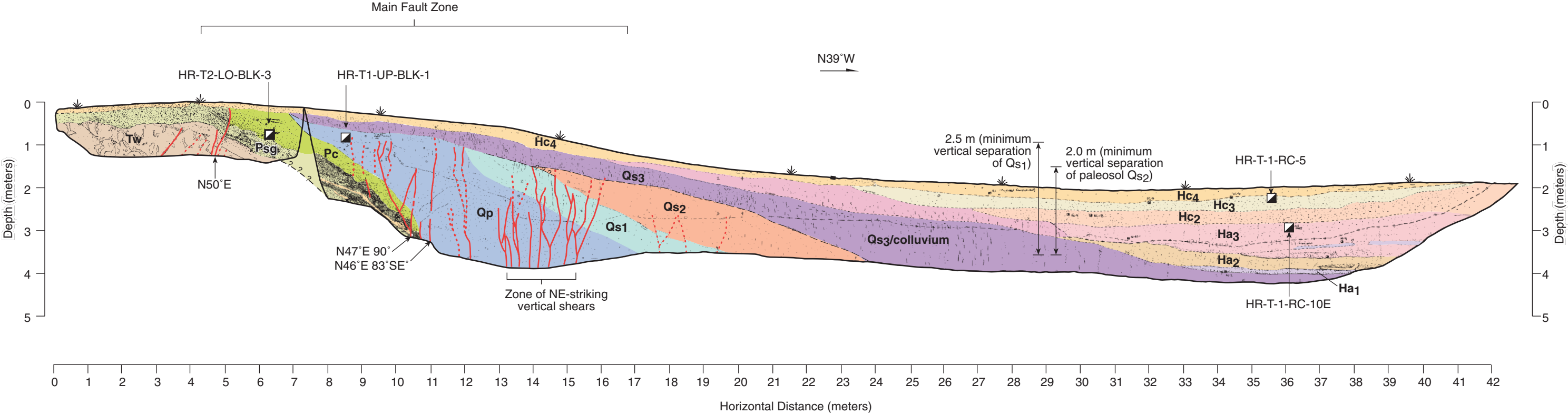


Figure 8. GPR-1 is preliminarily interpreted as imaging moderately dipping Eocene Wilcox (T_W) and Pleistocene (Qp) loess that are inset by a sequence of buried paleochannel deposits and undeformed overlying alluvium. Hyperbolic feature in GPR-1 interpreted as an artifact from a telephone pole. Preliminary interpretation of GPR-2 depicts folded and faulted bedding along the southeast part of the profile and a sequence of nested paleochannel deposits in the axis of the linear valley. See Figure 6 for section location.



Explanation

- Fault

----- Contact

▣ Radiocarbon sample location and designation (see Table 1) for results of radiocarbon analysis)
- Hc4** Holocene colluvium (modern)

Hc3 Holocene colluvium

Hc2 Holocene colluvium

Ha3 Holocene alluvium

Hc1 Holocene colluvium

Ha2 Holocene alluvium

Ha1 Holocene alluvium
- Qs3** Middle to late Holocene paleosol/colluvium

Qs2 Late Pleistocene to early Holocene paleosol/colluvium

Qs1 Late Pleistocene to early Holocene paleosol

Qp Pleistocene Peoria Loess

Pc Pleistocene colluvium/reworked Mounds Gravel

Psg Pleistocene reworked Mounds Gravel with occasional Sangamon Geosol

Tw Eocene Wilcox Formation

COMMERCE GEOPHYSICAL LINEAMENT
IDALIA, MISSOURI

Trenches T-1 and T-2


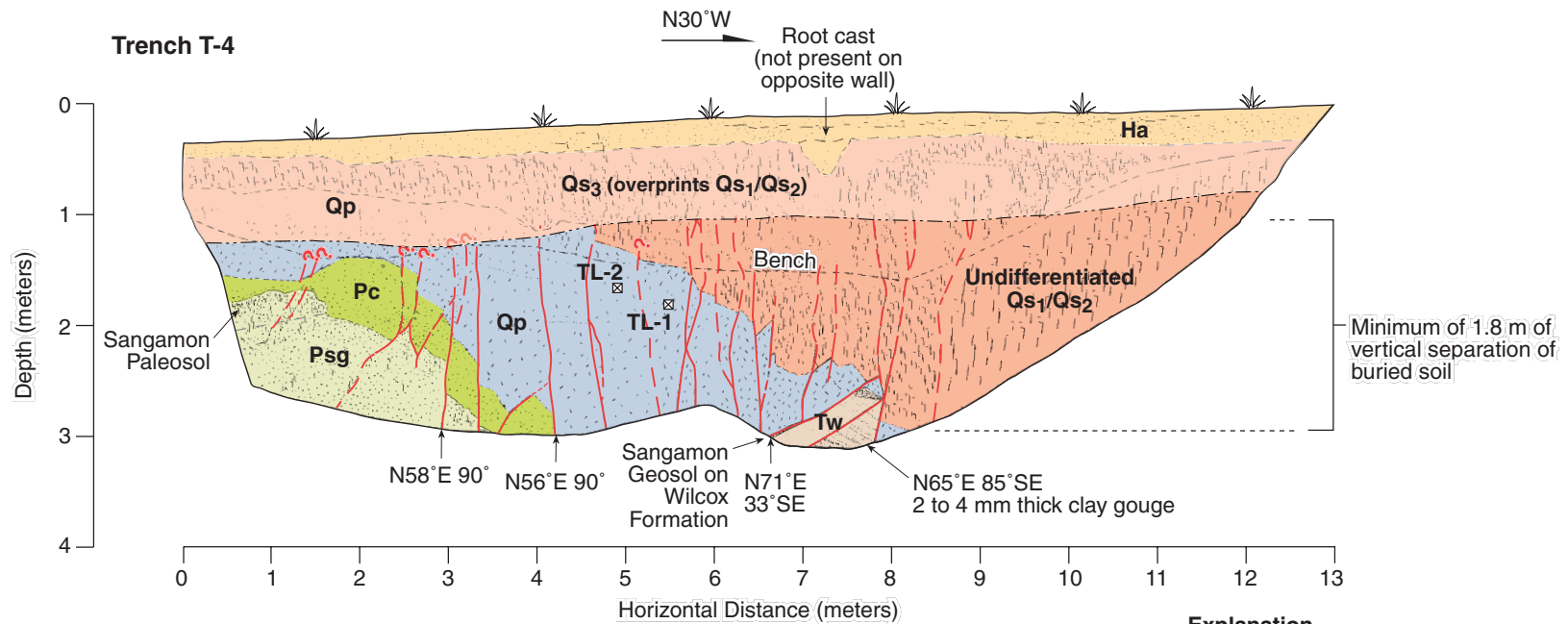
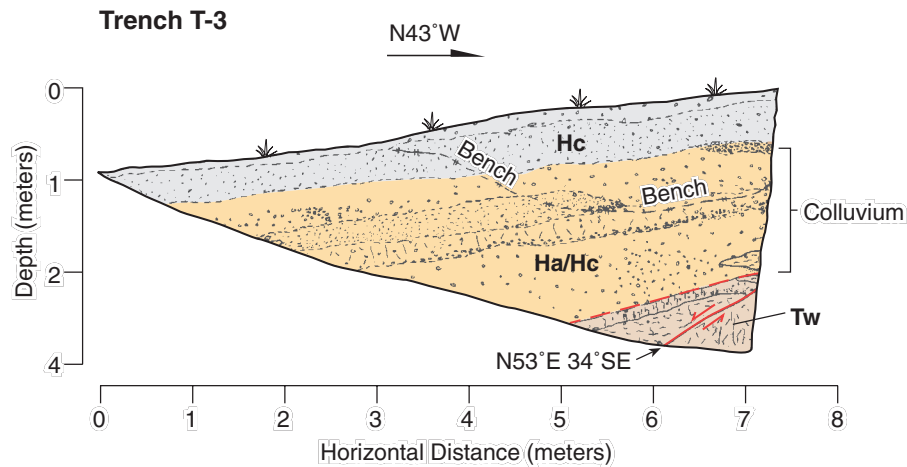
 William Lettis & Associates, Inc.


Figure 9

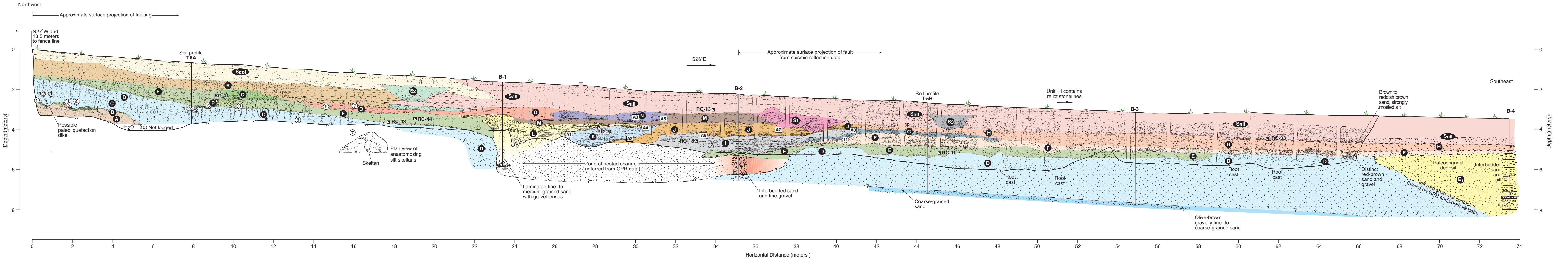


Explanation

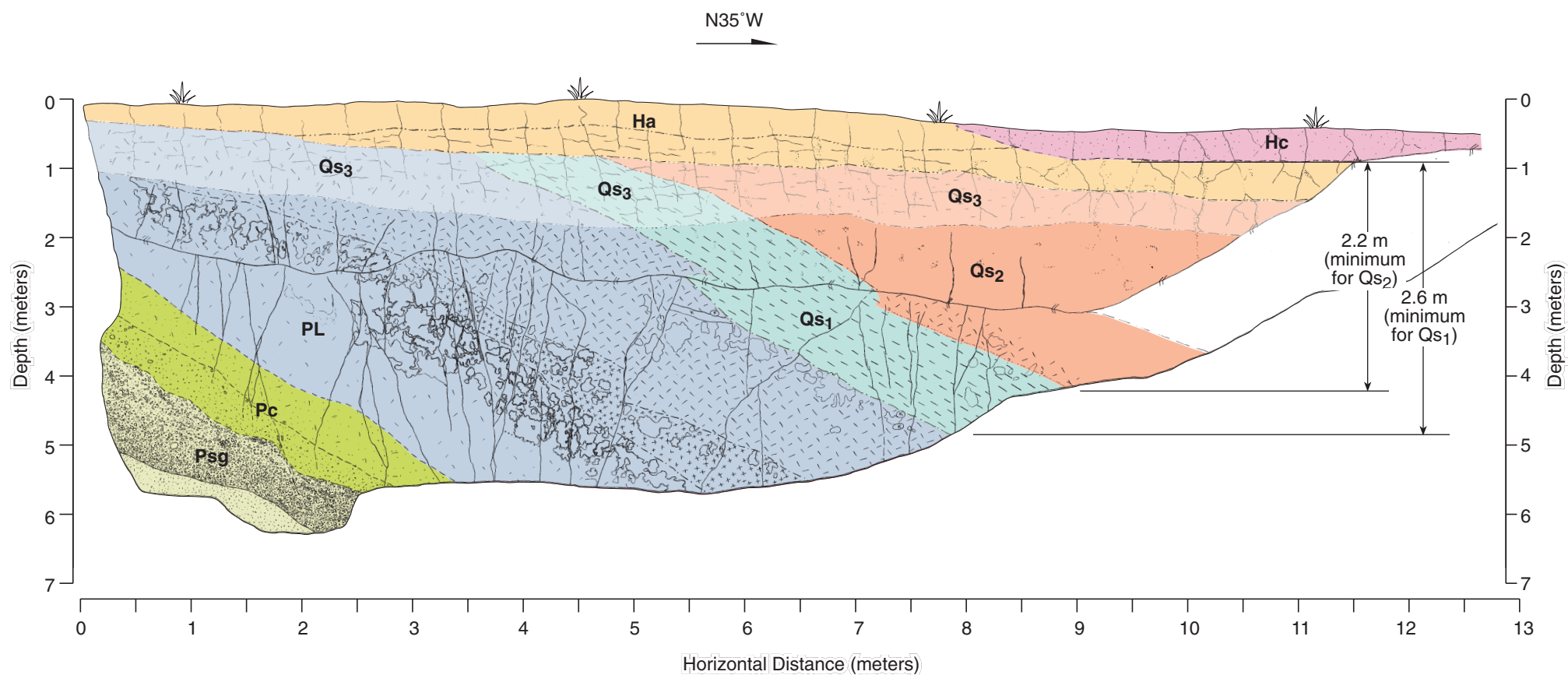
—	Fault
TL-1 ☒	Thermoluminescence sample location and designation (see Table 1)
Hc	Holocene colluvium
Ha/Hc	Holocene alluvium/colluvium
Qs₃	Middle to late Holocene paleosol/colluvium
Qs₁/Qs₂	Undifferentiated late Pleistocene to early Holocene paleosol
Qp	Pleistocene Peoria Loess
Pc	Pleistocene colluvium/reworked Mounds Gravel
Psg	Pleistocene reworked Mounds Gravel with occasional Sangamon Geosol
Tw	Eocene Wilcox Formation



COMMERCE GEOPHYSICAL LINEAMENT IDALIA, MISSOURI	
Trenches T-3 and T-4	
WZA  William Lettis & Associates, Inc.	Figure 10



Unit Descriptions		Unit Descriptions (continued)		Unit Descriptions (continued)		Unit Descriptions (continued)		Notes		Symbols	
A	Eocene Wilcox Formation White (10YR 6/4) medium- to coarse-grained sand; unit consists of banded or "tiger-striped" red and white sand with strong FeO ₂ staining; well-sorted; generally massive, firm to friable; contains fine FeO ₂ stained laminae; saturated at northwest end of trench; no basal contact observed.	F	Holocene alluvial fan deposits Interbedded strong brown (7.5YR 5/6 to 10YR 5/4) fine-grained sand with lenticular lenses of reddish brown gravelly sand (strong brown fine-grained sand is diagnostic of the basal part of the unit); massive to slightly bedded with sand and fine gravel; fines upsection to a massive silty sand; gravelly sand lenses are matrix supported; gravel contains chert; grades laterally into silty sand, but also represents an unconformity in places. strong FeO ₂ staining especially in upper part of the unit; clear basal contact along much of its length.	L	Holocene channel deposits White fine- to medium-grained sand with reddish brown (7.5YR5/6) silt laminae and gravel of 1 to 3 cm in thickness; well-bedded and prominent cross-bedding; concentration of pebbles common in thin lenses; FeO ₂ and MnO ₂ staining along bedding planes; gravel clasts up to 10 cm long and rare rip-up clasts of Porter Creek clay; contains a diagnostic strong brown basal sand; fines upward and becomes coarser-grained to north; clear basal contact that unconformably overlies Holocene alluvium.	R	Holocene colluvium Dark brown to yellowish brown (10YR 5/6) silty fine- to medium-grained sand with gravel; several discontinuous stone lines present in the middle section of the unit; gradesto east to fine-grained sand to silty sand; vertical grayish white silt vienlets or "bleached zones" cut across unit; contains <10% randomly distributed fine gravel; basal contact is gradational and wavy across 6 to 10 cm.	①	N12°W, 40° NE bedding between Tertiary Wilcox Fm and reworked Mounds Gravel.	⊗	Soil sample location and designation (see Appendix C)
B	Pleistocene Rework Mounds Gravel Strong reddish brown (7.5YR 5/8) clayey silty gravel; well-rounded pebbles within a clayey matrix; poorly sorted; massive; little or no relict bedding; cohesive; clasts consist predominantly of chert and < 2 cm in diameter; faint Sangamon paleosol preserved in gravel(?); clear basal contact that unconformably overlies Wilcox Formation.	G	Holocene alluvial fan deposits Strong brown (7.5 YR 4/6) sandy gravel to gravelly sand; contains medium to coarse, rounded to subrounded gravel; matrix supported by a silty to clayey sand; discontinuous to lenticular; unit becomes truncated to north by younger channel sequences; clear erosional basal contact, wavy to undulatory.	M	Holocene overbank deposits Yellowish-brown sandy silt to silty sand with occasional fine gravel (reworked Mounds Gravel) with abundant chert clasts; massive and fines upward; contains subvertical streaks of greyish-white silt stringers or "bleached zones"; faint MnO ₂ staining; moderate soil development; clear to gradational and smooth basal contact.	Scol	Holocene colluvium Dark brown (7.5YR 4/4) silty sand with trace of clay and 10 to 15% gravel; gravel up to 2 cm long; massive and fines upward; contains 5-10 mm diameter friable MnO ₂ nodules; faint light silty blotches; gradational wavy basal contact.	②	N40°E, 3°NE trend and plunge of fold axis	RC-11	Radiocarbon sample location and designation (see Table 1)
C	Pleistocene Peoria Loess Strong reddish brown (7.5YR 5/8) silt with a trace of clay; massive; hard to very stiff; moderate amount of FeO ₂ and MnO ₂ staining, but less than overlying reworked loess (Unit D); contains abundant near-vertical silt vienlets; rare vertical vienlets contain clean sand derived from underlying Wilcox Formation; near basal contact loess contains trace of fine gravel presumably from former ground surface (i.e., loess mantles surface); unit appears to conformably drape underlying reworked Mounds Gravel (Unit B).	H	Holocene alluvial fan deposits Yellowish brown (10YR 5/6) sandy silt (20% fine-grained sand) and trace of fine gravel; faint planar bedding from fine-grained sand laminae; mottled with fine to medium MnO ₂ black blotches; subvertical streaks of FeO ₂ and whitish reduction zones; interpreted, in part, as a buried soil; clear basal contact that conformably drapes underlying coarse alluvial fan deposit.	N	Holocene channel deposit White medium- to coarse-grained sand, well to moderately sorted with thin discontinuous lenses of silty sand; prominent lenticular white sand channel; cross-bedded and fines upward; coarse-grained sand and gravel concentrated near base of unit; contains a basal red sand between 3 to 5 cm thick; basal contact is clear smooth and wavy; unconformably cuts into underlying overbank deposits of Unit M.	S1	Holocene channel deposits White fine- to medium-grained sand; fines upward into silty sand to sandy silt; weak concentration of coarse-grained sand and pebbles; very friable; no cross-bedding; clear to sharp basal contact that cuts into underlying fine-grained units; appears to grade laterally to the south into a silty facies; this unit is contemporaneous with overbank deposits that cover much of the site.	③	0.20 to 0.30 m apparent vertical separation (north side up) of reworked Mounds Gravel	Channel Orientations A1 Unit L Channel margin S18°W A2 Unit K Channel margin S42°W A3 Unit N Channel margin S30°W A4 Unit L Channel margin S37°E A5 Unit N Channel margin S32°W A6 Unit J Channel margin S58°E A7 Unit S1 Channel thalweg S07°W A8 Unit J Channel margin S12°W	
D	Reworked Peoria Loess Strong reddish brown (7.5YR 5/8) silt with trace of fine sand and clay; generally massive; however contains rare faint stone line near Station 8 m and contains traces of fine sand and gravel to the south near the basal contact; very soft; strongly mottled (dark yellowish brown [10YR 4/4] to pale brown [10YR 6/3]); spherical reduction and oxidation zones throughout; common vertical silt vienlets or bleached zones that anastomose laterally and vertically; based on darker color, strong staining, and an increase in clay (10 to 20%) content, the upper part of the unit also interpreted as a buried soil horizon; basal contact is clear to gradational, planar and wavy.	I	Holocene channel deposit Strong brown silty sand and medium- to coarse-grained sand with fine gravel; dominated by lenticular interbeds of sand, silty sand and clayey sand, as well as occasional clean white sand; coarse-grained deposits separated by silty sand and silt laminae; some cross-bedding; massive; rare round rip-up clasts of Porter Creek clay; weak FeO ₂ and MnO ₂ staining; channel deposits are draped by a mottled yellowish-brown to light brownish gray sand to silty sand with rare coarse sand and pebbles; faint FeO ₂ and MnO ₂ stains as well as "blotchy" gray reduced zones; clear basal contact cuts into reworked Peoria Loess.	O	Holocene overbank deposits Sandy and clayey silt to silt (7.5 YR 5/4 to 5/6) with trace of gravel; 10 to 15% clay; 10 to 20% fine-grained sand; massive; fine gray mottling as well as black to dark brown MnO ₂ nodules and FeO ₂ zones of oxidation that fines subvertical and planar vienlets of bleached zones; basal contact is clear to gradational, smooth and wavy.	S2	Holocene channel deposits White fine- to medium-grained sand with mottled (7.5YR 4/4) sections; fines upward into silty sand to sandy silt; weak concentration of coarse-grained sand and pebbles; no cross-bedding; clear to sharp basal contact that cuts into underlying fine-grained units; appears to grade laterally to the south into a silty facies.	④	Two variations of fill within vertical skeltans or "bleached" zones: a. grayish white anastomosing vienlets in loess that contain sandy silt b. reddish-brown fine-grained sand cutting across loess (rare)		
E	Holocene channel deposits Dark reddish brown to reddish brown interbedded silt, silty fine-grained sand, and fine- to medium-grained sand, silt units contain <10% clay; FeO ₂ and MnO ₂ staining common; basal contacts of interbeds clear to abrupt and smooth.	J	Holocene channel deposit White (10YR 6/4) medium- to coarse-grained sand with lenses of strong brown (7.5YR 4/6) silty sand; occasional pockets of fine pebbly gravel derived from reworked Mounds Gravel and coarse-grained sand; fines upward into a silty sand with poorly bedded white sand channels and relict sand lenses; MnO ₂ staining along bedding and coats some clasts; contains pedogenic clay near base of unit; faint FeO ₂ and MnO ₂ mottling suggests pedogenic soil development; basal contact clear and wavy.	P	Holocene channel deposit Relatively clean white to slightly mottled orangish brown fine-grained sand with trace of coarse granules and fine gravel; massive, lenticular, truncates several vertical silt vienlets or "bleached zones"; does not appear to be linked with underlying sand bodies suggesting unrelated to liquefaction; clear basal contact.	S3	Holocene channel deposits Silty sand to fine-grained sand with thin gravel laminations; fines upward into a silty sand as it grades into overlying overbank deposits; weak planar bedding of coarse-grained sand and gravel near base of unit; clean to abrupt basal contact.	⑤	Wide fracture of silty fine- to medium-grained sand that projects upward to base of Unit P, where it appears to be truncated (soil samples 1 and 2 collected at this location).		
E	Holocene alluvium Strong brown (7.5YR 5/6; 10YR 5/6 to 5/4) gravelly silty sand; 10 to 15% fine to medium gravel; clasts derived from Mounds Gravel; trace to 15% clay interpreted as poorly developed paleosol that is truncated by overlying Holocene alluvium (Units P and Q) and colluvium (Unit R); moderately to strongly mottled from FeO ₂ and MnO ₂ staining; basal contact often noted by a thin discontinuous stone-line of pebbles; clear to gradational basal contact that unconformably overlies reworked Peoria loess. To the southeast, unit grades to a yellowish brown to light brown sandy silt with 10 to 15% clay; increase in sand content with depth to a silty fine- to medium-grained sand; <10% fine gravel and granules; generally massive but contains faint planar bedding and rare discontinuous stonelines near base, as well as a thin (1cm thick) fine-grained sand stinger near top of unit; strongly mottled with strong MnO ₂ nodules giving the unit a speckled appearance; unit often truncates vertical silt vienlets or "bleached zones" developed in Unit D; note that numerous vertical silt vienlets also cut across unit suggesting separate development histories; irregularly shaped patterns from FeO ₂ and MnO ₂ staining.	K	Holocene channel deposits Interbedded white "sugar" sand and strong reddish brown sand with lenticular yellowish brown sandy silt laminae; concentration of pebbles common in thin lenses; well-bedded; FeO ₂ -MnO ₂ staining along bedding planes and coats pebbles; pebbles typically rounded and <1cm in diameter; upsection unit becomes mottled, yellowish brown (10YR 5/6 to 5/4) silty fine-grained sand to sandy silt (appears to resemble reworked Peoria loess); relict sand and fine gravel lenses 2 to 3 cm thick, otherwise massive; charcoal common; clear and wavy basal contact.	Q	Holocene colluvial deposits Reddish-brown (7.5YR 5/6) silty fine- to medium-grained sand with 10 to 15% gravel; FeO ₂ staining common; gravel content increases near buried break-in-slope and decreases to south; subvertical grayish white silt vienlets scattered throughout unit; contains <10% fine gravel dispersed throughout unit; fines upsection as it approaches B-horizon of Unit R; base of unit is defined by a silty medium-grained sand; unconformably overlies Units E and P; clear to gradational basal contact.	Sall	Holocene alluvium (distal fan and overbank deposits) Yellowish brown sandy silt with faint dark mottling from MnO ₂ staining; massive but with concentration of fine sand and trace gravel at base; light grey mottling from skeltans common; basal contact is gradual and smooth.	⑥	Bowl-shaped feature consisting of sandy silt with reduced gray and iron oxide mottles; shape of feature suggestive of liquefaction feature; however no source identified.		
								⑦	Three-dimensional view of skeltans showing anastomosing and planar nature of fractures.		
								⑧	Sandy silt dike-like feature with coarse-grained sand and granules (liquefaction-related dike or skeltan)		
								⑨	Silty vienlets a. larger more continuous skeltans continue across Units D, E, and Q into younger overlying colluvium and alluvium. b. Numerous silty vienlets truncated by Unit E; lesser truncations at Units P, Q and O. c. Most prominent and prevalent fractures located in northern end of trench.		
								⑩	No fault observed at Tertiary Wilcox and Pleistocene loess contact prior to submergence.		
								⑪	Equivalent alluvial fan units project south across trench.		



Explanation

Ha	Holocene alluvium	PL	Pleistocene Peoria Loess
Hc	Holocene colluvium	Pc	Pleistocene colluvium/reworked Mounds Gravel
Qs3	Middle to late Holocene paleosol/colluvium	Psg	Pleistocene reworked Mounds Gravel with occasional Sangamon Geosol
Qs2	Late Pleistocene to early Holocene paleosol	Tw	Eocene Wilcox Formation
Qs1	Late Pleistocene to early Holocene paleosol		

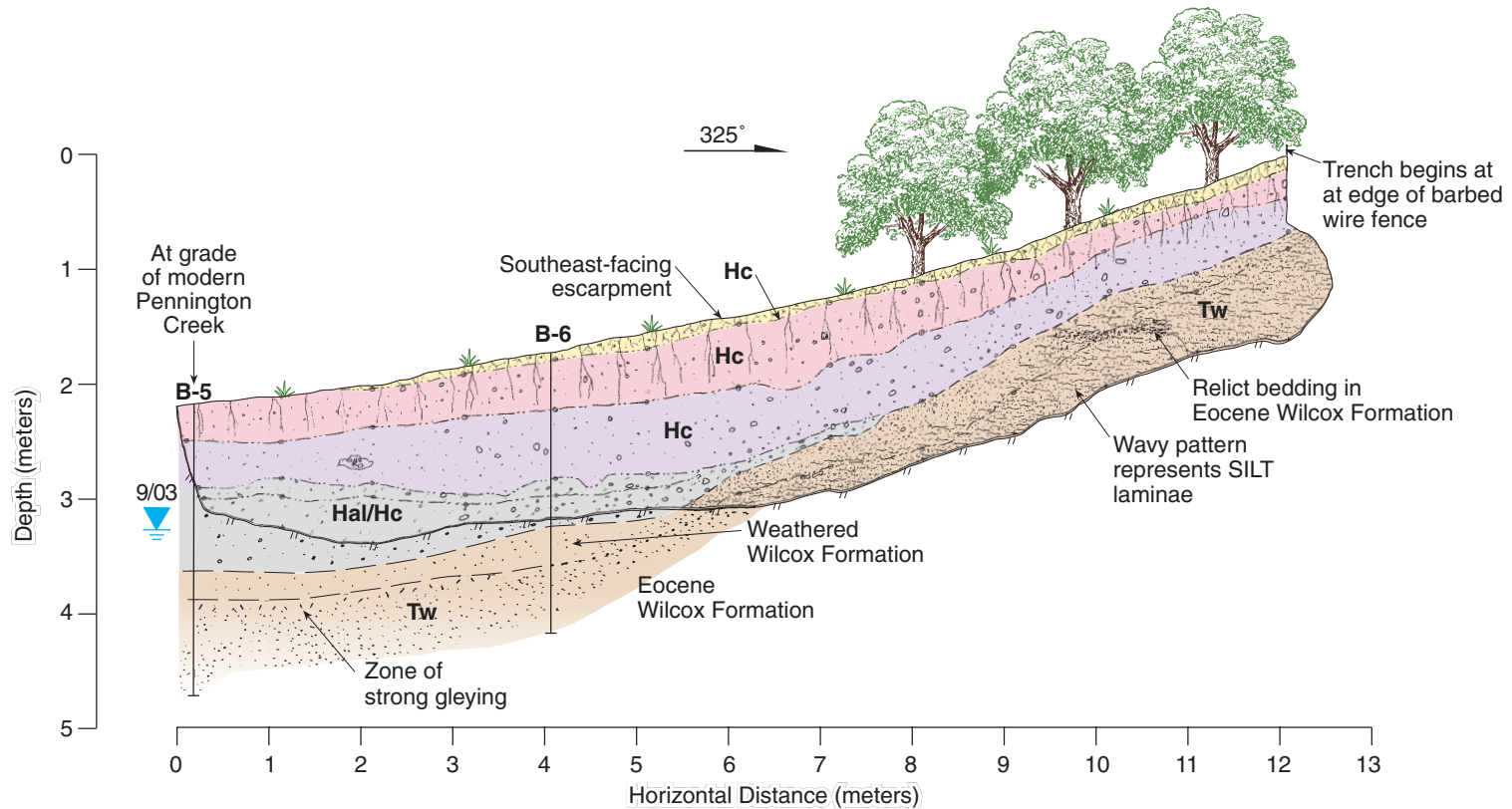
COMMERCE GEOPHYSICAL LINEAMENT
IDALIA, MISSOURI

Trench T-6



William Lettis & Associates, Inc.

Figure 12



Explanation

- Hc** Modern colluvial soil
Dark brown to black modern soil (10YR 4/4) check; silty sand with abundant roots; gravel randomly distributed throughout unit; massive; fines downslope.
- Hc** Upper Holocene colluvium with soil development
Dark brown (10YR 4/4) silty sand with gravel (<15%); fines upsection and downslope; massive; increase in clay content with pedogenic Bt horizon; gradational basal contact over 10 cm downslope and 5 cm upslope; roots common.
- Hc** Middle Holocene colluvial deposit
Strong brown (10YR 6/3) fine sand with trace of silt and 15 to 30% gravel; gravel content decreases downslope; predominantly pebble-sized gravel with few cobbles; massive; some gravel appear to dip downslope (faint imbrication); lower basal contact is gradational over 10 cm; trace of FeO₂ staining and faint "tiger stripe" laminae near contact with weathered bedrock; pebbles concentrated along slope and decrease to the southeast.

- Hal/Hc** Oldest Holocene colluvial unit (base of trench in water)
Strongly mottled grey to yellow-brown (10YR 6/2), fine- to medium-grained sand with gravel (<20%) and clay (5 to 10%); gravel is coated with FeO₂ staining; massive; fines toward the southeast (distal); gray color is from groundwater; weathered colluvium influenced by shallow water table; unconformable basal contact is gradational across about 6 cm.
- Tw** Weathered Wilcox Formation
Mixed light brown to strong brown (10YR 6/4) fine sand with trace of silt; contains randomly oriented distributed pebbles; 10 to 15 % gravel; slightly more cohesive than underlying unit because of greater silt content; gradational weathering contact 6 to 10 cm.
- Tw** Eocene Wilcox Formation-Holly Springs
White fine- to medium-grained sand (10YR 6/4), sugar texture; well sorted with <10% gravel; massive "tiger stripe" weathering pattern as thin silty 0.5 to 1.0 cm thick laminae; coarsens upsection; generally massive but has relict horizontal bedding(?) preserved as a thin discontinuous fine gravel lens; very loose and unconsolidated.

COMMERCE GEOPHYSICAL LINEAMENT
IDALIA, MISSOURI

Trench T-7



William Lettis & Associates, Inc.

Figure 13

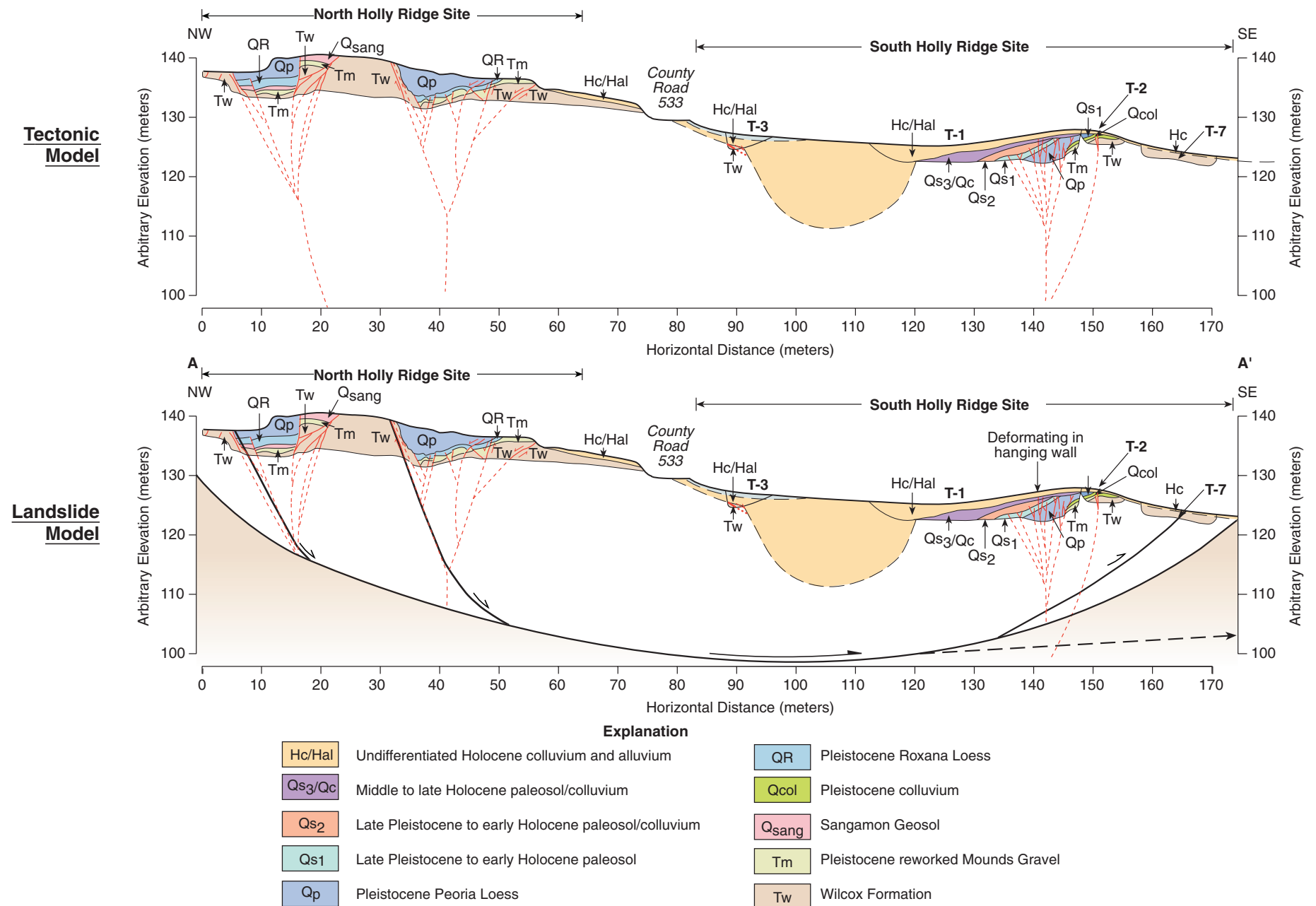


Figure 14. Schematic cross section A-A' across North and South Holly Ridge sites showing shallow surface faults connecting with faults interpreted from seismic profiles HR-1 and HR-2. See Figure 6 for section location. Tectonic model assumes deformation as primary tectonic deformation. Landslide model assumes faulting interpreted at both sites is related to landsliding.

APPENDIX A

DETAILED PEDOLOGIC DESCRIPTIONS OF TRENCH T-5

Soil Profile T-5A; Site description: Gentle southeast dipping alluvial fan surface with grasses.
Profile is from the north wall of Trench T-5 at station 8 m. Described by J. D. Vaughn 7/18-19/03. See log of T-5 for location.

Horizon	Depth (cm)	Horizon boundary	Munsell Color		Structure	% Gravel	Consistence Moist	Texture	Clay films	%Clay (est.)	Notes
			Moist	Mottles							
Ap	0-15	cs	10YR 4/3		wk., fine, gran.	<2%	friable	sandy loam	few reworked; on pebbles	14-15	sand is well graded from alluvial/colluvial material
BA	15-27	gs	10YR 4/4; (10YR4/3 tongues)		wk., fine, gran.	<2%	friable	loam	none	15	scattered worm c pebs derived from Wilcox and Mou alluvial/colluvial
B1	27-52	gs	10YR 4/6	10YR 5/4; 10YR 6/3 and 6/4	wk.; fine to med. subang. Blocky	<1%	friable to slightly firm	loam	few, thin on ped faces and pores	16-17	few worm casts;
Bt1	52-83	gs	7.5YR 4/4	10YR 6/3 to 6/4	wk.; fine to med. subang. Blocky	<2%	slightly firm	loam	thin on ped faces and pores	18-20	common fn-med. patchy clay
Bt2 & E	83-140	cs	10YR 4/4; 10YR 6/3 and 6/4	10YR 6/3; 6/4; 6/2	wk.; fine to med. subang. Blocky	n/a	firm to friable	loam	patchy thin on some peds and pores	16-18	Bt2 is being destroyed by eluviation; 1-10 cm tongues of 10YR 6/4 loam every 20 cm
2Bt1b	140-160	gs	10YR 5/4 and 4/4	common 10YR 6/1 and 6/2	wk.; fine to med. subang. Blocky	n/a	firm	silt loam	thin patchy on ped faces; med. continuous on pores	20-22	Buried soil horizon; few black (10YR 4/4) stains on peds; very few cracks with 10YR 5/4 silt; 10-30 cm wide
2Bt2b	160-188	gs	7.5YR 4/4; 10YR 6/1 and 6/2		wk.; fine to med. subang. Blocky	n/a	firm	silt loam	thin patchy on ped faces; med. continuous on pores	18	Few fn to med. b (10YR2/1) Mn stains <5% Tm pebs and grains in lower section
3Bt3b	188-213	gs	10YR 4/4; 10YR 6/1 and 6/2	common 7.5YR 4/6	wk., fine subang. Blocky to massive	n/a	firm	loam	few on pores and peds; thick on vesic. Pores	16	Reworked loess/loam common black (10YR 4/4) stains and soft no 10YR6/1 and 6/2 20cm wide; krotos
3Bt4b	213-241	as	7.5YR 4/6; 10YR 6/1		wk., fine to med. subang. Blocky	n/a	firm	loam	few on pores and peds; thick on vesic. Pores	18-20	Few fn Fe-Mn so stains; krotos and above; loess. Mo

Bottom of trench @ 300 cm

TABLE A-2: SOIL PROFILE DESCRIPTION FOR TRENCH T-5 (Central Part): South Holly Ridge site, Idalia, Missouri.

Soil Profile T-5B; Site description: Gentle southeast dipping alluvial fan surface with grasses.

Profile is from the north wall of Trench T-5 at station 44.5 m. Described by J. D. Vaughn 7/14/03.; BOT probed between 304 and 444 cm.

Classification: Coarse loamy to fine loamy, mixed, thermic, Typic Hapludlfs.

Horizon	Depth (cm)	Horizon boundary	Munsell Color		Structure	Consistence Moist	Texture	Clay films	%Clay (est.)	Roots	Pores	Notes	Corresponding Unit
			Moist	Mottles									
Ap	0-18	as	10YR 4/3	n/a	1f-m gr	n/a	sandy loam	none	not noted	3 f-m grass and herbs	n/a	none	Unit Sall (Plow Zone)
B1	18-28	cs	10YR 5/6; w/4/3 -4/4)	n/a	1m sbk & 1fgr	n/a	sandy loam	none	not noted	2 f-m grass roots	1 f tub	none	Unit Sall
Bt1	28-57	gs	7.5YR 4/6	n/a	1f-m sbk	n/a	loam	1 thin patchy on peds and tub. Pores	not noted	2 fine	1 f tub	MnO stains on peds (2-3); 10YR 2/1 and 3/1	Unit Sall
Bt2	57-84	gs	7.5YR 5/6	n/a	1f-m sbk	n/a	loam	1 thin patchy on peds and tubular pores	not noted	1 fine	1 f tub	MnO stains on peds (2-3); 10YR 2/1 and 3/1	Unit Sall
2Bt3	84-123	gs to gw	7.5YR 4/4	n/a	1f-m sbk	n/a	sandy loam	2 thin patchy on peds and in pores	not noted	1 fine to very fine	2 vf-f tub and 1 m ves.	(1-2) dark MnO stains on peds	Unit Sall
2Bt4	123-149	cs	10YR 4/4 to 5/4	10YR 6/2 to 6/4; 7.5YR 5/6	1f-m sbk	n/a	loam	2 thin patchy on peds and in pores	not noted	1 fine	2 vf-f tub	(1-2) dark MnO stains on peds; 1 f in pores; 1 f Fe-Mn soft nod	Unit H
2Bt5	149-168	cs	7.5YR 4/4	10YR 6/2 and 6/3	1m-c sbk to massive	n/a	gravelly loam	patcy on peds and pebbles; bridge grains	not noted	very few to f to vf	1 f-m tub and 1 f ves.	1 f m MnO stains (patchy); slightly gravelly to gravelly	Unit G
3Bt6	168-217	cs	7.5YR 4/4	10YR 6/3	1m-c sbk	n/a	sandy loam	bridge grains; 1 patchy on peds and in pores	not noted	none	1 f-m tub and 2 m-c ves.	1 f MnO stains	Unit F
4Bt1b	217-244	gs	7.5YR 4/4	10YR 6/2 to 6/3; 7.5YR 5/6	1f-m sbk	n/a	silty loam	1 patchy on peds; nearly continuous in pores	24-26	none	none	1 f-m black Fe-Mn stains	Unit E
4Bt2b	244-275	gs	7.5YR 4/6-5/6 and 6/2	n/a	1-2 f-m sbk	n/a	silty loam to loam	few thin patchy on some peds and in some pores	18-20	none	none	1 c-m 10YR 2/1 MnO stains on some peds and in some pores	Unit E
4Bt3b	275-304	gs	10YR 4/4	10YR 6/2 to 6/3	1f-m sbk	n/a	silty loam to loam	1 thin patcy on peds and in some pores	20	none	none	1 10YR 2/1 MnO stain on some peds and pores	Unit D
4Bt4b	304-341	n/a	10YR 4/4 to 5/4	10YR 6/2; 7.5YR 4/6	1f-m sbk	n/a	silty loam	1 thin patcy on peds and in some pores	22-26	none	none	Soil Probe: 1 10YR 2/1 MnO stain on some peds and pores	Unit D
4Bt5b	341-359	n/a	7.5YR 4/4	10YR 6/2 to 6/3	1f sbk	n/a	loam	1 thin patcy on peds and in some pores	not noted	none	none	Soil Probe: 1 f Fe-Mn nodules	Unit D
4Bt6b	359-432	n/a	7.5YR 4/4	10YR 6/2 to 6/3	1f sbk	n/a	loam to silty loam	1 thin patcy on peds and in some pores	not noted	none	none	Soil Probe:1 f Fe-Mn nodules	Unit D
5BC1b	432-444	n/a	7.5YR 4/4	10YR 6/2	1f sbk	n/a	sandy loam	n/a	not noted	none	none	Soil Probe: massive; dense and saturated	Unknown
Bottom of trench @ 304 cm													

SERVICE

PEDON DESCRIPTION

Print Date: 06/17/2004
Description Date: 09/30/2003
Describer: KD, LT, BB, RT

Site ID: 03M0207 022
Site Note:
Pedon ID: 03M0207 022
Pedon Note:
Lab Source ID: MCL Lab Pedon #: M0320719

Soil Name as Described/Sampled: Teksob
Soil Name as Correlated:
Classification: Fine-loamy, mixed, active, thermic Typic Hapludalfs

Pedon Type: Pedon Purpose: full pedon
description:
Taxon Kind:
Associated Soils:

Location Information:
Country:
State: Missouri
County: Stoddard
MLRA: 134 -- Southern Mississippi Valley Loess
Soil Survey Area: M0207 -- Stoddard County, Missouri
Map Unit: 6F -- Eustis-Memphis complex, 14 to 40 percent slopes
Quad Name: Dexter, Missouri

Location Description: Dexter Quad
Legal Description:

Latitude: degrees minutes seconds
Longitude: degrees minutes seconds
Datum: NAD83
UTM Zone: 16
UTM Easting: 243334 meters
UTM Northing: 4082630 meters

Physiographic Division:
Physiographic Province:
Physiographic Section:
State Physiographic Area:
Local Physiographic Area:

Geomorphic Setting: None Assigned
Upslope Shape: Cross Slope Shape:

Primary Earth Cover: Grass/herbaceous cover
Secondary Earth Cover: Tame pastureland
Plant Association Name:
Existing Vegetation:

Parent Material: loamy colluvium
Bedrock Kind:
Bedrock Depth:
Bedrock Hardness:
Bedrock Fracture Interval:

Surface Fragments:

Particle Size Control Section: 48 to 98 cm.

Diagnostic Features: argillic horizon 48 to 160 cm.

Top	Bottom	Restriction	Restriction
Depth (cm)	Depth (cm)	Kind	Hardness

Cont. Site ID: 03M0207 022

Pedon ID: 03M0207 022

Slope	Elevation	Aspect	MAAT	MSAT	MWAT	MAP	Frost-	Drainage
Slope	Upslope						Free Days	Class
Length	Length	(deg)	(C)	(C)	(C)	(mm)		
(%)	(meters)							
(meters)	(meters)							
5.0	111.3	190						well

Ap1--0 to 14 centimeters; brown (10YR 4/3) loam, pale brown (10YR 6/3), dry; moderate medium platy structure, and moderate fine subangular blocky structure; many very fine and fine roots; many very fine tubular pores; abrupt smooth boundary.

Ap2--14 to 48 centimeters; brown (7.5YR 4/4) loam; weak medium prismatic structure, and moderate fine and medium subangular blocky structure; many very fine and fine roots; many very fine and fine vesicular and common fine and medium tubular pores; clear smooth boundary.

Bt1--48 to 83 centimeters; dark yellowish brown (10YR 4/4) loam; weak medium prismatic structure, and moderate fine and medium subangular blocky structure; common very fine roots; common fine and medium tubular and many very fine vesicular pores; clear smooth boundary.

Bt2--83 to 106 centimeters; dark yellowish brown (10YR 4/4) silt loam; weak medium prismatic structure, and moderate fine and medium subangular blocky structure; common very

fine roots; many
very fine and fine vesicular and common fine and medium tubular pores; abrupt wavy
boundary.

Bt3--106 to 127 centimeters; dark yellowish brown (10YR 4/4) sandy clay loam;
moderate fine and
medium subangular blocky structure; many fine and medium tubular pores; abrupt wavy
boundary.

Bt4--127 to 160 centimeters; dark yellowish brown (10YR 4/4) clay loam; strong
medium prismatic
structure, and weak medium subangular blocky structure; many very fine and fine
tubular pores; 20
percent light gray (10YR 7/2) silt coats; 1 percent fine distinct black (10YR 2/1)
manganese masses
and 2 percent fine distinct light brownish gray (10YR 6/2) iron depletions and 5
percent fine
distinct strong brown (7.5YR 5/6) masses of oxidized iron; abrupt wavy boundary.

BC1--160 to 183 centimeters; light yellowish brown (10YR 6/4) loamy sand; single
grain; many fine
tubular pores; 1 percent fine prominent black (10YR 2/1) manganese masses and 2
percent fine
distinct light brownish gray (10YR 6/2) iron depletions and 10 percent medium
distinct strong brown
(7.5YR 5/6) masses of oxidized iron; abrupt wavy boundary.

BC2--183 to 203 centimeters; yellowish brown (10YR 5/4) silt loam; moderate medium
subangular blocky
structure; many very fine and fine vesicular and many very fine and fine tubular
pores; 1 percent
fine distinct black (10YR 2/1) manganese masses and 2 percent fine distinct light
brownish gray
(10YR 6/2) iron depletions and 10 percent medium distinct strong brown (7.5YR 5/6)
masses of
oxidized iron.

USDA - NATURAL RESOURCES CONSERVATION

SERVICE

PEDON DESCRIPTION

Print Date: 06/17/2004
Description Date: 09/30/2003
Describer: KG

Site ID: 03M0207 023
Site Note:
Pedon ID: 03M0207 023
Pedon Note:
Lab Source ID: MCL Lab Pedon #: M0320720

Soil Name as Described/Sampled: Teksob
Soil Name as Correlated:
Classification: Fine-loamy, mixed, active, thermic Typic Hapludalfs

Pedon Type: Pedon Purpose: full pedon
description
Taxon Kind:
Associated Soils:

Location Information:
Country:
State: Missouri

Slope		Elevation	Aspect	i d a l i a u s d a s o i l s . t x t				Frost- Free Days	Drai nage Cl ass
Slope	Upslope	Length (%)		Length (meters)	MAAT (C)	MSAT (C)	MWAT (C)		
5.0	109.7	190							well

Ap--0 to 10 centimeters; grayish brown (10YR 5/2) loam, pale brown (10YR 6/3), dry; moderate fine and medium subangular blocky structure; friable; many very fine and fine roots; many fine interstitial pores; abrupt smooth boundary.

BA--10 to 28 centimeters; dark yellowish brown (10YR 4/4) loam; moderate medium subangular blocky structure; friable; common very fine and fine roots; many very fine and fine tubular pores; clear smooth boundary.

Bt1--28 to 64 centimeters; dark yellowish brown (10YR 4/4) sandy clay loam; moderate medium subangular blocky structure; friable; common very fine and fine roots; many very fine and fine tubular pores; 10 percent prominent brown (7.5YR 4/4) clay films; clear smooth boundary.

Bt2--64 to 86 centimeters; dark yellowish brown (10YR 4/4) sandy clay loam; moderate medium prismatic structure parting to moderate medium subangular blocky structure; firm; few very fine and fine roots; many very fine and fine tubular pores; clear smooth boundary.

Bt3--86 to 107 centimeters; yellowish brown (10YR 5/4) sandy clay loam; moderate medium prismatic structure parting to moderate medium subangular blocky structure; firm; few very fine and fine roots; many very fine and fine tubular pores; 1 percent well rounded 2- to 5-millimeter chert fragments; clear smooth boundary.

Bt4--107 to 140 centimeters; dark yellowish brown (10YR 4/6) silt loam; weak medium
 and coarse
 prismatic structure parting to moderate medium subangular blocky structure; firm;
 few very fine
 roots; many fine tubular and few medium tubular pores; 1 percent distinct yellowish
 brown (10YR 5/4)
 clay films; 1 percent fine and medium prominent black (10YR 2/1) iron-manganese
 masses and 4 percent
 fine prominent light brownish gray (10YR 6/2) iron depletions; clear smooth
 boundary.

Bt5--140 to 178 centimeters; dark yellowish brown (10YR 4/6) silt loam; weak medium and coarse prismatic structure parting to moderate medium subangular blocky structure; firm;

many fine tubular
and few medium tubular pores; 5 percent distinct yellowish brown (10YR 5/4) clay
films; clear smooth
boundary.

BC--178 to 203 centimeters; dark yellowish brown (10YR 4/6) loam; weak medium and
coarse prismatic
structure parting to moderate medium subangular blocky structure; firm; 1 percent
well rounded 2- to
5-millimeter chert fragments.

USDA - NATURAL RESOURCES CONSERVATION

SERVICE

PEDON DESCRIPTION

Print Date: 06/17/2004
Description Date: 10/02/2003
Describer: RT, BB

Site ID: 03M0207 024
Site Note:
Pedon ID: 03M0207 024
Pedon Note:
Lab Source ID: MCL Lab Pedon #: M0320721

Soil Name as Described/Sampled: Teksob
Soil Name as Correlated:
Classification: Fine-loamy, mixed, active, thermic Typic Hapludal fs

Pedon Type: Pedon Purpose: full pedon
description
Taxon Kind:
Associated Soils:

Location Information:
Country:
State: Missouri
County: Stoddard
MLRA: 131 -- Southern Mississippi Valley Alluvium
Soil Survey Area: M0207 -- Stoddard County, Missouri
Map Unit: 74B -- Malden sand, 0 to 4 percent slopes
Quad Name: Dexter, Missouri

Location Description: Dexter Quad
Legal Description:

Latitude: degrees minutes seconds
Longitude: degrees minutes seconds
Datum: NAD83
UTM Zone: 16
UTM Easting: 243533 meters
UTM Northing: 4082582 meters

Physiographic Division:
Physiographic Province:
Physiographic Section:
State Physiographic Area:
Local Physiographic Area:

Geomorphic Setting: None Assigned
Upslope Shape: Cross Slope Shape:

Primary Earth Cover: Grass/herbaceous cover

Secondary Earth Cover: Tame pastureland
 Plant Association Name:
 Existing Vegetation:

Parent Material: loamy colluvium
 Bedrock Kind:
 Bedrock Depth:
 Bedrock Hardness:
 Bedrock Fracture Interval:

Surface Fragments:

Particle Size Control Section: 8 to 58 cm.

Diagnostic Features: ? to ? cm.

Top	Bottom	Restriction	Restriction
Depth (cm)	Depth (cm)	Kind	Hardness

Cont. Site ID: 03M0207 024

Pedon ID: 03M0207 024

Slope	Elevation	Aspect	MAAT	MSAT	MWAT	MAP	Frost-Free Days	Drainage Class
Slope	Upslope							
Length (%)	Length (meters)	(deg)	(C)	(C)	(C)	(mm)		
(meters)	(meters)							
6.0	103.6	95						well

Ap--0 to 8 centimeters; brown (10YR 4/3) fine sandy loam, brown (10YR 5/3), dry; weak fine granular structure; friable; many very fine and fine roots; many very fine and fine tubular pores; abrupt smooth boundary.

Bt1--8 to 43 centimeters; dark yellowish brown (10YR 4/4) loam; moderate fine subangular blocky structure; friable; many very fine and fine roots; many very fine and fine tubular pores; 10 percent

distinct brown (10YR 4/3) organic stains; clear smooth boundary.

Bt2--43 to 69 centimeters; dark yellowish brown (10YR 4/4) fine sandy loam; moderate fine and medium subangular blocky structure; friable; many very fine and fine roots; many very fine and fine tubular pores; 5 percent distinct brown (10YR 4/3) organic stains; clear smooth boundary.

Bt3--69 to 91 centimeters; brown (10YR 4/3) silt loam; moderate fine and medium subangular blocky structure; firm; common very fine roots; many very fine and fine tubular pores; 10 percent prominent light gray (10YR 7/1) sand coats; clear smooth boundary.

Bt4--91 to 117 centimeters; 60 percent yellowish brown (10YR 5/6) and 40 percent dark yellowish brown (10YR 4/4) silt loam; weak medium prismatic structure parting to moderate fine subangular blocky structure; firm; common very fine roots; many very fine and fine tubular pores; 10 percent prominent light gray (10YR 7/1) sand coats; gradual smooth boundary.

Bt5--117 to 145 centimeters; dark yellowish brown (10YR 4/4) loam; weak medium prismatic structure parting to moderate fine subangular blocky structure; firm; few very fine roots; many very fine and fine tubular pores; 10 percent prominent light gray (10YR 7/1) sand coats; clear smooth boundary.

Bt6--145 to 165 centimeters; dark yellowish brown (10YR 4/4) fine sandy loam; weak medium subangular blocky structure; friable; many very fine and fine tubular pores; 10 percent prominent light gray (10YR 7/1) sand coats; 2 percent well rounded 2- to 5-millimeter chert fragments; clear smooth boundary.

Bt7--165 to 180 centimeters; dark yellowish brown (10YR 4/4) fine sandy loam; weak medium subangular blocky structure; friable; many very fine vesicular pores; 2 percent well rounded 2- to 5-millimeter chert fragments; clear smooth boundary.

BC--180 to 213 centimeters; dark yellowish brown (10YR 4/4) loam; weak medium prismatic structure parting to moderate medium subangular blocky structure; firm; many very fine and fine tubular pores; 3 percent prominent light gray (10YR 7/1) sand coats; gradual smooth boundary.

C1--213 to 244 centimeters; dark yellowish brown (10YR 4/4) sandy loam; weak medium subangular blocky structure; friable; many very fine and fine tubular pores; 5 percent prominent light gray (10YR 7/1) sand coats; 1 percent well rounded 2- to 5-millimeter chert fragments; gradual smooth boundary.

C2--244 to 279 centimeters; dark yellowish brown (10YR 4/4) sandy loam; weak medium subangular blocky structure; friable; many very fine and fine tubular pores; 5 percent prominent light gray (10YR 7/1) sand coats; gradual smooth boundary.

idalia usda soils.txt

C3--279 to 305 centimeters; dark yellowish brown (10YR 4/4) sandy loam; weak medium subangular blocky structure; friable; many very fine and fine tubular pores; 5 percent prominent light gray (10YR 7/1) sand coats.

APPENDIX B

RESULTS OF PARTICLE SIZE ANALYSES

MOISTURE CONTENT AND DRY DENSITY

Client Name: WILLIAM ZETTIS & ASSOC
 Project Name: COMMENCE GEOPHYSICAL LINEAMENT
 Client Project No: 1573

oven dry 50.0g taken for Hyd before take off
 CF = 1140
 MATL
 DRY WT OF #40 MATL

Date Sampled: _____ Date Received: _____
 Date Tested: 9/16/03
 Tested by: RLF

Boring No.	Depth (ft)	Sample Length (in)	Sample Diameter (in)	Cup No.	Cup Weight (g)	Wet Weight + Cup (g)	Dry Weight + Cup (g)	Sample Dry Density (pcf)	Moisture Content (%)	Material Description (Soil type is based on visual/manual examination; classification test results may modify soil type.)
T-5	#1		+40 -40 P-5	F-409 F-307		TARE	50.0 + 215.7 - 16.0	249.7g		YEL BR (10YR 5/4) W/LT YEL BRN (10YR 6/4) AND YEL BRN (10YR 5/6) SANDY SILT (ML) VFG SAND
T-5	#2		+40 -40 P-6	F-406 F-201			50.0 + 211.3 - 16.5	241.8		DK YEL BRN (10YR 4/4) W/YEL BRN (10YR 5/4) CLAYEY SILT (ML/CL) TR VFG SAND
T-5	#3		+40 EXTRA (3) -40 P-2	F-401 F-308			50.0 + 192.7 - 16.0	220.7		YEL BRN (10YR 5/4) W/DK YEL BRN (10YR 4/4) AND PALE BRN (10YR 6/3) SILT (ML) DK YEL BRN (10YR 4/4) VARI ?
T-5	#4		+40 EXTRA (3) -40 P-1	F-400 F-310			50.0 + 210.0 - 16.0	241.0		DK YEL BRN (10YR 4/4) W/PALE BRN (10YR 6/3) AND YEL BRN (10YR 5/4) CLAYEY SILT (ML/CL)
COMMENTS										
	#1			#1						SMALL DK YEL BRN MOD CLAY FRAG SLID TO BREAK / CRUNCH W/FINGERS BEDDING APPARENT, WEATH SILTSTONE?
	#2			#2						
	#3			#3						

Client: William Lettis and Associates
Project: Commerce Geophysical Lineament
Project No.: 1573

can no.	Plastic Limit			Liquid Limit				
wet soil + can (g)	44.2	43.2		26.7	24.1	22.3		
dry soil + can (g)	38.2	37.3		21.9	19.8	18.3		
can (g)	3.5	3.5		3.5	3.5	3.5		
dry soil (g)	34.7	33.8	0.0	18.4	16.3	14.8	0.0	0.0
moisture (g)	6.0	5.9	0.0	4.8	4.3	4.0	0.0	0.0
water content (%)	0.173	0.175	#DIV/0!	0.261	0.264	0.270	#DIV/0!	#DIV/0!

	Plastic Limit			Liquid Limit				
can no.								
wet soil + can (g)	23.7	35.6		26.6	22.2	23.1	26.0	
dry soil + can (g)	20.2	31.0		20.1	16.8	17.3	19.1	
can (g)	3.5	7.9		3.5	3.5	3.5	3.5	
dry soil (g)	16.7	23.1	0.0	16.6	13.3	13.8	15.6	0.0
moisture (g)	3.5	4.6	0.0	6.5	5.4	5.8	6.9	0.0
water content (%)	0.210	0.199	#DIV/0!	0.392	0.406	0.420	0.442	#DIV/0!

	Plastic Limit			Liquid Limit				
can no.								
wet soil + can (g)								
dry soil + can (g)								
can (g)								
dry soil (g)	0.0	0.0	0.0	0.0	0.0	0.0	0.0	0.0
moisture (g)	0.0	0.0	0.0	0.0	0.0	0.0	0.0	0.0
water content (%)	#DIV/0!	#DIV/0!	#DIV/0!	#DIV/0!	#DIV/0!	#DIV/0!	#DIV/0!	#DIV/0!

Client: William Lettis and Associates
Project: Commerce Geophysical Lineament
Project No.: 1573

can no.	Plastic Limit			Liquid Limit				
wet soil + can (g)	34.2	24.7		24.8	26.0	22.5	22.3	18.6
dry soil + can (g)	29.9	21.8		20.1	20.9	18.0	17.8	14.8
can (g)	3.5	3.5		3.5	3.5	3.5	3.5	3.5
dry soil (g)	26.4	18.3	0.0	16.6	17.4	14.5	14.3	11.3
moisture (g)	4.3	2.9	0.0	4.7	5.1	4.5	4.5	3.8
water content (%)	0.163	0.158	#DIV/0!	0.283	0.293	0.310	0.315	0.336

can no.	Plastic Limit			Liquid Limit				
wet soil + can (g)	26.3	40.5		24.4	19.4	18.6	22.5	19.8
dry soil + can (g)	22.1	33.6		18.7	15.0	14.3	16.9	14.9
can (g)	3.5	3.5		3.5	3.5	3.5	3.5	3.5
dry soil (g)	18.6	30.1	0.0	15.2	11.5	10.8	13.4	11.4
moisture (g)	4.2	6.9	0.0	5.7	4.4	4.3	5.6	4.9
water content (%)	0.226	0.229	#DIV/0!	0.375	0.383	0.398	0.418	0.430

	Plastic Limit			Liquid Limit				
can no.								
wet soil + can (g)								
dry soil + can (g)								
can (g)								
dry soil (g)	0.0	0.0	0.0	0.0	0.0	0.0	0.0	0.0
moisture (g)	0.0	0.0	0.0	0.0	0.0	0.0	0.0	0.0
water content (%)	#DIV/0!	#DIV/0!	#DIV/0!	#DIV/0!	#DIV/0!	#DIV/0!	#DIV/0!	#DIV/0!

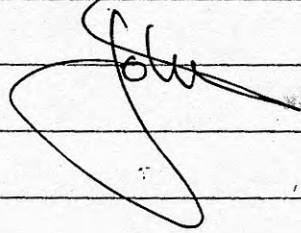
RECEIVED
9/5/03

9.4-03.

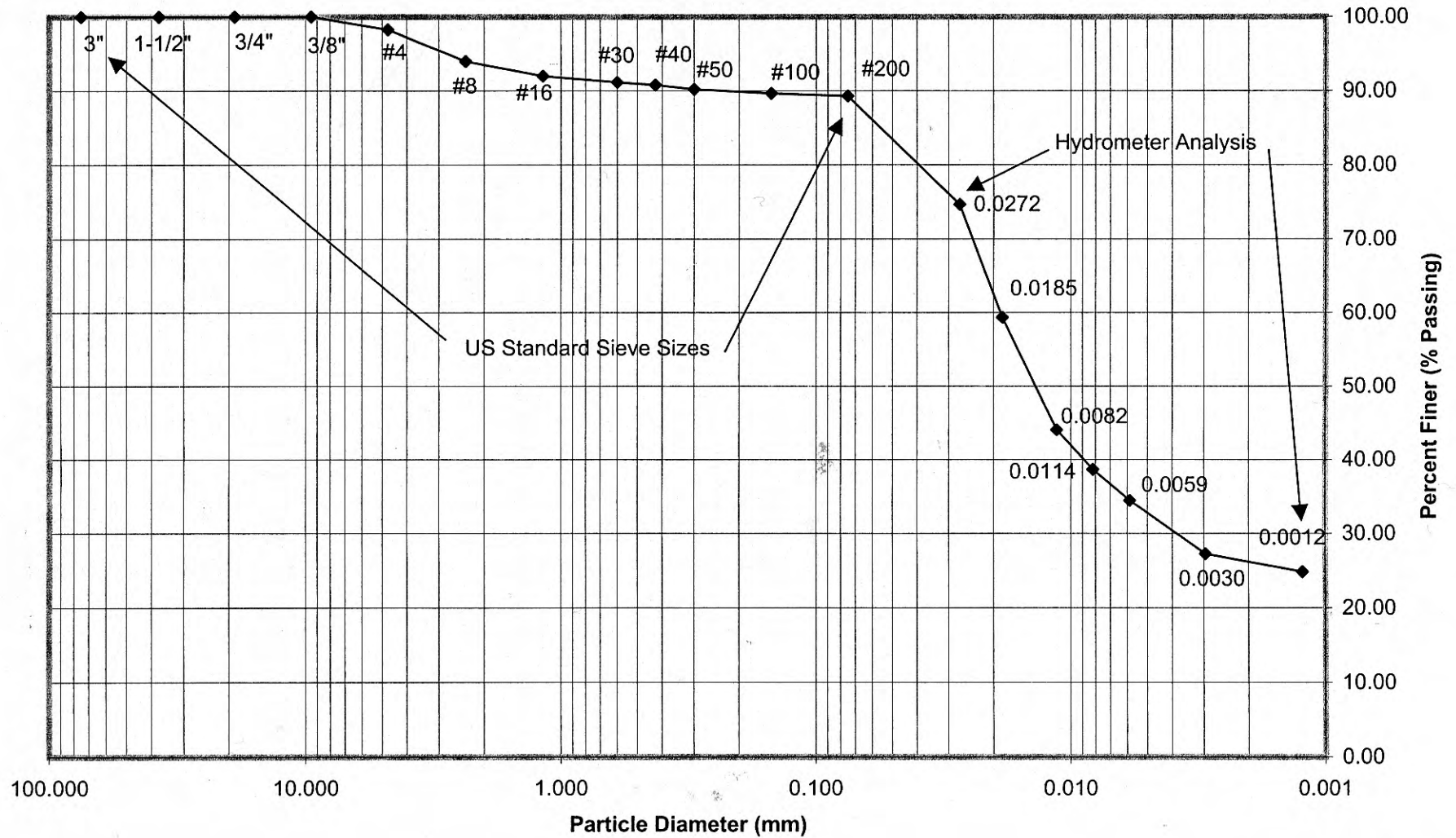
Hi Ray

PLEASE RUN SLEWS, HYDRAULICS and
PI TESTS ON THE SIX SAMPLES. I have
enclosed log + photographs to give you
a feel of depositional environment and
texture. PLEASE give me a cost
estimate before proceeding on all six.
May have you do samples 1-4 first.

Thanks -



Partial - Size Analyses Results
Commerce Geophysical Lineament, Project 1573
Trench T-5, Sample No. 3



CLIENT: WILLIAM LETTIS AND ASSOCIATES

RAYMOND L. FISHER, P.E.
SOIL TESTING LABORATORY

PARTICLE SIZE ANALYSES DATA SHEET					ASTM D422			
CLIENT:		William Lettis and Associates						
PROJECT:		Commerce Geophysical Lineament			PROJ. NO.:		1573	
BORING:		T-5	Sample #:		3	DEPTH:		NA
Before #40 Wash								
Dry Wt. +	Can Wt	Dry Wt.						
Can Wt.(g)	(g)	(g)						
250.6	1	249.6						
After #40 Wash					Percent Material Passing #40 Sieve =			
					90.83			
Dry Wt. +	Can Wt	Dry Wt.						
Can Wt.(g)	(g)	(g)						
32.1	9.2	22.9						
Hydrometer Sample								
Dry Wt. +	Can Wt	Dry Wt.						
Can Wt.(g)	(g)	(g)						
53.5	3.5	50.0						
Sieve Analysis after #40 Wash (Entire Sample)								
Sieve	Diameter	Dry Wt. +	Can Wt	Dry Wt.	%Retained	%Passing	Plot Values	
Number	(mm)	Can Wt.(g)	(g)	(g)			Dia. (mm)	%passing
3"	75.000	7.8	7.8	0	0.00	100.00	75.000	100.00
1-1/2"	37.500	7.8	7.8	0	0.00	100.00	37.500	100.00
3/4"	19.000	7.8	7.8	0	0.00	100.00	19.000	100.00
3/8"	9.500	7.8	7.8	0	0.00	100.00	9.500	100.00
4	4.750	12.0	7.7	4.3	1.72	98.28	4.750	98.28
8	2.360	18.4	7.7	10.7	4.29	93.99	2.360	93.99
16	1.180	12.7	7.7	5	2.00	91.99	1.180	91.99
30	0.600	9.8	7.7	2.1	0.84	91.15	0.600	91.15
40	0.425	8.6	7.7	0.9	0.36	90.79	0.425	90.79
Pan: add % ret. to #50)		7.8	7.7	0.1	0.04		0.300	90.20
Sieve Analysis after #200 Wash (Hydrometer Portion ~ 50g)								
(percent passing value includes sample correction factor for entire sample)								
50	0.300	8	7.7	0.3	0.6	90.20	0.0272	74.63
100	0.150	8	7.7	0.3	0.5	89.66	0.0185	59.35
200	0.075	7.9	7.7	0.2	0.4	89.29	0.0114	44.06
Pan				0.0			0.0082	38.66
HYDROMETER RESULTS								
Particle	Percent			Percent Passing				
Dia. (mm)	Finer (50g sample)			Adjusted for Entire Sample				
0.0272	82.17			74.63				
0.0185	65.34			59.35				
0.0114	48.51			44.06				
0.0082	42.57			38.66				
0.0059	37.92			34.44				
0.0030	30.00			27.24				
0.0012	27.32			24.82				

HYDROMETER ANALYSIS										
Meniscus Correction ¹			0.5							
Specific Gravity of Solids			2.70							
Unit Weight Correction Factor ²			0.99							
Dry Wt. Of Sample			50.0	grams						
Elapsed	Reading	Zero	Zero Cor	Temp	Temp Cor	Percent	K	L	Dia. (mm)	
Time, T (min)	R(actual)	Correction	Reading	Deg C	Factor ³	Passing ⁴	Table 3	Table 2 ⁵	D=K(L/T) ^{1/2}	
2	44	3.5	40.5	24	1.00	82.17	0.01282	9.00	0.0272	
5	35.5	3.5	32	24	1.00	65.34	0.01282	10.39	0.0185	
15	27	3.5	23.5	24	1.00	48.51	0.01282	11.79	0.0114	
30	24	3.5	20.5	24	1.00	42.57	0.01282	12.28	0.0082	
60	21.5	3.5	18	24.5	1.15	37.92	0.01275	12.69	0.0059	
240	17	3.5	13.5	26	1.65	30.00	0.01253	13.43	0.0030	
1440	16	3.5	12.5	25	1.30	27.32	0.01267	13.59	0.0012	
Notes										
1 Diff between top and bottom of meniscus in clear solution										
2 See Table 1 ASTM D422										
3 See Table 6-3 Bowles										
4 $P = [R(\text{actual}) - \text{zero cor. Factor} + \text{Temp Cor}] \times \text{unit wt cor} / \text{dry wt of solids}$										
5 use actual hydrom reading and add meniscus correction to get										

ATTERBERG LIMITS (ASTM D 4318)

300
P-2

Client WILLIAM LETTIS & ASSOCIATES Client Project No. 1573
 Project COMMERCE GEOPHYSICAL LINEAMENT
 Boring No. T-5 Sample No. 3 Sample Depth _____
 Material Description _____
 Date Tested _____ Tested By RLF

PLASTIC LIMIT DETERMINATION

can no.	C-5	F-53	
mass of wet soil + can (g)	23.7	35.6	
mass of dry soil + can (g)	20.2	31.0	
mass of can (g)	3.5	7.9	
mass of dry soil (g)	16.7	23.1	
mass of moisture (g)	3.5	4.6	AVE
water content, ω (%)	21.0	19.9	20.45

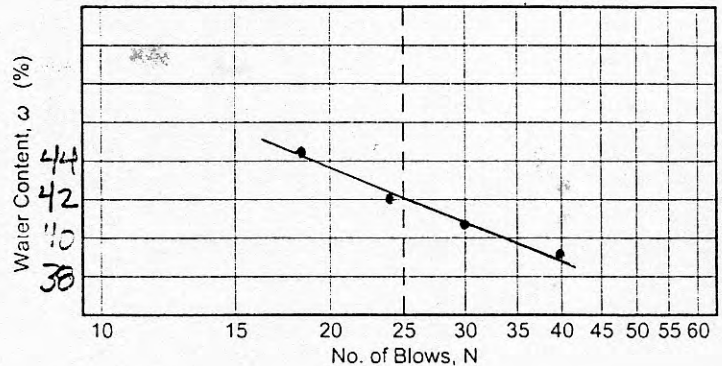
LIQUID LIMIT DETERMINATION

can no.	C-4	C-1	C-3	C-8	
mass of wet soil + can (g)	26.6	22.2	23.1	26.0	
mass of dry soil + can (g)	20.1	16.8	17.3	19.1	
mass of can (g)	3.5	3.5	3.5	3.5	
mass of dry soil (g)	16.6	13.3	13.8	15.6	
mass of moisture (g)	6.5	5.4	5.8	6.9	
water content, ω (%)	39.2	40.6	42.0	44.2	
no. of blows, N	40	30	24	18	

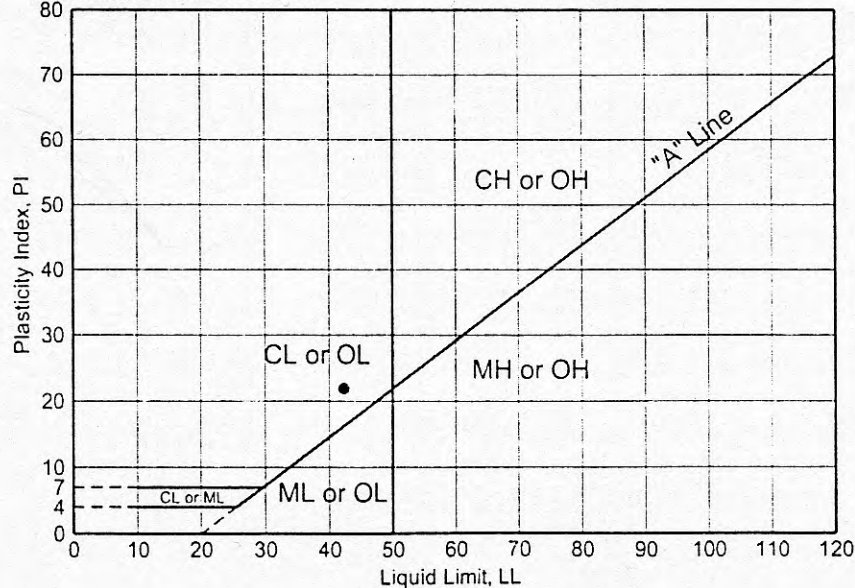
ATTERBERG LIMITS

Liquid Limit, LL 42
 Plastic Limit, PL 20
 Plasticity Index, PI 22

FLOW CURVE



PLASTICITY CHART



F-401

F-308

GRAIN SIZE ANALYSIS-MECHANICAL

Data Sheet 5

Project COMMERCE GEOPHYSICAL Job No. 1573Location of Project _____ Boring No. T-5 Sample No. #3

Description of Soil _____ Depth of Sample _____

Tested By RLF Date of testing _____

Soil Sample Size (ASTM D1140)

Nominal diameter of largest particle _____ Approximate minimum Wt. of sample, g

No. 10 sieve 200

No. 4 sieve 500

3/4 in. 1500

BEFORE WASH

AFTER
~~20~~ 40
WASH

Wt. of dry sample + container		32.1
Wt. of container <u>CAN#</u>		9.2
Wt. of dry sample, W.	249.6	22.9

TOTAL DRY WT. BEFORE WASH

$$226.7 + 22.9 = 249.6$$

CAN# F-401

Sieve analysis and grain shape

Sieve no.	Diam. (mm)	Wt. retained	% retained	% passing
#4		12.0 - 7.7		
#8		18.4 - 7.7		
#16		12.7 - 7.7		
#30		9.8 - 7.7		
#40		8.6 - 7.7		
#60		7.8 - 7.7		

$$\% \text{ passing} = 100 - \sum \% \text{ retained.}$$

F-308
#3

Job No. 1573

Job Name COMMERCE GEOPHYSICAL LN

Boring No. T-5 Depth #3

Date _____ Tested by RLF

Sample Description _____

WHOLE SAMPLE

Air Dry Sample Wt. = _____ (A1)

Air Dry Water Content

Can no. _____

wet + can _____

dry + can _____

can wt. _____

w.c. (dec) _____ (A2)

Oven Dry Sample Wt. = $\frac{A1}{1+A2}$ = _____ (A3)

<NO. 10 PORTION

Air Dry Wt. Passing No. 10 = _____ (B1)

Air Dry Water Content

can no. _____

wet + can _____

dry + can _____

can wt. _____

w.c. (dec) _____ (B2)

Oven Dry Wt. Passing No. 10 = $\frac{B1}{1+B2}$ = _____ (B3)

Air Dry Wt. of Hydrometer Sample = _____ (B4)

Oven Dry Wt. of Hydrometer Sample = $\frac{B4}{1+B2}$ = _____ (B5)

SCF, Sieve Correction Factor = $\frac{A3}{100 \times B5} \times B6$ = _____

HPF, Hydrometer Percentage Factor = $\frac{1000}{B5/B6} \times \frac{G}{G-1} = \frac{1600}{B5/B6}$ = _____

Specific Gravity, G = 2.65

DRY SIEVE

Original Dry Sample Wt. (A3) = _____ gm

U.S. Standard Sieve Size	Can No.	Sample Wt. (SW)	Corrected Sample Wt. = SW-SCF (#18-#200 only)	Cumulative Wt. Retained	Cumulative % Retained	% Passing
1"						
3/4"						
3/8"						
#4						
#8						
#10						
#16						
#30						
#40						
#50						
#100						
#200						

Hydrometer Correction

clear water reading _____ (C1)

water + diap (top) _____ (C2)

water + diap (bottom) _____ (C3)

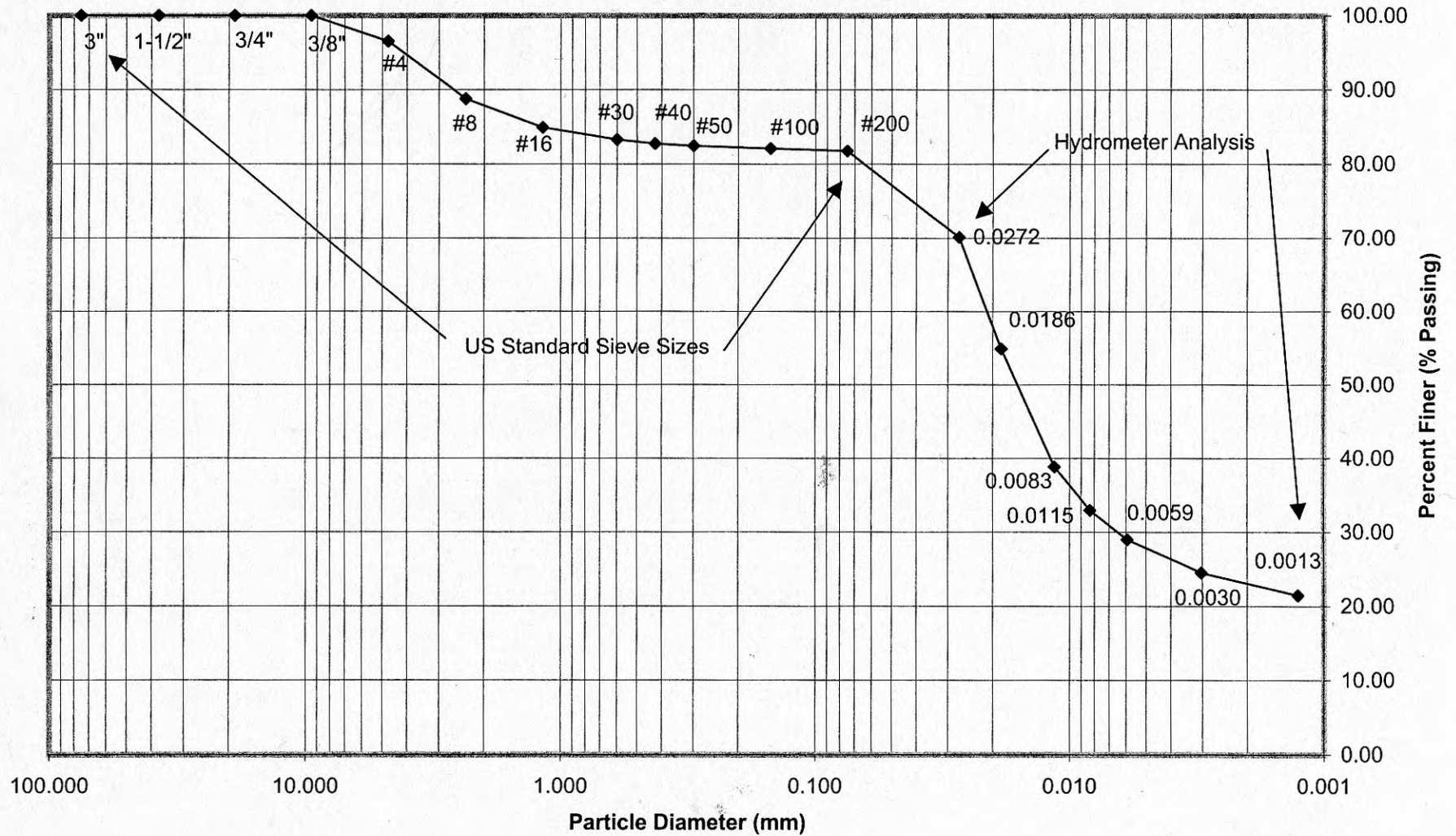
Hyd Corr = $1 \times (2 \times C2 - C1 - C3)$ = _____

START 6:03 PM

Date	Time	T Elapsed Time	Hydrometer Reading	Hydrometer Correction	R Corrected Reading	Temp. (C)	P HPF · (R-1)	K Table 3, pg. 93	L Table 2, pg. 92	D (mm) D = K√L/T
10/5	6:05 PM	2	44			24.0°				
	6:08 PM	5	35.5							
	6:18 PM	15	27.0							
	6:33 PM	30	24.0							
	7:03 PM	60	21.5			24.5				
	10:03 PM	240 (4h)	17.0			26.0				
10/6	6:03 PM	1440 (24h)	16.0			25.0				
10/5	6:04	1	49			24.0°				

AFTER #200
WASH
F-105 7.7g CAN
DRY CAN 8.5
8.5 - 7.7 = 0.8g

Partial - Size Analyses Results
Commerce Geophysical Lineament, Project 1573
Trench T-5, Sample No. 4



CLIENT: WILLIAM LETTIS AND ASSOCIATES

RAYMOND L. FISHER, P.E.
SOIL TESTING LABORATORY

PARTICLE SIZE ANALYSES DATA SHEET					ASTM D422							
CLIENT:		William Lettis and Associates										
PROJECT:		Commerce Geophysical Lineament			PROJ. NO.:		1573					
BORING:		T-5	Sample #:	4	DEPTH:		NA					
Before #40 Wash												
Dry Wt. +	Can Wt	Dry Wt.										
Can Wt.(g)	(g)	(g)										
296.1	1	295.1										
After #40 Wash					Percent Material Passing #40 Sieve =		85.33					
Dry Wt. +	Can Wt	Dry Wt.										
Can Wt.(g)	(g)	(g)										
51.1	7.8	43.3										
Hydrometer Sample												
Dry Wt. +	Can Wt	Dry Wt.										
Can Wt.(g)	(g)	(g)										
53.5	3.5	50.0										
Sieve Analysis after #40 Wash (Entire Sample)												
Sieve	Diameter	Dry Wt. +	Can Wt	Dry Wt.	%Retained	%Passing						
Number	(mm)	Can Wt.(g)	(g)	(g)							Plot Values	
											Dia. (mm) %passing	
3"	75.000	7.8	7.8	0	0.00	100.00					75.000 100.00	
1-1/2"	37.500	7.8	7.8	0	0.00	100.00					37.500 100.00	
3/4"	19.000	7.8	7.8	0	0.00	100.00					19.000 100.00	
3/8"	9.500	7.8	7.8	0	0.00	100.00					9.500 100.00	
4	4.750	17.9	7.7	10.2	3.46	96.54					4.750 96.54	
8	2.360	30.6	7.7	22.9	7.76	88.78					2.360 88.78	
16	1.180	19.1	7.7	11.4	3.86	84.92					1.180 84.92	
30	0.600	12.5	7.7	4.8	1.63	83.29					0.600 83.29	
40	0.425	9.3	7.7	1.6	0.54	82.75					0.425 82.75	
Pan: add % ret. to #50)		8.1	7.7	0.4	0.14						0.300 82.45	
Sieve Analysis after #200 Wash (Hydrometer Portion ~ 50g)											0.150 82.10	
(percent passing value includes sample correction factor for entire sample)											0.075 81.76	
50	0.300	7.8	7.7	0.1	0.3	82.45					0.0272 70.11	
100	0.150	7.9	7.7	0.2	0.3	82.10					0.0186 54.91	
200	0.075	7.9	7.7	0.2	0.3	81.76					0.0115 38.86	
Pan				0.0							0.0083 32.94	
HYDROMETER RESULTS											0.0059 28.97	
Particle	Percent			Percent Passing						0.0030 24.50		
Dia. (mm)	Finer (50g sample)			Adjusted for Entire Sample						0.0013 21.46		
0.0272	82.17					70.11						
0.0186	64.35					54.91						
0.0115	45.54					38.86						
0.0083	38.61					32.94						
0.0059	33.96					28.97						
0.0030	28.71					24.50						
0.0013	25.15					21.46						

HYDROMETER ANALYSIS										
Meniscus Correction ¹			0.5							
Specific Gravity of Solids			2.70							
Unit Weight Correction Factor ²			0.99							
Dry Wt. Of Sample			50.0	grams						
Elapsed	Reading	Zero	Zero Cor	Temp	Temp Cor	Percent	K	L	Dia. (mm)	
Time, T (min)	R(actual)	Correction	Reading	Deg C	Factor ³	Passing ⁴	Table 3	Table 2 ⁵	D=K(L/T) ^{1/2}	
2	44	3.5	40.5	24	1.00	82.17	0.01282	9.00	0.0272	
5	35	3.5	31.5	24	1.00	64.35	0.01282	10.47	0.0186	
15	25.5	3.5	22	24	1.00	45.54	0.01282	12.03	0.0115	
30	22	3.5	18.5	24	1.00	38.61	0.01282	12.61	0.0083	
60	19.5	3.5	16	24.5	1.15	33.96	0.01275	13.02	0.0059	
240	17	3.5	13.5	24	1.00	28.71	0.01282	13.43	0.0030	
1440	15.5	3.5	12	23	0.70	25.15	0.01297	13.67	0.0013	
Notes										
1	Diff between top and bottom of meniscus in clear solution									
2	See Table 1 ASTM D422									
3	See Table 6-3 Bowles									
4	P= [R(actual) - zero cor. Factor + Temp Cor] x unit wt cor / dry wt of solids									
5	use actual hydrom reading and add meniscus correction to get									

ATTERBERG LIMITS (ASTM D 4318)

#4 F-3

Client WILLIAM LETTIS & ASSOCIATES Client Project No. 1573
 Project COMMERCE GEOPHYSICAL LINEAMENT
 Boring No. T-5 Sample No. 4 Sample Depth _____
 Material Description _____
 Date Tested _____ Tested By RLF

PLASTIC LIMIT DETERMINATION

can no.	C-7A	C-2A
mass of wet soil + can (g)	26.3	40.5
mass of dry soil + can (g)	22.1	33.6
mass of can (g)	3.5	3.5
mass of dry soil (g)	18.6	30.1
mass of moisture (g)	4.2	6.9
water content, ω (%)	22.6	22.9

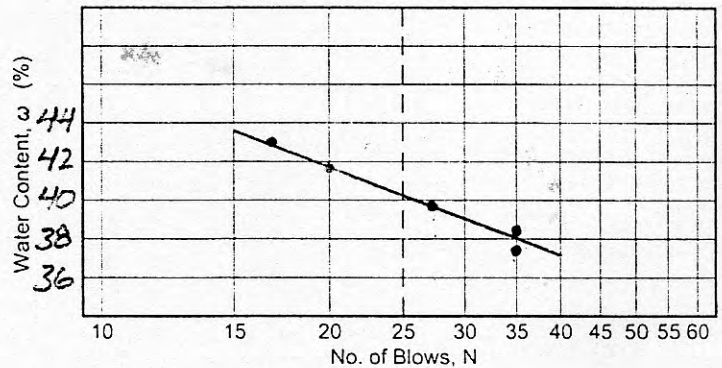
LIQUID LIMIT DETERMINATION

can no.	C-1	C-5	C-12	C-10	C-4
mass of wet soil + can (g)	24.4	19.4	18.6	22.5	19.8
mass of dry soil + can (g)	18.7	15.0	14.3	16.9	14.9
mass of can (g)	3.5	3.5	3.5	3.5	3.5
mass of dry soil (g)	15.2	11.5	10.8	13.4	11.4
mass of moisture (g)	5.7	4.4	4.3	5.6	4.9
water content, ω (%)	37.5	38.3	39.8	41.8	43.0
no. of blows, N	35	35	27	20/21	17

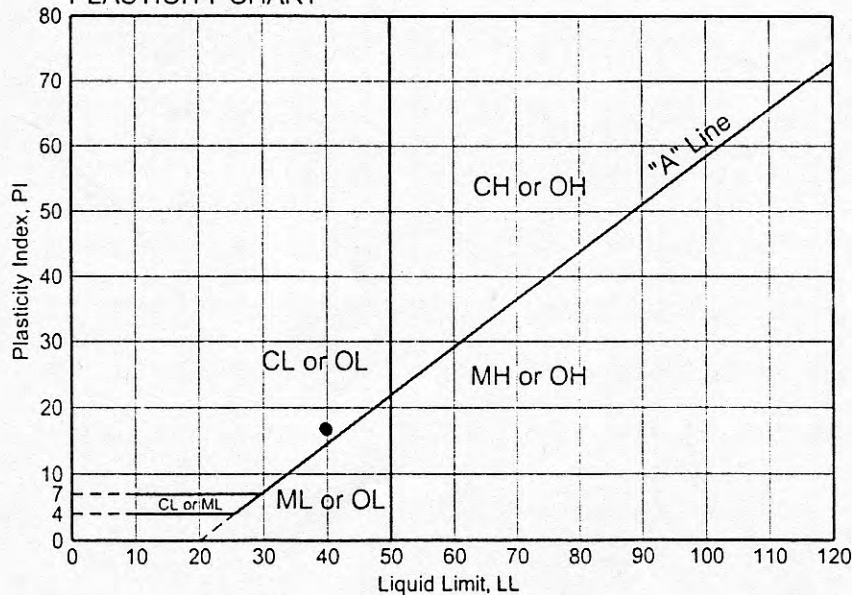
ATTERBERG LIMITS

Liquid Limit, LL	<u>40</u>
Plastic Limit, PL	<u>23</u>
Plasticity Index, PI	<u>17</u>

FLOW CURVE



PLASTICITY CHART



GRAIN SIZE ANALYSIS-MECHANICAL

F-48
F-310

Data Sheet 5

Project COMMERCE GEOPHYSICAL Job No. 1573
Location of Project _____ Boring No. T-5 Sample No. #4
Description of Soil _____ Depth of Sample _____
Tested By RLF Date of testing _____

Soil Sample Size (ASTM D1140)

TOTAL DRY WT. BEFORE WASH
244.0 + 51.1

Nominal diameter of largest particle
No. 10 sieve
No. 4 sieve
3/4 in.

Approximate minimum Wt. of sample, g
200
500
1500

AFTER
#200-40
WASH

Wt. of dry sample + container		58.9
Wt. of container <u>CAN#</u>		7.8
Wt. of dry sample, W _s	295.1	51.1

CAN# F48

Sieve analysis and grain shape

Sieve no.	Diam. (mm)	Wt. retained	% retained	% passing
#4		17.9 - 7.7 10.2	3.46	96.54
#8		30.6 - 7.7 22.9	7.76	88.78
#16		19.1 - 7.7 11.4	3.86	84.92
#30		12.5 - 7.7 4.5	1.63	83.90
#40		9.3 - 7.7 1.6	0.54	82.75
PAW		8.1 - 7.7 0.4	0.14	

% passing = 100 - Σ % retained.

Job No. 1573

F-310

Job Name COMMERCE GEOPHYSICALBoring No. T-5Depth #4Date 11/15/63Tested by RLF

Sample Description

WHOLE SAMPLE

Air Dry Sample Wt. = _____ (A1)

Air Dry Water Content

Can no. _____

wet + can _____

dry + can _____

can wt. _____

w.c. (dec) _____ (A2)

Oven Dry Sample Wt. = $\frac{A1}{1+A2} = \frac{245.1}{1+0.40} = 245.1$ (A3)

NO. 40 PORTION

Air Dry Wt. Passing No. 10 = _____ (B1)

Air Dry Water Content

can no. _____

wet + can _____

dry + can _____

can wt. _____

w.c. (dec) _____ (B2)

Oven Dry Wt. Passing No. 10 = $\frac{B1}{1+B2} = \frac{51.1}{1+0.40} = 51.1$ (B3)

Air Dry Wt. of Hydrometer Sample = _____ (B4)

Oven Dry Wt. of Hydrometer Sample = $\frac{B4}{1+B2} = \frac{50.0}{1+0.40} = 50.0$ (B5)SCF, Sieve Correction Factor = $\frac{A3}{100 \times B5} \times B6 = \frac{245.1}{100 \times 50.0} \times 82.5 = 0.49$ HPF, Hydrometer Percentage Factor = $\frac{1000}{B5/B6} \times \frac{G}{G-1} = \frac{1000}{50.0/82.5} \times \frac{2.65}{2.65-1} = 1806$

Specific Gravity, G = 2.65

START 6:21 PM 11/15/63

 $G_s = 2.65 \quad \alpha = 0.10$

Hydrometer Correction 26°
 clear water reading 0.0 (C1) 0.5
 water + disp (top) 4.0 (C2)
 water + disp (bottom) 4.5 (C3)
 Hyd Corr $-1 \times (2 \times C2 - C1 - C3) = -3.5$

Date	T	Hydrometer	Hydrometer	R	Temp. (C)	P	K	L	D (mm)
Time	Elapsed Time	Reading	Correction	Corrected Reading		HPF (R-1)	Table 3, pg. 93	Table 2, pg. 92	D=K/V/LIT
10/3 6:23 PM	2	44	-3.5	40.5	24.0	0.8217	0.01282	9.0	0.0272
6:26 PM	5	35	-3.5	31.5	24.0	0.6435	0.01282	10.5	0.0185
6:36 PM	15	25.5	-3.5	22.0	24.0	0.4752	0.01282	12.0	0.0147
6:51 PM	30	22	-3.5	18.5	24.0	0.3861	0.01282	12.6	0.0093
7:21 PM	60	19.5	-3.5	16.0	24.5	0.3396	0.01275	13.0	0.0059
10/4 7:21 PM	240 (4h)	17.	-3.5	13.5	24.0	0.2871	0.01282	13.4	0.0030
10/3 7:21 PM	1440 (24h)	15.5	-3.5	12.0	23.0	0.2515	0.01291	13.7	0.0013
10/3 6:23 PM	1	48	-3.5	44.5	24.0				

$$P = \frac{(R_{ACTUAL} - ZERO CORR + C_T) \times W_s}{W_s}$$

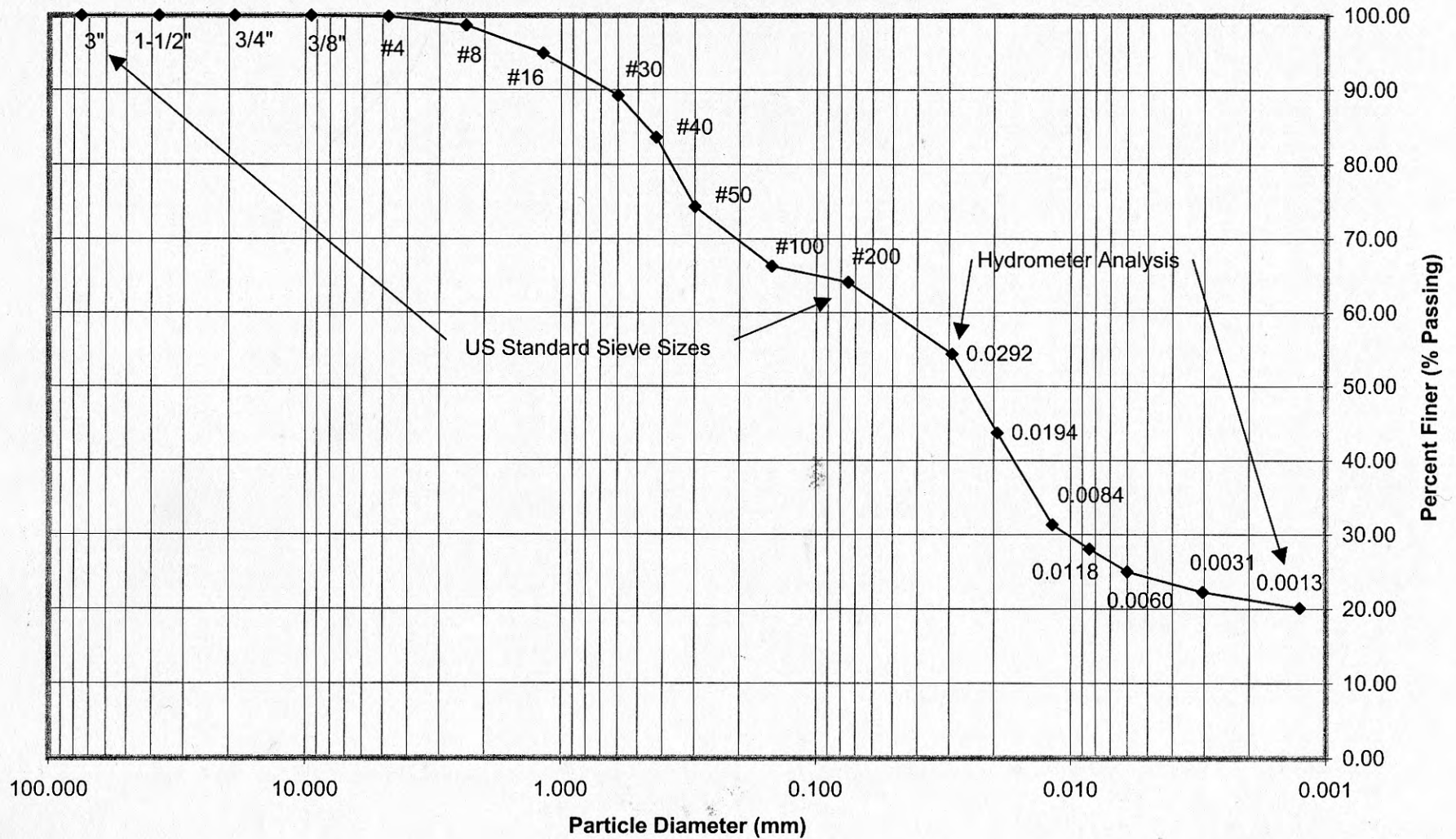
 $C_T = 1.0, 24^\circ$ $C_T = 1.15, 24.5^\circ$ $C_T = 0.70, 23^\circ$

CORRECTED
 FOR MULTISCALE
 MD 0.5 TO
 1.0 RAIL

F-405 9.2

DRY + CAN
 9.6g

Grain Size Analyses Results
Commerce Geophysical Lineament, Project 1573
Trench T-5, Sample No. 2



RAYMOND L. FISHER, P.E.
SOIL TESTING LABORATORY

CLIENT: WILLIAM LETTIS AND ASSOCIATES

PARTICLE SIZE ANALYSES DATA SHEET				ASTM D422					
CLIENT:		William Lettis and Associates							
PROJECT:		Commerce Geophysical Lineament				PROJ. NO.:		1573	
BORING:		T-5	Sample #:		2	DEPTH:		NA	
Before #40 Wash									
Dry Wt. +	Can Wt	Dry Wt.							
Can Wt.(g)	(g)	(g)							
294.9	1	293.9							
After #40 Wash									
Dry Wt. +	Can Wt	Dry Wt.		Percent Material Passing #40 Sieve =		83.29			
Can Wt.(g)	(g)	(g)		Wash Water and Soil Retained and Dehydrated					
58.3	9.2	49.1							
Hydrometer Sample									
Dry Wt. +	Can Wt	Dry Wt.							
Can Wt.(g)	(g)	(g)							
53.5	3.5	50.0							
Sieve Analysis after #40 Wash (Entire Sample)									
Sieve	Diameter	Dry Wt. +	Can Wt	Dry Wt.	%Retained	%Passing	Plot Values		
Number	(mm)	Can Wt.(g)	(g)	(g)			Dia. (mm)	%passing	
3"	75.000	7.8	7.8	0	0.00	100.00	75.000	100.00	
1-1/2"	37.500	7.8	7.8	0	0.00	100.00	37.500	100.00	
3/4"	19.000	7.8	7.8	0	0.00	100.00	19.000	100.00	
3/8"	9.500	7.8	7.8	0	0.00	100.00	9.500	100.00	
4	4.750	8.2	7.8	0.4	0.14	99.86	4.750	99.86	
8	2.360	11.4	7.9	3.5	1.19	98.67	2.360	98.67	
16	1.180	18.8	7.8	11	3.74	94.93	1.180	94.93	
30	0.600	24.7	8.0	16.7	5.68	89.25	0.600	89.25	
40	0.425	24.4	7.9	16.5	5.61	83.63	0.425	83.63	
Pan: add % ret. to #50)		8.7	7.7	1	0.34		0.300	74.30	
Sieve Analysis after #200 Wash (Hydrometer Portion ~ 50g)							0.150	66.30	
(percent passing value includes sample correction factor for entire sample)							0.075	64.14	
50	0.300	13.1	7.7	5.4	9.3	74.30	0.0292	54.42	
100	0.150	12.5	7.7	4.8	8.0	66.30	0.0194	43.70	
200	0.075	9	7.7	1.3	2.2	64.14	0.0118	31.34	
Pan				0.0			0.0084	28.04	
HYDROMETER RESULTS							0.0060	24.99	
Particle	Percent			Percent Passing			0.0031	22.26	
Dia. (mm)	Finer (50g sample)			Adjusted for Entire Sample			0.0013	20.12	
0.0292	65.34					54.42			
0.0194	52.47					43.70			
0.0118	37.62					31.34			
0.0084	33.66					28.04			
0.0060	30.00					24.99			
0.0031	26.73					22.26			
0.0013	24.16					20.12			

HYDROMETER ANALYSIS											
Meniscus Correction ¹		0.5									
Specific Gravity of Solids		2.70									
Unit Weight Correction Factor ²		0.99									
Dry Wt. Of Sample		50.0 grams									
Elapsed	Reading	Zero	Zero Cor	Temp	Temp Cor	Percent	K	L	Dia. (mm)		
Time, T (min)	R(actual)	Correction	Reading	Deg C	Factor ³	Passing ⁴	Table 3	Table 2 ⁵	D=K(L/T) ^{1/2}		
2	35.5	3.5	32	24	1	65.34	0.01282	10.39	0.0292		
5	29	3.5	25.5	24	1	52.47	0.01282	11.46	0.0194		
15	21.5	3.5	18	24	1	37.62	0.01282	12.69	0.0118		
30	19.5	3.5	16	24	1	33.66	0.01282	13.02	0.0084		
60	17.5	3.5	14	24.5	1.15	30.00	0.01275	13.35	0.0060		
240	16	3.5	12.5	24	1	26.73	0.01282	13.59	0.0031		
1440	15	3.5	11.5	23	0.7	24.16	0.01297	13.76	0.0013		
Notes											
1		Diff between top and bottom of meniscus in clear solution									
2		See Table 1 ASTM D422									
3		See Table 6-3 Bowles									
4		P= [R(actual) - zero cor. Factor + Temp Cor] x unit wt cor / dry wt of solids									
5		use actual hydrom reading and add meniscus correction to get									

ATTERBERG LIMITS (ASTM D 4318)

Client WILLIAM LETTIS & ASSOCIATES Client Project No. 1573

Project COMMERCE GEOPHYSICAL LINEAMENT

Boring No. T-5 Sample No. 2 Sample Depth _____

Material Description _____

Date Tested _____ Tested By RLF

PLASTIC LIMIT DETERMINATION

can no.	C-8	C-6	
mass of wet soil + can (g)	34.2	24.7	
mass of dry soil + can (g)	29.9	21.8	
mass of can (g)	3.5	3.5	
mass of dry soil (g)	26.4	18.3	
mass of moisture (g)	4.3	2.9	
water content, ω (%)	16.3	15.8	

LIQUID LIMIT DETERMINATION

can no.	C-11	C-3	C-2	C-9	C-7
mass of wet soil + can (g)	24.6	26.0	22.5	22.3	18.6
mass of dry soil + can (g)	20.1	20.9	18.0	17.8	14.8
mass of can (g)	3.5	3.5	3.5	3.5	3.5
mass of dry soil (g)	16.6	17.4	14.5	14.3	11.3
mass of moisture (g)	4.7	5.1	4.5	4.5	3.8
water content, ω (%)	28.3	29.3	31.0	31.5	33.6
no. of blows, N	39	34	26	20	16

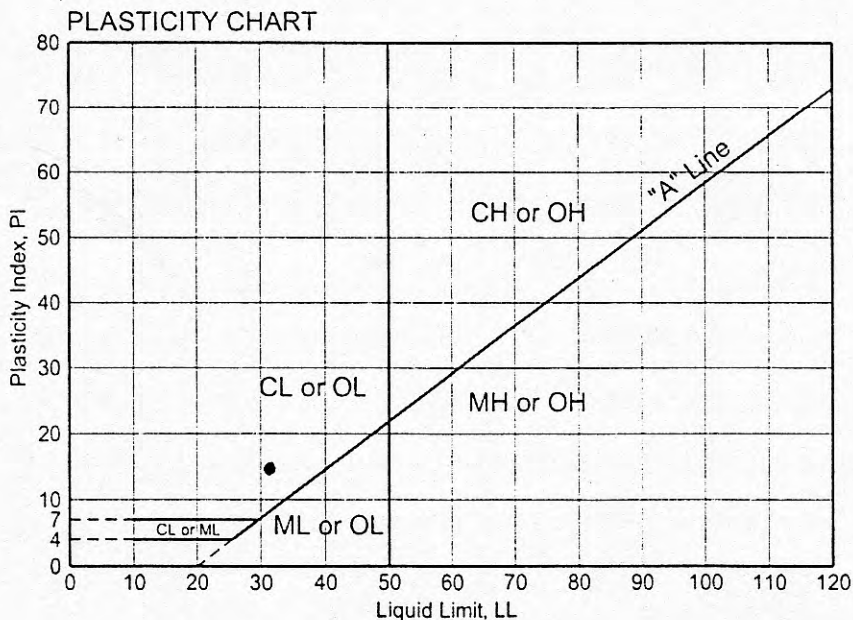
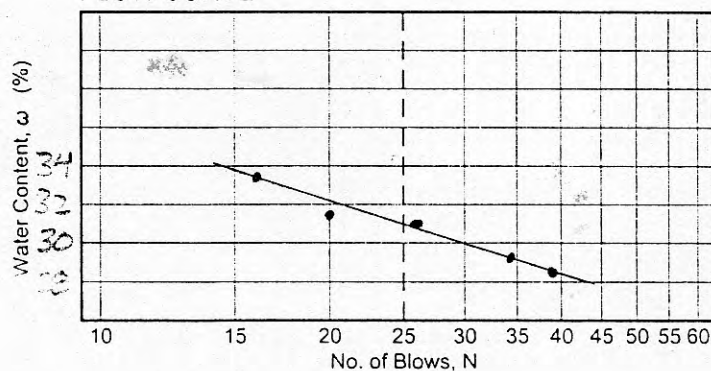
ATTERBERG LIMITS

Liquid Limit, LL 31

Plastic Limit, PL 16

Plasticity Index, PI 15

FLOW CURVE



F-406

GRAIN SIZE ANALYSIS-MECHANICAL

Data Sheet 5

Project COMMERCE GEOPHYSICAL Job No. 1573

Location of Project _____ Boring No. T-5 Sample No. #2

Description of Soil _____ Depth of Sample _____

Tested By RLF Date of testing _____

Soil Sample Size (ASTM D1140)

Nominal diameter of largest particle _____ Approximate minimum Wt. of sample, g

No. 10 sieve 200

No. 4 sieve 500

3/4 in. 1500

TOTAL BEFORE WASH
244.8 + 49.1 = 293.9

AFTER
#200-#40
WASH

Wt. of dry sample + container		58.3
Wt. of container <u>CAN#</u>		9.2
Wt. of dry sample, W _s	293.9	49.1

CAN#F-406

Sieve analysis and grain shape

Sieve no.	Diam. (mm)	Wt. retained	% retained	% passing
4		8.2 - 7.8		
8		11.4 - 7.9		
16		18.6 - 7.8		
30		24.7 - 8.0		
40		24.4 - 7.9		
PAN		8.7 - 7.7		

% passing = 100 - Σ % retained.

Job No. 1573 F-201
 Job Name COMMERCE GEOPHYSICAL LI. #2
 Boring No. T-5 Depth #2
 Date 10/3/03 Tested by RLF

Sample Description

WHOLE SAMPLE

Air Dry Sample Wt. = _____ (A1)

Air Dry Water Content

Can. no. _____

wet + can _____

dry + can _____

can wt. _____

w.c. (dec) _____ (A2)

$$\text{Oven Dry Sample Wt.} = \frac{A1}{1+A2} = \text{_____ (A3)}$$

<NO. 10 PORTION

Air Dry Wt. Passing No. 10 = _____ (B1)

Air Dry Water Content

can no. _____

wet + can _____

dry + can _____

can wt. _____

w.c. (dec) _____ (B2)

$$\text{Oven Dry Wt. Passing No. 10} = \frac{B1}{1+B2} = \text{_____ (B3)}$$

Air Dry Wt. of Hydrometer Sample = _____ (B4)

$$\text{Oven Dry Wt. of Hydrometer Sample} = \frac{B4}{1+B2} = \text{_____ (B5)}$$

$$\text{SCF, Sieve Correction Factor} = \frac{A3}{100 \times B5} \times B6 = \text{_____}$$

$$\text{HPF, Hydrometer Percentage Factor} = \frac{1000}{B5/B6} \times \frac{G}{G-1} = \frac{1606}{B5/B6} = \text{_____}$$

Specific Gravity, G = 2.65

DRY SIEVE

Original Dry Sample Wt. (A3) = _____ gm

U.S. Standard Sieve Size	Can No.	Sample Wt. (SW)	Corrected Sample Wt. = SW-SCF (#18-#200 only)	Cumulative Wt. Retained	Cumulative % Retained	% Passing
1"						
3/4"						
3/8"						
#4						
#8						
#10						
#18						
#30						
#40						
#50						
#100						
#200						

Hydrometer Correction
 clear water reading 0.0 (C1)
 water + disp (top) 4.0 (C2)
 water + disp (bottom) 4.5 (C3)
 Hyd Corr $-1 \times (2 \times C2 - C1 - C3) = \text{_____}$

START 6:30 10/3/03 P = R/B5

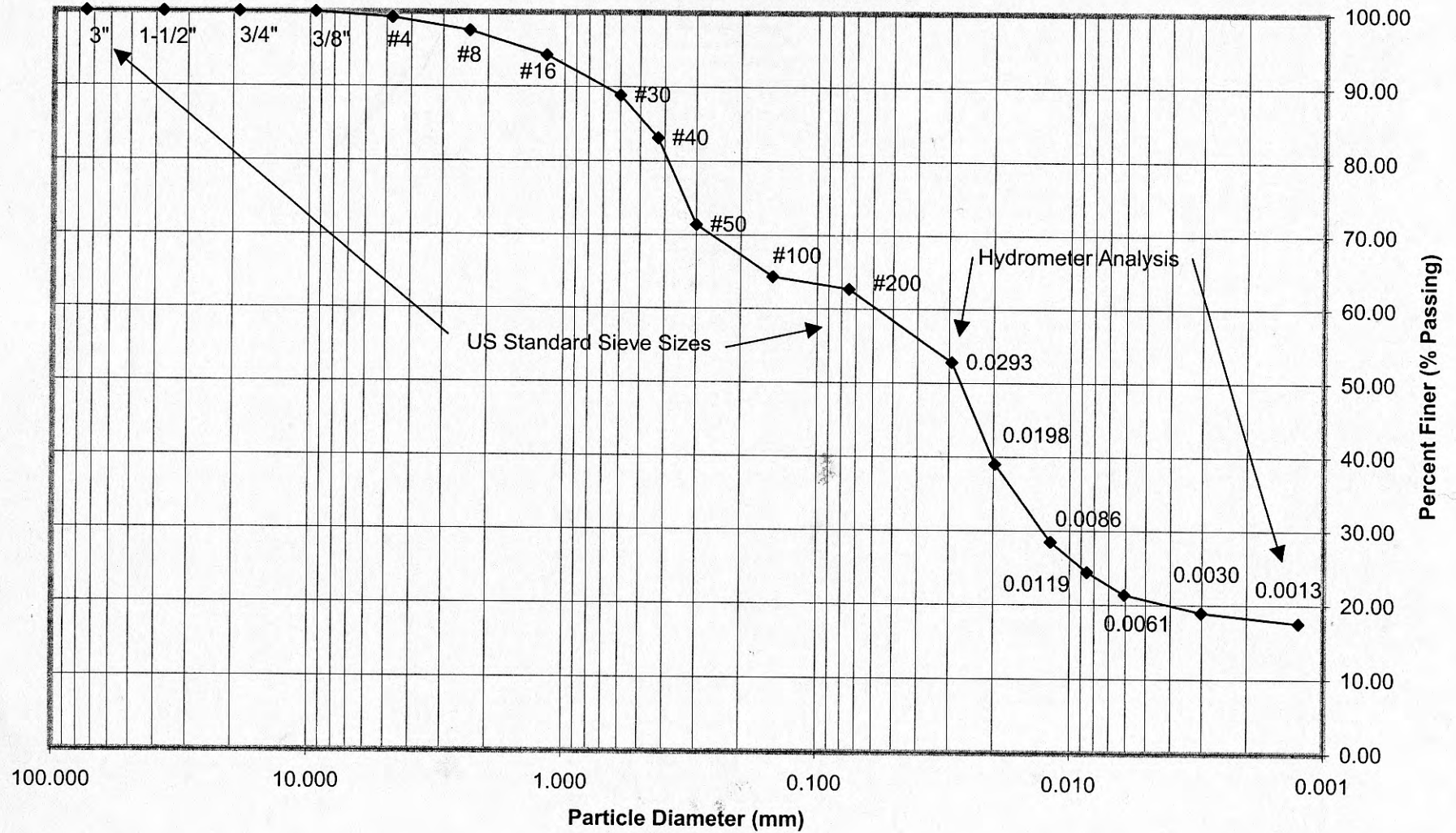
Date	Time	T Elapsed Time	Hydrometer Reading	Hydrometer Correction	R Corrected Reading	Temp. (C)	P HPF · (R-1)	K Table 3, pg. 93	L Table 2, pg. 92	D (mm) D = K√L/T
10/3	6:30 pm	2	35.5	-3.5	32.0	24.0			10.4	
	6:33 pm	5	29	-3.5	25.5	24.0			11.45	
	6:43 pm	15	21.5	-3.5	18.0	24.0			12.7	
	6:58 pm	30	19.5	-3.5	16.0	24.0			13.0	
	7:25 pm	60	17.5	-3.5	14.0	24.5			13.3	
	10:28 pm	240 (4h)	16.	-3.5	12.5	24.0			13.6	
10/4	T 6:28 pm	1440 (24h)	15	-3.5	11.5	25.0			13.75	
10/3	6:29 pm	1	39	-3.5	35.5	24.0			19.8	

$$P = \frac{(R_{act} - \text{ZERO COR} + C_1) \times W_s}{\text{_____}}$$

USING R
 CORRECTED
 FOR
 VISCOSITY
 ADD
 0.5 P
 RACT

200 WASH
 F-104 7.63
 DRY + CAN
 19.19

Partial - Size Analyses Results
Commerce Geophysical Lineament, Project 1573
Trench T-5, Sample No. 1



CLIENT: WILLIAM LETTIS AND ASSOCIATES

RAYMOND L. FISHER, P.E.
SOIL TESTING LABORATORY

PARTICLE SIZE ANALYSES DATA SHEET				ASTM D422					
CLIENT:		William Lettis and Associates							
PROJECT:		Commerce Geophysical Lineament				PROJ. NO.:		1573	
BORING:		T-5		Sample #:		1		DEPTH: NA	
Before #40 Wash									
Dry Wt. +	Can Wt	Dry Wt.							
Can Wt.(g)	(g)	(g)							
305.1	1	304.1							
After #40 Wash				Percent Material Passing #40 Sieve =		82.11			
Dry Wt. +	Can Wt	Dry Wt.							
Can Wt.(g)	(g)	(g)							
63.6	9.2	54.4							
Hydrometer Sample									
Dry Wt. +	Can Wt	Dry Wt.							
Can Wt.(g)	(g)	(g)							
53.5	3.5	50.0							
Sieve Analysis after #40 Wash (Entire Sample)									
Sieve	Diameter	Dry Wt. +	Can Wt	Dry Wt.	%Retained	%Passing	Plot Values		
Number	(mm)	Can Wt.(g)	(g)	(g)			Dia. (mm)	%passing	
3"	75.000	7.8	7.8	0	0.00	100.00	75.000	100.00	
1-1/2"	37.500	7.8	7.8	0	0.00	100.00	37.500	100.00	
3/4"	19.000	7.8	7.8	0	0.00	100.00	19.000	100.00	
3/8"	9.500	7.8	7.8	0	0.00	100.00	9.500	100.00	
4	4.750	10.0	7.7	2.3	0.76	99.24	4.750	99.24	
8	2.360	12.9	7.7	5.2	1.71	97.53	2.360	97.53	
16	1.180	17.7	7.7	10	3.29	94.25	1.180	94.25	
30	0.600	24.1	7.7	16.4	5.39	88.85	0.600	88.85	
40	0.425	25.2	7.7	17.5	5.75	83.10	0.425	83.10	
Pan: add % ret. to #50)		10.8	7.7	3.1	1.02		0.300	71.40	
Sieve Analysis after #200 Wash (Hydrometer Portion ~ 50g)									
(percent passing value includes sample correction factor for entire sample)									
50	0.300	14.2	7.7	6.5	11.7	71.40	0.0293	52.84	
100	0.150	12	7.7	4.3	7.1	64.34	0.0198	39.02	
200	0.075	8.7	7.7	1.0	1.6	62.70	0.0119	28.45	
Pan				0.0			0.0086	24.39	
HYDROMETER RESULTS									
Particle	Percent			Percent Passing					
Dia. (mm)	Finer (50g sample)			Adjusted for Entire Sample					
0.0293	64.35			52.84					
0.0198	47.52			39.02					
0.0119	34.65			28.45					
0.0086	29.70			24.39					
0.0061	26.04			21.38					
0.0030	23.07			18.94					
0.0013	21.38			17.56					

HYDROMETER ANALYSIS									
Meniscus Correction ¹		0.5							
Specific Gravity of Solids		2.70							
Unit Weight Correction Factor ²		0.99							
Dry Wt. Of Sample		50.0 grams							
Elapsed	Reading	Zero	Zero Cor	Temp	Temp Cor	Percent	K	L	Dia. (mm)
Time, T (min)	R(actual)	Correction	Reading	Deg C	Factor ³	Passing ⁴	Table 3	Table 2 ⁵	D=K(L/T) ^{1/2}
2	35	3.5	31.5	24	1.00	64.35	0.01282	10.47	0.0293
5	26.5	3.5	23	24	1.00	47.52	0.01282	11.87	0.0198
15	20	3.5	16.5	24	1.00	34.65	0.01282	12.94	0.0119
30	17.5	3.5	14	24	1.00	29.70	0.01282	13.35	0.0086
60	15.5	3.5	12	24.5	1.15	26.04	0.01275	13.67	0.0061
240	13.5	3.5	10	26	1.65	23.07	0.01253	14.00	0.0030
1440	13	3.5	9.5	25	1.30	21.38	0.01267	14.08	0.0013
Notes									
1 Diff between top and bottom of meniscus in clear solution									
2 See Table 1 ASTM D422									
3 See Table 6-3 Bowles									
4 P= [R(actual) - zero cor. Factor + Temp Cor] x unit wt cor / dry wt of solids									
5 use actual hydrom reading and add meniscus correction to get									

ATTERBERG LIMITS (ASTM D 4318)

F-307
P-5

Client WILLIAM LETTIS & ASSOCIATES Client Project No. 1573

Project COMMERCE GEOPHYSICAL LINEAMENT

Boring No. T-5 Sample No. 1 Sample Depth _____

Material Description _____

Date Tested _____ Tested By RLF

PLASTIC LIMIT DETERMINATION

can no.	C-11	C-9
mass of wet soil + can (g)	44.2	43.2
mass of dry soil + can (g)	38.2	37.3
mass of can (g)	3.5	3.5
mass of dry soil (g)	34.7	33.8
mass of moisture (g)	6.0	5.9
water content, ω (%)	17.3	17.5

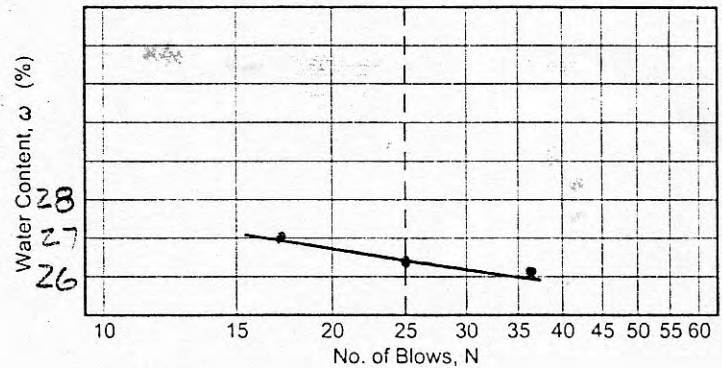
LIQUID LIMIT DETERMINATION

can no.	C-12	C-10	C-7
mass of wet soil + can (g)	26.7	24.1	22.3
mass of dry soil + can (g)	26.9	19.8	18.3
mass of can (g)	3.5	3.5	3.5
mass of dry soil (g)	18.4	16.3	14.8
mass of moisture (g)	4.8	4.3	4.0
water content, ω (%)	26.1	26.4	27.0
no. of blows, N	36	25	17

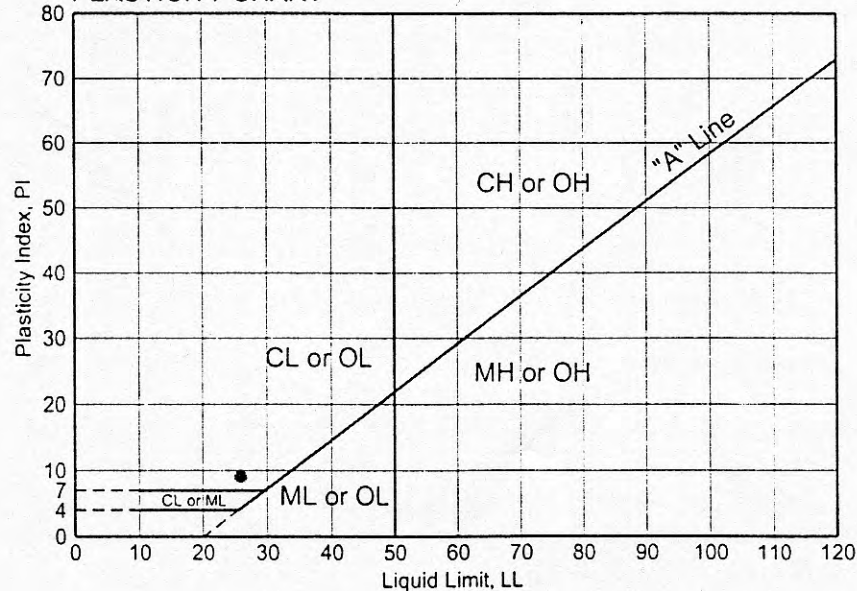
ATTERBERG LIMITS

Liquid Limit, LL 26
Plastic Limit, PL 17
Plasticity Index, PI 9

FLOW CURVE



PLASTICITY CHART



Job No. 1573Job Name COMMERCE GEOPHYSICAL LIN.Boring No. T-5 Depth # 1Date 1/15/72 Tested by RLFF-307
#1

Sample Description

WHOLE SAMPLE

Air Dry Sample Wt. = _____ (A1)

Air Dry Water Content

Can no. _____

wet + can _____

dry + can _____

can wt. _____

w.c. (dec) _____ (A2)

Oven Dry Sample Wt. = $\frac{A1}{1+A2} = \frac{304.1}{1+0} = 304.1$ (A3)

CNO. 10 PORTION

Air Dry Wt. Passing No. 10 = _____ (B1)

Air Dry Water Content

can no. _____

wet + can _____

dry + can _____

can wt. _____

w.c. (dec) _____ (B2)

Oven Dry Wt. Passing No. 10 = $\frac{B1}{1+B2} = \frac{249.7}{1+0} = 249.7$ (B3)

Air Dry Wt. of Hydrometer Sample = _____ (B4)

Oven Dry Wt. of Hydrometer Sample = $\frac{B4}{1+B2} = \frac{50.0}{1+0} = 50.0$ (B5)SCF, Sieve Correction Factor = $\frac{A3}{100 \times B5} \times B6 = \frac{304.1}{100 \times 50.0} \times 100 = 5.053$ HPF, Hydrometer Percentage Factor = $\frac{1000}{B5/B6} \times \frac{G}{G-1} = \frac{1000}{50.0/1.0} \times \frac{2.65}{2.65-1} = 1606$

Specific Gravity, G = 2.65

607 START

X = 0.99

DRY SIEVE						
Original Dry Sample Wt. (A3) = 304.1 gm						
U.S. Standard Sieve Size	Can No.	Sample Wt. (SW)	Corrected Sample Wt. = SW-SCF (+18-200 only)	Cumulative Wt. Retained	Cumulative % Retained	% Passing
1"						100
3/4"						100
3/8"						100
#4						99.24
#8						97.53
#10						94.24
#16						88.85
#30						83.09
#40						72.43
#50		14.2	6.5	10.67	7.24	65.36
#100		12.0	4.3	7.06	6.37	63.72
#200		8.7	1.0	1.64	63.72	

Hydrometer Correction

clear water reading 0.0 (C1) TOPwater + disp (top) 4.0 (C2)water + disp (bottom) 4.5 (C3)Hyd Corr = $-1 \times (2 \times C2 - C1 - C3) = -3.5$

Date	T	Hydrometer	Hydrometer	R	Temp. (C)	P	K	L	D (mm)
Time	Elapsed Time	Reading	Correction	Corrected Reading		HPF (R-1)	Table 3, pg. 93	Table 2, pg. 92	D = K/V ^{1/3} T
6:09 PM	2	35	-3.5	31.5	24.0°	0.6435	0.01282	10.5	0.0294
6:12 PM	5	26.5		23.0		0.4752	0.01282	11.9	0.0198
6:22 PM	15	20.0		16.5		0.3465	0.01282	12.95	0.0119
6:37 PM	30	17.5		14.0		0.2970	0.01282	13.3	0.0095
7:07 PM	60	15.5		12.0	24.5	0.2604	0.01275	13.7	0.0061
10:07 PM	240 (4h)	13.5		10.0	26.0	0.2307	0.01253	14.0	0.0030
6:07 PM	1440 (24h)	13.0		9.5	25.0	0.2138	0.01267	14.7	0.0013

$$P = (R_{actual} - \text{zero corr} + C_T) \alpha \quad \checkmark W/S PAWD \quad 6 \text{ HOURS}$$

F-410 AFTER #22

20.9-9.2

$C_T = 1.0, 24.0$
 $C_T = 1.15, 24.5$
 $C_T = 1.65, 26.0$
 $C_T = 1.30, 25.0$

NOTED TO ADT

GRAIN SIZE ANALYSIS-MECHANICAL

Data Sheet 6

Project COMMERCE GEOPHYSICAL Job No. 1573Location of Project _____ Boring No. T-5 Sample No. #1

Description of Soil _____ Depth of Sample _____

Tested By RLF Date of testing _____

Soil Sample Size (ASTM D1140)

Nominal diameter of largest particle Approximate minimum Wt. of sample, g

No. 10 sieve 200

No. 4 sieve 500

3/4 in. 1500

BEFORE WASH

AFTER
#200 40
WASH

TOTAL DRY WT BEFORE WASH

249.7 + 54.4 = 304.1

Wt. of dry sample + container		63.6
Wt. of container <u>CAN#</u>		9.2
Wt. of dry sample, W _s	304.1	54.4

CAN# F-409

Sieve analysis and grain shape

Sieve no.	Diam. (mm)	Wt. retained	% retained	% passing
#4		10.0 - 7.7 2.3	0.76	99.24
#8		12.9 - 7.7 5.2	1.71	97.53
#16		17.7 - 7.7 10.0	3.29	94.24
#30		24.1 - 7.7 16.4	5.39	88.85
#40		25.2 - 7.7 17.5	5.76	83.09
PAN		10.0 - 7.7 3.1	1.02	

% passing = 100 - \sum % retained.